A study of mitochondrial biogenesis in the rodent nervous system

Radha Desai

Institute of Neurology

University College London

Supervisor: Professor Kenneth J Smith

2014

Declaration

I, Radha Desai confirm that the work presented in this dissertation is my own, unless stated otherwise.

Intraspinal injections were carried out in collaboration with Andrew Davies and Gregory Delattre.

Cell culture was carried out in collaboration with Joseph Jebelli and Jennifer Pocock.

Signature:

_____

RADHA DESAI

Date:

_____

Acknowledgements

I would like to express deep gratitude to my supervisor Ken, for his patience, guidance and most of all encouragement to follow unexplored ideas in this thesis. The work has only been possible because he was willing to venture down a scientifically risky, but interesting path.

I am extremely thankful to members of the Smith group who made this journey enjoyable and have been great compatriots in the face of sometimes gloomy science. I'm especially grateful to Kim Chisholm, Jamie Cartland, Renee Ewe, Maya Gimalova, Gregory Delattre, Andrew Davies, Roshni Desai and Joseph Jebelli who helped with aspects of this project which required more than one set of hands on the bench as well as provided the intellectual fodder that is banter. I would also like to thank Sharmeen Haque and Charlotte Burt who have been very helpful with all sorts of paperwork and administrative responsibilities.

Lastly I want to thank my family. My mum and dad who inspired me to move away from biophysics and towards biomedical research and for their support during my PhD. Supriya, who is my sounding board for ideas that seemed crazy even to me. And finally, my husband Nayan who has been patient, encouraging and unrelenting in his championing of my scientific career in spite of me.

Abstract

This thesis investigates the process of mitochondrial biogenesis in the rodent CNS in the context of neuroinflammatory and neurodegenerative disease. There is mounting evidence of mitochondrial damage in neuroinflammation but very little is known about the turnover of mitochondria in neurones. We developed a method to assess mitochondrial biogenesis by tagging replicating mitochondrial DNA with bromodeoxyurine (BrdU), and used the method to examine mitochondrial biogenesis. In healthy motor neurons, mitochondria were distributed throughout the cell, including the axons, but the DNA replication signal initially only appeared in the cell body, subsequently becoming distributed away from the soma suggesting the presence of a mitochondrial 'nursery' in the cell body of long neurones. Furthermore, neuronal DNA replication increased in response to raised energy demand resulting from unilateral electrical stimulation of the sciatic nerve, indicating that mitochondrial biogenesis is promptly responsive to energy demand.

Mitochondrial biogenesis was also examined in spinal cord neurons in a model of multiple sclerosis (experimental autoimmune encephalomyelitis; EAE), and the degree of mtDNA replication was compared with the amount of inflammation in the tissue. We found that in severely inflamed tissue mitochondrial biogenesis was significantly reduced in the motor neurones. However, under subtle inflammation in EAE as well as with local intraspinal

injection of LPS (lipopolysaccharide), there was an increase in mitochondrial biogenesis, which may be a compensatory mechanism.

In separate experiments the CNS was examined globally using the BrdU method, which revealed the presence of hotspots of neuronal mtDNA replication indicating marked differences in mitochondrial turnover. Interestingly, these hotspots represented regions known to undergo degeneration in neurological diseases, especially those known or suspected to have a mitochondrial component in their aetiology.

The current findings reveal that mitochondrial biogenesis is substantial in neurons with long axons, and that it is promptly responsive to changing energy and disease conditions.

Table of Contents

Abbreviations

5-HT	5-hydroxytryptamine (Serotonin)
AD	Alzheimer's disease
AMPK	AMP-activated protein kinase
Ara-C	cytosine furanoarabinoside
ATP	adenosine triphosphate
BrdU	bromodeoxyuridine
CA1	Cornu Ammonis 1 (Hippocampal Region)
CA2	Cornu Ammonis 2 (Hippocampal Region)
CA3	Cornu Ammonis 3 (Hippocampal Region)
CGC	cerebellar granule cells
ChAT	choline acetyl transferase
CNS	central nervous system
DA	Dark Agouti
DG	dentate gyrus
EBSS	Earle’s balance salts solution
FBS	fetal bovine serum
GFAP	glial fibrillary acidic protein
HCl	Hydrochloric acid
HD	Huntington's disease
HIF-1α	hypoxia inducible factor - 1α
MEM	modified Eagle's medim
Mfn 1, 2	Mitofusin 1,2

mtDNA	mitochondrial DNA
NeuN	Feminising Locus
NRF-1,2	nuclear respiratory factor
OCT	optimal cutting temperature
OPA1	optic atrophy -1
OPA2	optic atrophy -2
OXPHOS	oxidative phosphorylation
PBS	phosphate buffered saline
PD	Parkinson's disease
PDL	poly d-lysine
PFA	paraformaldehyde
PGC	PPAR coactivator
PPAR	peroxisome proliferator activated receptor
RC	respiratory chain
ROS	reactive oxygen species
SBTI	soybean trypsin inhibitor
SN	substantia nigra
SOD-1	superoxide dismutase 1
TFAM	mitochondrial transcription factor A
TH	tyrosine hydroxylase
UCP	uncoupling protein
VDAC - 1	voltage dependent anion channel - 1
Vta	ventral tegmental area
β III Tub	beta III tubulin

Chapter 1: Introduction

Mitochondria are aptly termed the ‘powerhouses of the cell’ and are major contributors to the production of ATP – the energy molecule. ATP is the end product of a series of pathways predominantly - oxidative phosphorylation (OXPHOS) and glycolysis. Mitochondria carry out OXPHOS via respiratory chain complexes arranged on the inner membrane of mitochondria. Apart from this, mitochondrial are also the seat of many housekeeping functions of the cell, including biosynthesis of amino acids and steroids, β-oxidation of fatty acids, maintenance of cytosolic calcium homeostasis, and production and modulation of reactive oxygen species (ROS). Mitochondrial also play a vital role in apoptosis (Davis and Williams, 2012). Considering the intense energy demands of neurones, improper functioning of mitochondria can have devastating effects on neuronal survival. There is ample evidence particularly from genetic forms of disease, to suggest that impaired mitochondrial function is a cause rather than a consequence of neurodegeneration (Zsurka and Kunz, 2013).

Mitochondrial are double-membrane, dynamic organelles that are organized in a reticular network in the cell. They fuse and divide (fusion is mediated by OPA1, Mfn1, and Mfn 2, and fission is mediated by proteins fission 1 and Drp1), fragment, swell, extend and are recycled (mitophagy or vesicle formation) constantly and in a regulated fashion. Part of the lifecycle of mitochondria also includes the generation of new mitochondria known as

mitochondrial biogenesis – a process that is only beginning to be understood and explored in the context of disease. Unbalanced fusion leads to mitochondrial elongation, and unbalanced fission leads to excessive mitochondrial fragmentation and small mitochondria, both of which impair the function of mitochondria. It has been shown that exchange of mitochondrial contents is important for mitochondrial function as well as organelle distribution in neurons (Vidoni et al., 2013). Mitochondrial fusion, in particular that mediated by Mfn2, is required for proper development and maintenance of the cerebellum (Chen et al., 2007a). The picture that emerges is that the delicate balance between the different processes of fission, fusion, mitophagy, and biogenesis, is crucial for the functioning of the mammalian brain, and particularly in maintaining the health of the ageing brain. In this thesis, I studied the rodent central nervous system to shed light on the state of mitochondrial biogenesis in different neuronal types and in different tissue environments.

Mitochondrial DNA:

Mitochondria are unique organelles in that they are the only extra nuclear organelle in mammals to have their own genome - mitochondrial DNA (mtDNA). Mammalian MtDNA is a circular 16.5 kb molecule that encodes 13 essential peptides of the oxidative phosphorylation system, the main source of ATP for the eukaryotic cell. Secondary mtDNA mutations are typically caused by defects in nuclear genes that encode mtDNA processing proteins or those affecting nucleotide pools, leading to progressive accumulation of mtDNA deletions or mtDNA depletion, and subsequently to mitochondrial respiratory chain (RC) deficiency. MtDNA maintenance defects have been shown to be a

cause of neurodegenerative disorders (Corral-Debrinski et al., 1992). MtDNA replicates continuously in post-mitotic cells, but the mechanisms that regulate mtDNA replication initiation and copy number are not fully understood. Likewise, the consequences of increased mtDNA amount *in vivo* are not well characterized. Two mtDNA maintenance proteins, mitochondrial transcription factor A (TFAM) and the mitochondrial helicase Twinkle, are known to correlate linearly with mtDNA copy number but the mechanisms involved are only beginning to be understood (Ylikallio et al., 2010). Within the mitochondria, mtDNA exists as multi-molecular clusters called nucleoids. Nucleoid organization and mtDNA copy number are both important for the maintenance, inheritance and segregation of mtDNA.

TFAM (mitochondrial transcription factor A)- a high-mobility group-box protein, is an activator of mitochondrial transcription, and is required for mtDNA replication, probably through providing RNA primers for replication. However, it also serves a histone-like function by packaging mtDNA, and, as mtDNA levels follow TFAM levels, it is likely that naked mtDNA does not exist in mitochondria (Kanki et al., 2004). Visualizing TFAM (via immunohistochemistry) can be a useful read-out for the amount mtDNA in a cell. However, this is not a good indicator of mitochondrial biogenesis because the method does not indicate whether the amount of mitochondrial DNA has increased or decreased as a result of the regulation of mitochondrial biogenesis or mitophagy.

The respiratory chain, which is responsible for the process of oxidative phosphorylation, ultimately resulting in the production of ATP from ADP,

consists of complex I–complex IV. The mitochondrial genome holds 13 protein-encoding genes, which incorporate into complex1, III, IV, complex and ATP synthase. Complex II is the only complex with all subunits encoded by only nuclear DNA(Taylor et al., 2004). MtDNA point mutations and deletions lead to energy deficiency states frequently affecting the central nervous system (CNS) in patients with primary mitochondrial diseases (Goldstein et al., 2012).

The maintenance of mtDNA is crucial for normal cellular function (Wallace et al., 1988). A unique feature of mitochondrial genetics is the coexistence of both mutant and wild-type mtDNA in a single cell. Mutations in mtDNA accumulate over time and must reach a crucial threshold (~70-90% of total mtDNA) before associated neurological signs manifest (Wallace and Fan, 2009). Proper mitochondrial dynamics are important for the accurate segregation and transmission of mtDNA during mitosis, and numerous studies in yeast have shown that there is a relationship between mitochondrial dynamics and genomic stability (Hermann and Shaw, 1998; Rapaport et al., 1998). The results of subsequent studies in mammalian cells agreed with these findings and confirmed the roles of Mfn1, Mfn2 and Opa1 in mtDNA maintenance (Chen et al., 2007a).

It has been suggested that the exchange of mitochondrial contents mediated by mitochondrial fusion, enables the reduction of the influence of pathogenic mtDNA mutations. Introducing wild-type mtDNA dilutes the mutant mtDNA molecules and prevents them from reaching a crucial threshold in the cell

(Chen et al., 2007b; Sato et al., 2006, 2009) In a recent study conducted by Chen et al., muscle-specific *Mfn1*- and *Mfn2*-knockout mice were reported to have impaired mitochondrial function, abnormal mitochondrial proliferation and muscle loss (Chen et al., 2011). Furthermore, loss of mitochondrial fusion in skeletal muscle resulted in increased mtDNA point mutations and deletions as well as severe mtDNA depletion, which preceded the phenotypic changes observed in these mutant mice. This study supports the hypothesis that mitochondrial fusion through intramitochondrial exchange increases the tolerance of a cell to mutant mtDNA, and protects the integrity of the mitochondrial genome. Therefore, changes in the expression levels of both fusion and fission proteins can influence the mitotic segregation of mutant and wild-type mtDNA, and might be an important factor in the proliferation of dysfunctional mitochondria that is observed with ageing and mitochondrial disease. Recently, it has also been postulated that the size and complexity of mtDNA nucleoid structure can influence mtDNA damage accumulation during ageing of many somatic tissues (Bogenhagen, 2009). Although significant advances have been made in understanding the role of mitochondrial dynamics in mtDNA transmission, segregation and stability, additional work is required to link the aging process directly with the organization of mtDNA nucleoids and the proteins that regulate mitochondrial dynamics.

So far no reports have been published about the mitochondrial biogenesis process in neuroinflammation or neurodegeneration, largely because the process is not easy to probe *in vivo.* The techniques that have been used in

the past have mostly been in cell cultures (Calkins and Reddy, 2011a; Magnusson et al., 2003).

The understanding of the mitochondrial biogenesis landscape in the central nervous will enable the exploration of whether modulating the molecular mechanisms of biogenesis can facilitate the protection of neurones against their degenerative fate.

Understanding mitochondrial biogenesis from non-neuronal systems

Research regarding mitochondrial biogenesis has been ongoing for decades. Whether it is intrinsic to mitochondria themselves (fully autonomous), wholly separate from preexisting mitochondria (nonautonomous), or somewhere in between (partially autonomous)—has been continuously addressed starting from biochemical lipid synthesis studies beginning 40 years ago (Dennis and Kennedy, 1972). In addition, the more recent findings of mitochondrial network fission and fusion events has turned the simplistic concept that damaged mitochondria can be replaced into an open debate on the precise definition of ‘replacement.' Is there fission of existing mitochondria with selective replacement of damaged sections and constituents or complete replacement of proteins, lipids, and/or mtDNA? The prevailing sentiment generally supports a partially autonomous model of biogenesis (Michel et al., 2012), wherein newly synthesized proteins and other components (e.g., lipids) are incorporated into existing mitochondria, which is somehow linked to fission to restructure and/or divide. Despite these limitations, mitochondrial dynamics related to the term ‘biogenesis' can be assessed by the combined use of several outcomes, many of which are now investigated in the context of

brain pathology.

Mitochondrial proteins are encoded in both the nuclear and mitochondrial genomes, necessitating transcriptional activation in both organelles for fully functional mitochondria. This bigenomic origin of mitochondrial proteins is well documented and several critical components have been identified, but the exact mechanism and coordination of intra- and extra-mitochondrial processes are still poorly understood. The mitochondrial transcription factor A (TFAM) is encoded in the nucleus and is required for initiation of mtDNA replication, initiation of transcription of mitochondrial-encoded genes, as well as the organization, and possibly copy number, of the mtDNA genome (Falkenberg et al., 2007). Although several other mitochondrial transcription factors have been identified, TFAM appears to be the major regulator of transcription. The expression of TFAM is primarily under the control of the nuclear transcription factor NRF-1 (nuclear respiratory factor 1), which also induces the transcription of nuclear-encoded mitochondrial genes essential for the electron transport chain. The replication of mtDNA and the induction of both nuclear- and mitochondrial-encoded mitochondrial genes are necessary for mitochondrial biogenesis, and support the concept that induction of TFAM and possibly NRF-1 are indispensable elements in biogenesis. To this end, upregulation of Tfam has been observed under several neuroprotective settings (Mendelev et al., 2011).

Various upstream signalling pathways can contribute towards the activation of the transcriptional programme necessary for biogenesis. PGC1- α

(peroxisome proliferator-activated receptor (PPAR)- γ coactivator 1- α), nuclear factor- κ B (NF- κ B), and Nfe2l2 can translocate to the nucleus either by dissociation of tethering proteins or posttranslational modification, and are then capable of binding to the promoter region and promoting transcription of NRF-1. NRF-1 can then bind to and promote the transcription of mitochondrial transcription factor A (TFAM) and many other nuclear-encoded mitochondrial proteins, such as subunits of the electron transport machinery (Stetler et al., 2012). These proteins are then translated and imported into the mitochondria. TFAM then can bind to and initiate transcription of the mitochondrial genomes, which includes mitochondrial-encoded subunits of the electron transport machinery. Tfam, in addition to other proteins, also acts in the control of mitochondrial DNA (mtDNA) copy number, including replication when needed (Ngo et al., 2014).

Several elements of the above described pathway and associated proteins are implicated in neurodegenerative and neuroinflammatory conditions (Figure 1). However, what is not understood is:

- the constitutive rate of mitochondrial biogenesis in a neurone of interest
- whether this rate changes under the influence of changing metabolic demands
- whether modulating biogenesis can offer protection.

BrdU – historical use / pharmacokinetics

Bromodeoxyuridine (BrdU) is an often-used analogue of thymidine, which gets incorporated into the *de novo* strand during DNA synthesis or replication.

Introduction of BrdU complimented with immunohistochemistry has been used extensively to study cellular proliferation to mark the nuclear DNA of the replicating cell (Gratzner, 1982). This method has proved to be a particularly powerful tool in the study of neural stem cell (Kee et al., 2002). Although BrdU has been used extensively for studying proliferation of nuclear DNA, it is not a common probe for looking at mitochondrial DNA replication. One of the reasons may be that the widely used dose of BrdU (100-200 mg/kg) *in vivo* for cell proliferation does not provide a sufficient concentration of BrdU in the tissue to probe the much smaller signal for mitochondrial DNA. The other possibility is that there is very little mtDNA replication in most cells. The ability of BrdU to remain as part of the new strand of DNA provides a pulse and chase experimental tool, allowing the possibility of probing a specific point in time and space to evaluate the degree and pattern of mitochondrial DNA replication and, in turn, mitochondrial biogenesis. This method has been used successfully in the past for cultured cell studies (Amiri and Hollenbeck, 2008; Davis and Clayton, 1996; Lentz et al., 2010; Magnusson et al., 2003).

Incorporation of BrdU has been found to be deleterious to the fidelity of DNA, resulting in more mutations when BrdU containing DNA replicates in subsequent generations (Duque and Rakic, 2011). I was cautious in interpreting the fate of BrdU containing mtDNA for this reason, because it may behave differently than naturally occurring mtDNA. For the purpose of this study we restricted our observations to using the BrdU signal as a simple readout of the percentage of mitochondria undergoing DNA replication. All

quantitative studies were made against physiologically comparable, controlled conditions.

Mitochondrial pathology - neuroinflammation

Multiple Sclerosis is an inflammatory demyelinating disease of the CNS. Although available treatments are effective in controlling the neuroinflammatory pathology, the loss in neuronal tissue which underlies the symptoms of the disease continues to progress. In recent years, evidence has emerged to suggest that infiltrating inflammatory cells and activated microglia contribute towards damage to neuronal mitochondria (Witte et al., 2014), which eventually leads to axonal loss and ultimately neuronal death. Mitochondria were implicated in MS research with the observation that patients suffering from Leber's hereditary optic neuropathy (LHON), which is caused by mutations in mtDNA (Wallace et al., 1988) have an increased risk of developing an MS-like condition known as Harding's disease (Olsen et al., 1995). Studies have suggested a weak association between LHON, mtDNA mutations and MS susceptibility, whereas other studies failed to find any association. There is evidence that the presentation of severe optic neuritis in a subset of MS patients is linked strongly to mtDNA mutations. This may be due to the relation of both MS and LHON to a certain mtDNA haplotype (a distinct set of mtDNA polymorphism (Kalman et al., 1999).

So far one polymorphism in nuclear DNA encoding a mitochondrial protein has been linked to the susceptibility to MS. This was found to be associated with MS in two independent cohorts of German patients in the promoter

region of uncoupling protein 2 (UCP2) a mitochondrial protein that is able to separate the mitochondrial membrane potential from ATP synthesis and thereby decrease ATP and ROS production (Vogler et al., 2005). As more whole genome sequencing is performed, it is likely that other mitochondrial proteins may be identified. In the meanwhile, it is important to get a handle on the mitochondrial turnover dynamics in multiple sclerosis and animal models of neuroinflammation – experimental autoimmune excephalomyelitis (EAE).

It was reported that in mice, NRF-2 is induced in neurones by the drug dimethyl fumarate (DMF) (Linker et al., 2011). This effect has been proposed to contribute to an attenuated EAE disease course in DMF-treated mice, and might, therefore, partly underlie the beneficial effects of this drug in patients with MS. One of the key roles of NRF-2 is to increase mitochondrial biogenesis along with NRF-1 via the PGC-1α pathway (Ventura-Clapier et al., 2008a). It may be postulated that along with providing antioxidant-mediated protection, NRF-2 induced mitochondrial biogenesis to repair the pool of damaged mitochondria. One of the aims of the present work is to study the changes that occur to the rate of mitochondrial biogenesis under conditions of neuroinflammation.

Microarray analysis of the postmortem motor cortex from MS patients revealed decreased gene expression of 26 nuclear-encoded subunits of the RC (Dutta et al., 2006), which coincided with a significant reduction in activity of OXPHOS complexes I and III. *In situ* hybridisation showed that this decrease occurs specifically in cortical neurons. It was also observed that the

MS cerebral cortex contained neurons devoid of complex IV activity (Campbell et al., 2011). However, this does not explain the reduction of various nuclear-encoded respiratory chain complex subunits in the MS cortex (Dutta et al., 2006). The overall level of mitochondrial biogenesis may be reduced in inflamed tissue and we explored this possibility in the present work.

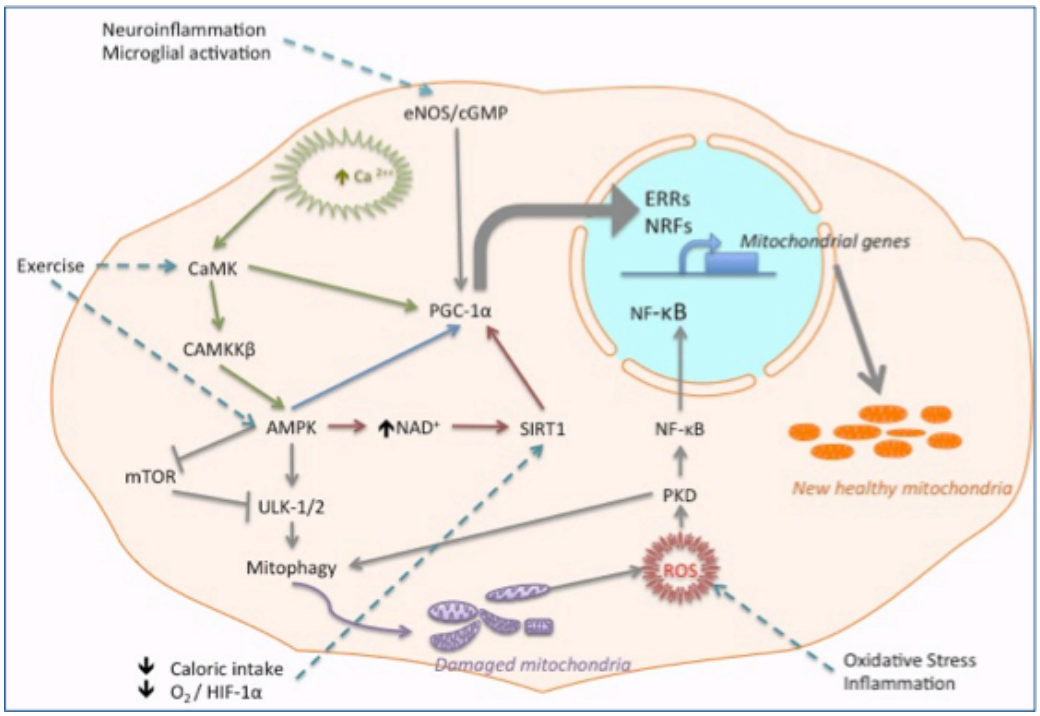

Figure 1: Schematic showing the molecular pathways at play, which dictate the mitochondrial environment in the diseased CNS. Stimuli that directly initiate biogenesis – oxidative stress, microglial activation, hypoxia are found to be active in neuroinflammatory and neurodegenerative disease. High levels of reactive oxygen species get released from damaged mitochondria and in turn activate the biogenesis machinery via signalling down the PKD and NF-κB cascade. Similarly hypoxia can stimulate mitochondrial biogenesis via the SIRT1 signalling pathway, which activates PGC-1α, one of the master regulators of mitochondrial biogenesis.

Why study mitochondrial biogenesis?

Peroxisome proliferator-activated receptor (PPAR)-γ co-activator (PGC)-1α is a transcriptional co-activator that interacts with a broad range of transcription factors involved in a wide variety of biological processes and/or responses including mitochondrial biogenesis, OXPHOS, antioxidant defense, adaptive thermogenesis, glucose /fatty acid metabolism, fibre type switching in skeletal muscle, and heart development (Liang and Ward, 2006; Puigserver and Spiegelman, 2003; St-Pierre et al., 2006). PGC-1α does not bind to DNA directly, but forms heteromeric complexes with transcription factors, including nuclear respiratory factors, NRF-1 and NRF-2, and the nuclear receptors, PPARα, PPARδ, PPARγ, and estrogen-related receptor α (Lin et al., 2003). These transcription factors, in turn, regulate the expression of many nuclear-encoded mitochondrial genes, such as cytochrome c, complexes I to V, and TFAM (Handschin and Spiegelman, 2006; Kelly and Scarpulla, 2004). In recent years, impaired PGC-1α expression and/or function has emerged as a common underlying cause of mitochondrial dysfunction in neurodegenerative diseases such as Huntington's disease (HD), Parkinson's disease (PD), and Alzheimer's disease (AD) and amyotrophic lateral sclerosis (ALS).

There is substantial evidence for the impairment of PGC-1α levels and activity in HD (Cui et al., 2006). The involvement of PGC-1α in HD was first indicated by the findings that PGC-1α knockout mice exhibited mitochondrial dysfunction, defective bioenergetics, a hyperkinetic movement disorder, and striatal degeneration, which are features also observed in HD (Lin et al.,

2003). Selective ablation of PGC-1α leads to increased striatal neuron degeneration and increased susceptibility to the mitochondrial toxin 3-NP in HD transgenic mice (Cui et al., 2006). Furthermore, impaired PGC-1α function and levels occur in striatal cell lines, transgenic mouse models of HD, and postmortem brain tissue from patients with HD ((Cui et al., 2006). This suggests that dysfunctional mitochondrial biogenesis signal can underlie the pathology of the large scale neurodegeneration occurring in HD.

It is not understood, why certain populations of neurones are far more susceptible to damage and death. The symptoms which manifest the disease are related to the function of these neurones. One prime example of this is Parkinsons disease. A meta-analysis of 17 independent genome-wide gene expression microarray studies revealed the strongest association between PD and nuclear genes encoding for OXPHOS subunits in mitochondria and enzymes involved in glucose metabolism, all of which are regulated by PGC-1α (Zheng et al., 2010b). These genes showed decreased expression in (laser microdissected) substantia nigra dopaminergic neurons even in the earliest stages of PD. Activation of PGC-1α results in increased expression of OXPHOS subunits and blocks the dopaminergic neuron loss induced by mutant α-synuclein, or the pesticide rotenone, in cultured dopaminergic neurons from embryonic rat midbrain and human catecholaminergic SH-SY5Y cells (Zheng et al., 2010b). Transgenic mice overexpressing PGC-1α in dopaminergic neurons are resistant against cell degeneration induced by the neurotoxin MPTP (1-methyl-4-phenyl-1,2,3,6-tetrahydropyridine) (Mudo et al.,

2012). Earlier, it was noted that genetic ablation of the PGC-1α gene markedly enhances MPTP-induced loss of tyrosine hydroxylase-positive neurons in the substantia nigra (St-Pierre et al., 2006). Recently, a parkin-interacting substrate was identified that accumulates in parkinsonian rodent models and the human PD brain. These tissues show reduction in the expression of PGC-1α and its target gene, NRF-1 (Clark et al., 2011; Shin et al., 2011). Furthermore, there is some evidence of an association of certain PGC-1α single-nucleotide polymorphisms with the risk or age of onset of PD. This suggests that perhaps transcriptional targeting of mitochondrial biogenesis may prove effective in protecting against PD pathology, leading to the question of why substantia nigra neurones are susceptible to damage. It was recently reported that selective mtDNA damage is a molecular marker of vulnerable nigral neurons in PD and suggested that this may result from intrinsic differences in how these neurons respond to complex I defects (Sanders et al., 2014).

Using genome-wide complementary DNA microarray analysis (Qin et al., 2009) showed that PGC-1α expression is decreased in the brain of patients with AD as a function of dementia severity. PGC-1α protein content was negatively associated with both AD-type neuritic plaque pathology and β-amyloid contents. Qin et al. also showed that adenoviral-mediated exogenous PGC-1α expression in Tg2576 neurons attenuated hyperglycemic-mediated β-amyloidogenesis. Recently, Liang et al. (2011) showed an age-dependent decrease in PGC-1α in SOD1-G93A mice. Moreover, they showed that

overexpression of PGC-1α slowed the progression of ALS, moderately extended lifespan, and improved motor (rotarod) performance (Liang and Ward, 2006). These improvements were associated with a significant decrease in motor neuron cell death and less neuromuscular junction damage in the G93A mice that overexpressed PGC-1α. In the same year, the Pasinetti laboratory also showed that PGC-1α overexpression significantly improved motor function and survival of SOD1-G93A mice (Zhao et al., 2011). Reduced blood glucose levels and protection against motor neuron loss, restoration of mitochondrial electron transport chain activities, and inhibition of stress signalling in the spinal cord accompanied the behavioral improvements.

In light of the literature in the field this present study was set to lay the ground -work for studying mitochondrial biogenesis *in vivo* in the adult mammalian CNS, with the hope that this will prove beneficial in understanding the important molecular players in modulating mitochondrial lifecycle and how this can be used for therapeutic benefit in the future. In the following chapters, along with a brief introduction and description of methodology, four key advances are presented:

1. Established a new method for probing mitochondrial biogenesis using mtDNA replication as a surrogate marker for the production of new mitochondria
2. Evaluated mitochondrial biogenesis under conditions of neuroinflammation
3. Evaluated mitochondrial biogenesis under altered energy demand and discovered a somatic mitochondrial nursery in long motor neurones

4. Finally, identified regions of the CNS which show constitutively high mitochondrial biogenesis

Chapter 2: Assessing mitochondrial DNA biogenesis in the CNS

Introduction

Mitochondria are key regulators of cellular energy and the focus of a large number of studies examining the regulation of mitochondrial dynamics and biogenesis in the CNS, both in healthy and diseased conditions. One approach to monitoring mitochondrial biogenesis is to measure the rate of mitochondrial DNA (mtDNA) replication. Here, we describe a sensitive technique to label newly synthesized mitochondrial DNA (mtDNA) in individual neurons *in vivo* by combining incorporation of the thymidine analogue bromodeoxyuridine (BrdU). This technique is a valuable tool for visualizing and measuring mtDNA biogenesis within individual neurons, and importantly, in specific compartments such as somas, dendrites, axons, and synapses. This is the first report using BrdU to visualize mtDNA biogenesis *in vivo,* whereas other reports have used BrdU *in vitro* (Amiri and Hollenbeck, 2008; Lentz et al., 2010; Salic and Mitchison, 2008). The ability to visualize and quantify mitochondrial biogenesis will afford new insight into the mechanisms underlying the pathogenesis of multiple mitochondrial-based neurological disorders and here this method has been developed to study mitochondrial biogenesis in the context of neuroinflammation. BrdU was administered

systemically and the signal was evaluated post mortem via immunohistochemistry. We have found that in CNS tissue using this protocol the signal is observed mainly in neuronal cell bodies. The technique has been optimized for the rate of mitochondrial turnover in spinal cord motor neurones. Adult neurones are post-mitotic and so nuclear DNA replication, which is abundant in proliferating cells, is absent and the desired neuronal mitochondrial replication can be observed very clearly. The BrdU signal was confirmed to be arising from mitochondria by co-localization with a mitochondrial protein marker VDAC-1 (voltage dependent anion channel-1) and ensuring that these signals were extra-nuclear. The abundance of BrdU positive mitochondria as a percentage of the total VDAC-1 particles was regarded as a of mitochondrial biogenesis in a cell.

Furthermore, the reagents used in the protocol were evaluated *in vitro* in cerebellar granule cell cultures in order to validate the method against previously described protocols. Two other methods were evaluated as supplementary to the BrdU protocol: first, immunohistochemical labeling for TFAM, which is a transcription factor that regulates mtDNA replication and, second, labeling with PicoGreen®, a fluorescent dye that intercalates into double stranded DNA.

Methods

Preparation and injection of BrdU

C57/BL6 mice were used weighing between 25-35 g. Bromodeoxyuridine (BrdU) (Sigma-Aldrich, USA) was injected at different doses for the first experiment testing the appropriate dose: 100mg/kg, 200 mg/kg, 400mg/kg and then finally two doses of 200mg/kg spaced 2 hours apart. The BrdU was

dissolved in 0.9% sodium chloride solution in distilled water (saline), at 60°C in a water bath for 30 minutes just before injecting. The dosing volume was kept constant at 5 ml/kg. Control animals were injected with plain saline. Injections were administered intra-peritoneally (i.p.) into the abdominal cavity of the animal, alternating sides for multiple doses. Animals were sedated lightly with isoflurane before injections (Figure 1).

Figure 1: Timeline of BrdU injections. The different protocols were tested to optimize the optimum dose needed to detect mitochondrial DNA replication in spinal motor neurons.

Perfusing, fixing, sectioning

Animals were anaesthetised with 5% isoflurane and then maintained at 2% isoflurane, passed with 100% oxygen into a nose cone. Cardiac perfusion was performed using rinse (heparinized buffered saline) until the blood had been drained, and then 4% paraformaldehyde solution (PFA; in phosphate-buffered saline) until the tissue was structurally fixed. The carcass was decapitated to facilitate removing the brain and eyes. The spinal cord and nerve roots were dissected out separately. A piece of the small intestine was harvested as a positive control for the BrdU. The inner crypt layer of the intestine undergoes rapid cell proliferation and is a good marker for DNA replication. The samples were post fixed in 4% PFA overnight. The samples were immersed in increasing concentrations of sucrose (10%, 20% and 30%) for

cryopreservation. Each step was maintained as long as it was needed for the samples to sink into the solution to ensure that the sucrose solution had fully replaced the water content in the samples and the relative density across the solution and sample was in equilibrium. This precaution ensures minimum freezing artifacts in the samples. Following this, the samples were dissected to appropriate smaller pieces and then placed in plastic molds and covered with OCT (Optimal Cutting Temperature compound, Tisse-Tek) tissue matrix gel. The molds were then frozen in a pot of isopentane pre-cooled in a bath of dry ice. The frozen molds were wrapped in aluminium and stored at -80℃ until sectioning. The samples were sectioned using a cryostat at -19℃ at a thickness of 12 µm on to positively charged glass slides. The glass slides were stored in sealed boxes at -20℃ before being processed and stained.

Cell culture

Cerebellar Granule Cell (CGC) Culture: Cerebellae were collected and CGCs were isolated as previously described by Courtney and colleagues (Courtney et al., 1990). Five day old Sprague Dawley rat pups were sacrificed and cerebellae collected on ice into a buffer consisting of 153 mM Na^+, 4 mM K^+, 1.5 mM Mg^{2+}, 139 mM CL^-, 10 mM PO_4^{2-}, 1.5 mM SO_4^{2-}, 14 mM glucose, and 50 µM BSA (pH 7.4). This solution is called solution B. The cerebellae were chopped up with a sterile razor blade and collected into solution B supplemented with 0.5 mg/ml trypsin to facilitate enzymatic digestion of the extracellular matrix. CGCs in trypsin were incubated for 5 minutes at 37^{o}C with gentle agitation every 1-2 minutes. Trypsin was neutralised by addition of 20 ml of solution B containing 8 μg/mL soybean tryspin inhibitor (SBTI) and 8 U/ml DNAase. The suspension was then centrifuged at 6 g for 5 minutes. The

supernatant was discarded, and the pellet resuspended and triturated in 3 ml of buffer (solution B containing 3 mM Mg^{2+} and SO_4^{2-} supplemented with 50 µg/mL SBTI and 50 U/ml DNAase) using three fire-polished glass pipettes of progressively decreasing diameter. Triturated, homogenous perikarya were layered onto 5 ml 4% BSA in Ca^{2+} -free Earle's Balance Salts Solution (EBSS) and centrifuged for 5 minutes at 100 g to remove debris. The pellet was resuspended in warmed CGC medium (MEM supplemented with 10% FBS, 20 mM KCl, 30 mM D-glucose, 2 mM L-glutamine, 25 mM $NaHCO_4$, 50 U/ml penicillin, 50 μM streptomycin, and 6 μg/ml ampicillin) at a density of $8x10^6$ cells/ml. CGCs were then plated at $8x10^5$ cells per well onto 13 mm diameter poly-D-lysine (PDL)-coated coverslips in a volume of 100 μl media. To give perikarya time to adhere, additional CGC medium (400 μl) was not added until at least 1 hour after plating (giving a total volume of 500 μl per well). After 24 hours, the cells were washed and half the media was replaced with MEM supplemented with 20 μM cytosine furanoarabinoside (Ara-C) to prevent further glial proliferation. The cultures were maintained at 37°C in 6% CO_2 and were available for use after 6 days *in vitro*. Either 1 µl or 0.5 µl of a BrdU stock in saline (10 mM) was added into the medium to give a final concentration of 20 µM or 10 µM. The BrdU was left in the medium for a minimum of 6 h and maximum of 24 h. Control wells were treated with equal volumes of plain saline.

Immunohistochemistry / immunocytochemistry

Immunohistochemistry:

BrdU was detected using fluorescence immunohistochemistry. The slide boxes were removed from the freezer and allowed to warm up to room temperature before opening the box, in order to avoid condensation and freezing on the slide. Then the sections were re-fixed with a few drops of 4% PFA on the slide for 15 minutes at room temperature. Phosphate buffered saline (PBS, sodium chloride 137 mM, potassium chloride 2.7 mM, di-sodium hydrogen phosphate 10 mM, potassium di-hydrogen phosphate 2mM, pH adjusted to 7.4) containing 0.3% TritonX-100 was applied to partially permeabilize the cell membranes. After a five-minute PBS wash the slides were put in a trough containing 2 N hydrochloric acid (HCl) for 90 minutes at 40℃. The HCL partially denatures DNA in cells so as to expose the BrdU and allow the primary antibody access to the epitope. At the end of 90 minutes, the slides were washed with PBS once and then with PBS containing 0.3% hydrogen peroxide (from 30% stock, Sigma-Aldrich USA) to quench all endogenous peroxidase activity. The slides were then laid out in a humid staining tray for further processing. Two washes for 5 minutes with PBS were performed following which 5% goat serum in PBS with 0.1% tween-20 was applied for one hour. The blocking serum buffer blocks the primary antibody from interacting with non-specific epitopes, and reduces background. After blocking, the slides were cleared of the solution simply by tilting them and then primary antibody solution in PBS was added. The following primary antibodies were used after optimization to determine the ideal dilution factors stated.

1. Rat anti BrdU (AbD Serotec MCA2060) at 1:200

2. Rabbit polyclonal anti VDAC-1 / Porin (Abcam) ab15895 at 1:600
3. Rabbit polyclonal Anti-NeuN (Abcam ab104225) at 1:500
4. Sheep polyclonal anti choline acetyltransferase (Abcam ab18736) at 1:100
5. Mouse monoclonal anti Beta III Tubulin (Abcam ab78078) at 1:400
6. Rabbit Polyclonal anti-TFAM (Abcam ab131607) at 1:400

Slides were incubated with antibody solutions over night at 4℃. The next morning, slides were washed stringently in troughs of PBS with 0.2% tween, 3 times, 15 minutes each at room temperature. A combination of the following secondary antibodies in PBS were applied for 2 hours at room temperature

1. Biotinylated goat anti rat antibody at 1:200 (Vector labs BA-9401)
2. Biotinylated anti rabbit at 1:200 (Vector Labs BA-4001)
3. Goat anti rabbit conjugated to Alexa fluor 546 (Life Technologies A11081) at 1:400
4. Goat anti mouse conjugated to Alexa fluor 546 (Life Technologies A11003) at 1:400
5. Donkey anti mouse conjugated to Alexa Fluor 546 (Life Technologies A10036) at 1:400
6. Donkey Anti sheep conjugated to Alexa fluor 546 (Life Technologies A21098) at 1:400

Slides were washed once again 3 times, each wash lasting 15 minutes with PBS and 0.2% tween. Finally, slides were incubated for 90 min at room temperature with Alexa Fluor 488 conjugated streptavidin (Life Technologies

S-11223). After a final set of PBS washes, the slides were mounted using Vectashield (Vector labs H-1000) and then stored at 4℃ until ready to be imaged.

To ensure that the streptavidin was not reacting with endogenous biotin, one set of slides was incubated with avidin (4 drops / ml) in the blocking serum followed by biotin (4 drops/ml) with the primary antibody step. This showed no difference in pattern of staining compared with the simpler protocol, so it was avoided for other protocols. For staining that did not include BrdU the HCl acid treatment was replaced by a quick antigen retrieval step using DAKO target retrieval solution (S1700) for 40 minutes at room temperature.

Immunocytochemistry:

With the CGC cultures, the cells were incubated with BrdU (see above) for either 6 hours or 24 hours and then used the next day. Coverslips were kept in the 24 well plates for staining. Cells were fixed with 4% PFA in the wells for 15 minutes at room temperature. Following this, phosphate buffered saline (PBS) containing 0.1% TritonX-100 was applied to partially permeabilize the cell membranes. After a five minute PBS wash 2N hydrochloric acid (HCl) was put in the wells for 90 minutes at 40℃. At the end of 90 minutes, cells were washed with PBS once and then with PBS containing 0.3% hydrogen peroxide (from 30% stock, Sigma-Aldrich USA). Two washes for five minutes with PBS were performed following which 5% goat serum in PBS was applied for one hour; this blocks the primary antibody from interacting with non-specific epitopes, and reduces background. After blocking, primary antibody solution in PBS was added. Primary and secondary antibody treatments were

carried out as described above in the stated dilutions. A 90 min incubation at room temperature with Alexa Fluor 488 conjugated streptavidin (Invitrogen) was followed with a final set of PBS washes. The coverslips were mounted on glass slides using Vectashield (Vector labs) and then stored at 4℃ until ready to be imaged.

Image capture and analysis:

Fluorescent labelling was observed through a LSM 5 Pascal confocal microscope (Zeiss, Oberkochen, Germany) and images were recorded with the Pascal software (Zeiss). All image analysis was done using Image J (NCBI, USA) and corresponding plug-ins. All staining was checked for non-specific antibody labelling using control slides without primary antibody or without secondary antibody or without fluorescently labelled streptavidin. None of the controls showed any signs of nonspecific fluorescence.

Staining with PicoGreen®

PicoGreen® (Life Technologies P7581) was used to try and quantify mitochondrial DNA in histological sections. Instead of using PFA-fixed tissue, this tissue was fresh frozen and sectioned. The sections were allowed to warm up to room temperature and then PicoGreen® was added in PBS (3 μl of stock in 1 ml) and applied directly onto the slides for 15-30 minutes. Following this the slides were mounted with Vectashield and imaged on the confocal microscope within 24 hours

Results

Dosing regimen-

Different doses of BrdU were initially tried and then followed up with immunohistochemistry to visualize extra-nuclear DNA replication. The immunohistochemistry protocol was based on a previously described protocol with different antibodies (Calkins and Reddy, 2011b). The single doses of 100 mg/kg of 200 mg/kg did not show any obvious non-nuclear BrdU incorporation into DNA in the CNS. The 400 mg/kg single dose showed some appearance of BrdU signal in the cytoplasm of neurons in spinal cord grey matter. When BrdU in saline is administered at 100 mg/kg i.p., the plasma concentration peaked at 2 hours and then slowly subsided after 4 hours (data not shown). On the basis of this pharmacokinetic profile, a new protocol was tested. First a loading dose of 200 mg/kg was administered, followed two hours later with another dose of 200 mg/kg (Figure 2).

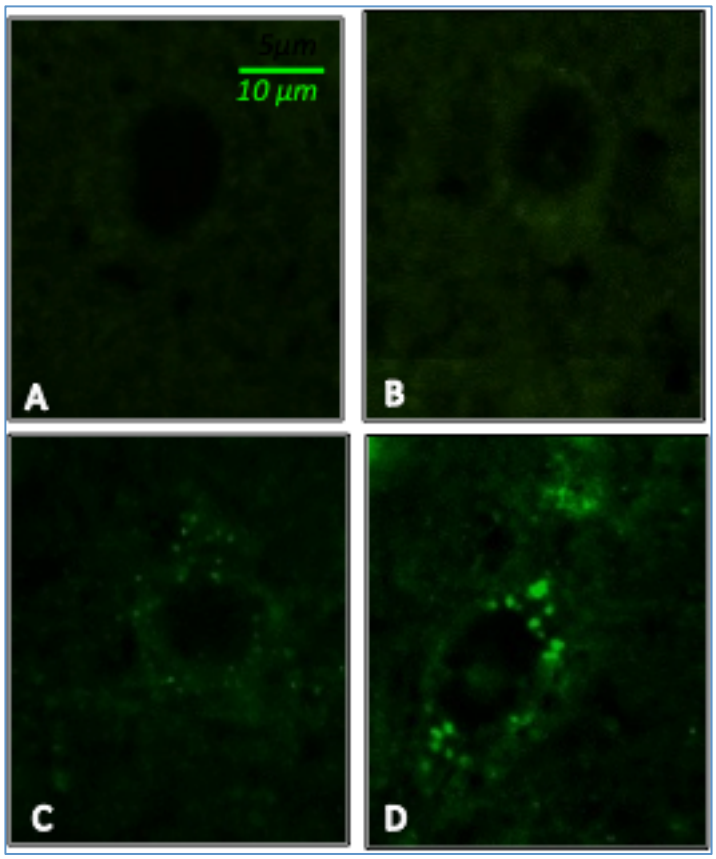

Figure 2: BrdU staining (Green) performed on sections of spinal cord in order to detect mitochondrial DNA replication. Each panel is a representative image of motor neurones in transverse section of the ventral horn of spinal cord from an animal that received the following dose of BrdU (A) received 100 mg/kg, (B) received 200 mg/kg, (C) received 400mg/kg, and (D) received 2 doses of 200 mg/kg.

This particular dosing regimen showed clear extra-nuclear BrdU labelling in neurones of the spinal cord (Figure 2). To ensure that the BrdU signal was arising from mitochondria, a double labeling of BrdU and VDAC-1/porin was performed. VDAC-1 is used as a mitochondrial marker protein. In most cases, the BrdU co-localized with the VDAC-1 signal, but not on every occasion. Figure 3 shows these signals from grey matter of the spinal cord. The cells of primary interest are motor neurons of the spinal cord, which are particularly large and energy-demanding neurons, which depend on a robust and

dynamic mitochondrial network for normal functioning. However, it is important to note that other cells in the CNS also do not show a large amount of BrdU in their cytoplasm indicating that the rate of replication of mtDNA is far greater in neurones as compared with other cells of the CNS.

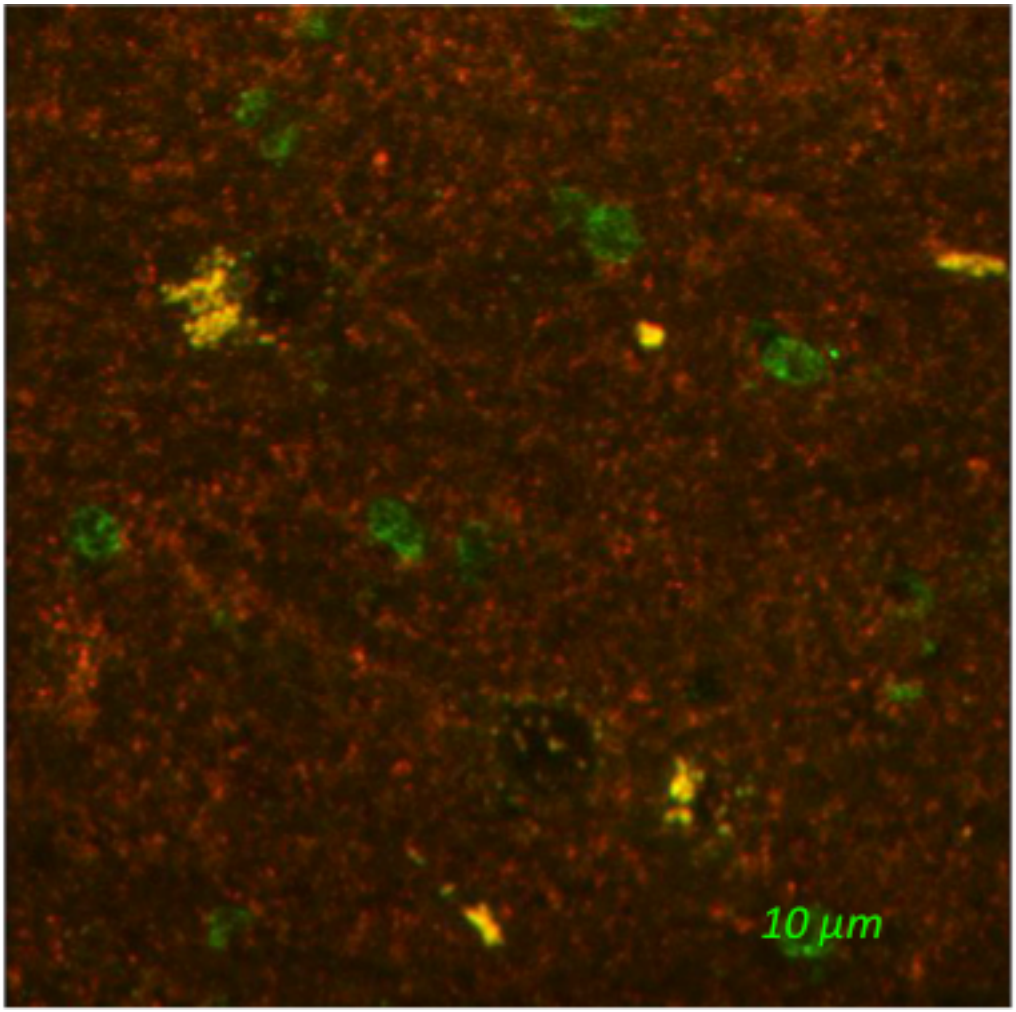
10 µm

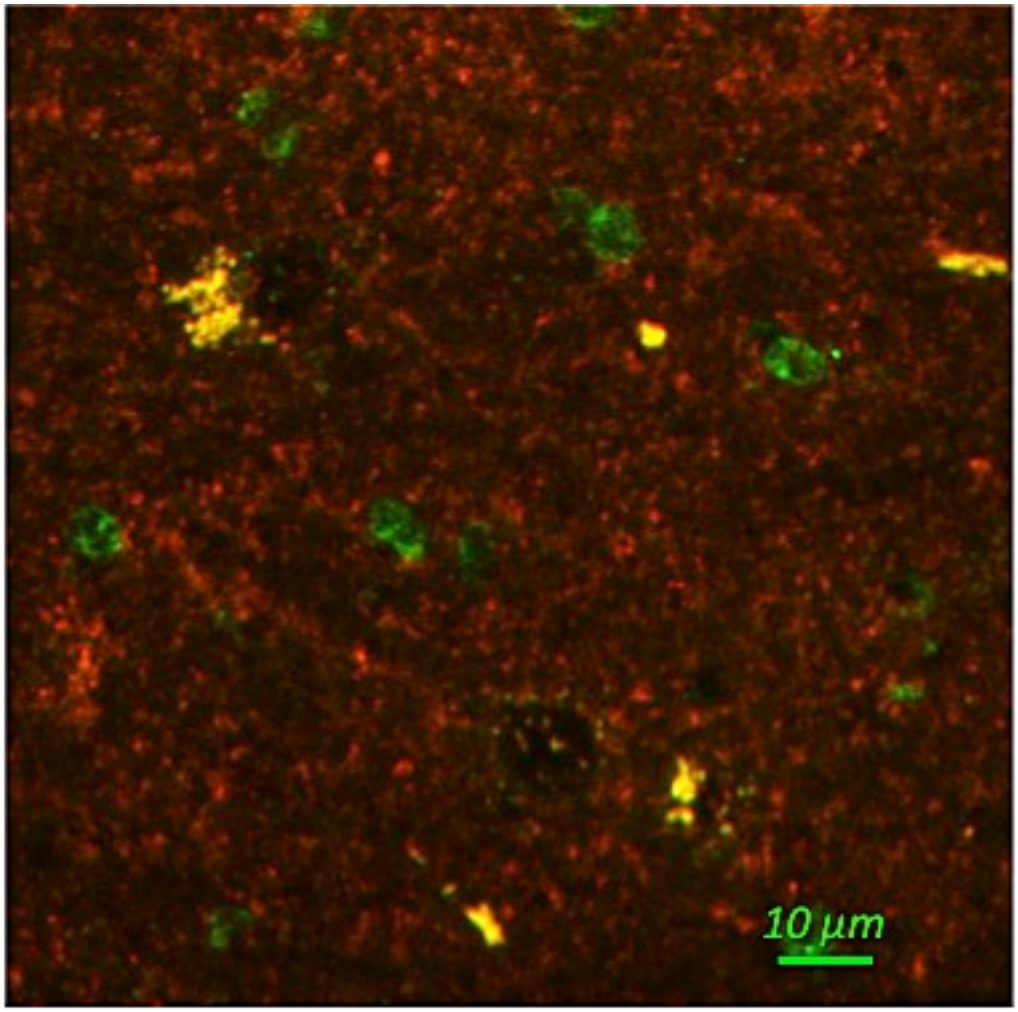

Figure 3: Confocal image of a section through the ventral horn of the spinal cord showing labelling of mitochondria with VDAC-1 (red), BrdU (green) and co-localized signal in yellow. The plain green spots represent mitotic cells. This image demonstrates that it is possible to get DNA replication signal from mitochondria using BrdU.

For subsequent experiments the 2 doses of 200 mg/kg were used along with an enhanced immunohistochemistry protocol. Two steps in the immunohistochemistry were vital in achieving clear staining; first, 90 minute incubation in 2N hydrochloric acid at 40 °C and, second, amplification using biotinylated secondary antibody with streptavidin conjugated with Alexa Fluor 488 (1:200). Without these two steps the signal was not clean even with a high dose of BrdU.

Colocalisation with VDAC-1, ChAT

Once the BrdU signal was confirmed to be arising from mitochondria, VDAC-1 was used as a marker of the abundance of mitochondrial. The extent of mitochondrial DNA replication was assessed as the fraction of VDAC-1 positive particles, which co-localized with BrdU (Explained in detail in Appendix) This analysis controls for the differences in mitochondrial content across cells attributed to differences in size or extent of arborization. In the following chapters similar analysis was performed in the where the extent of mitochondrial biogenesis was evaluated in different conditions where all other parameters of imaging and analysis were kept constant for images across experimental animals or samples.

In the spinal cord most of the mitochondrial biogenesis observed was found to occur in the cell bodies of neurones. The identity of these cells was established to be motor neurons by collocating the extra nuclear BrdU signal with motor neuron marker acetylcholine transferase (ChAT) (Figure 4).

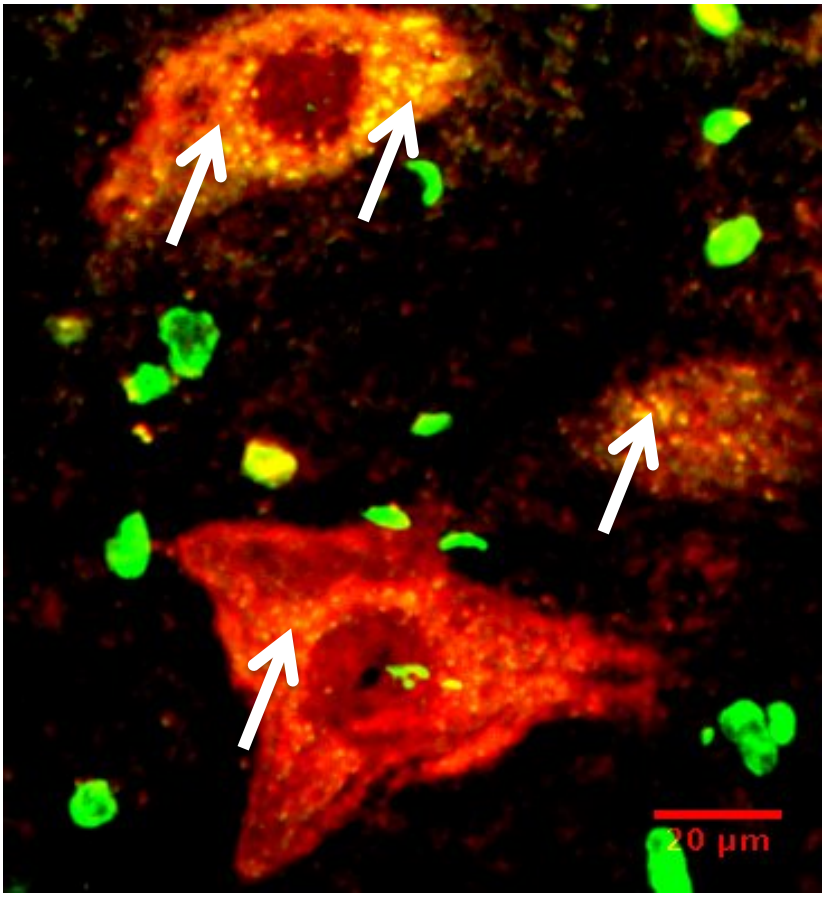

Figure 4: Confocal image of a section through the spinal cord which shows that the small cytoplasmic BrdU signal (white arrows) appears in motor neurones as identified by ChAT labeling (red).

In vitro validation – cerebellar granule cells culture

In order to validate the *in vivo* mitochondrial DNA replication technique, we tried to recreate the methods using cultured cells. Primary cell cultures from the cerebellum containing both neurons and glia were subjected to 10 μM (Figure 5A) or 20 μM BrdU for 6 hours (Figure 5B), commensurate to the expected duration of the BrdU *in vivo*, and 24 h (Figure 5C) as previously described (Calkins and Reddy, 2011b). We found a large amount of labelling for extra nuclear BrdU. Controls with no BrdU showed no signal. At 6 h there was substantial labelling of mitochondrial DNA containing BrdU. With samples incubated with BrdU for 24 hours (Figure 5) there seemed to be very dense

signal, suggesting that the signal was correlating with the duration of exposure to BrdU.

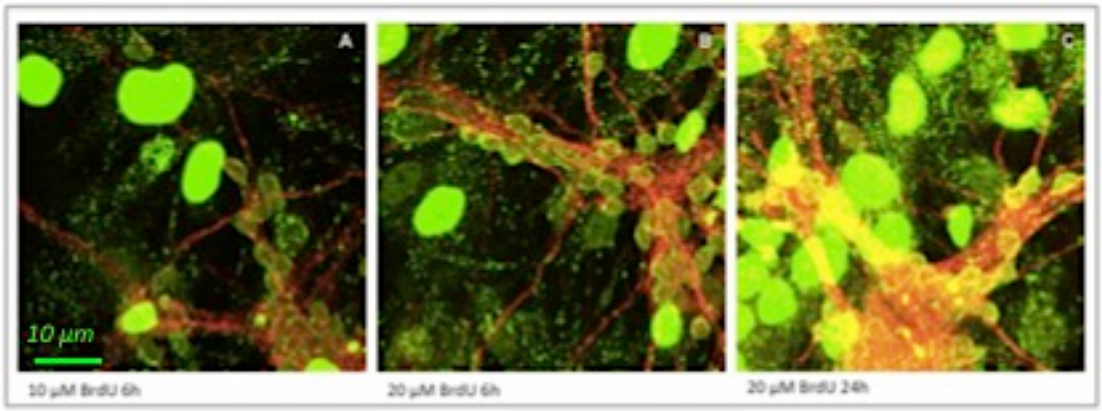

Figure 5: CGC cultures incubated with BrdU for 6 h or 24 hrs. BrdU (green) is seen in astrocyte nuclei as bright, saturated signal, and cytoplasmic, mitochondrial DNA appears as small green dots. The red marks VDAC-1, which appears in neuronal cell bodies and processes.

In these cultures, the astrocytes continued to proliferate and, accordingly, an extremely strong BrdU signal was observed in the nuclei of astrocytes (Figure 5). In order to image clearly, the much smaller mitochondrial DNA, the detection settings on the confocal microscope were optimized to collect a large saturating signal from proliferating nuclei. Unlike astrocytes, the neurons did not undergo cell division, and the entire BrdU signal arose from non-nuclear DNA.

The identity of neuronal cells in culture was established by labeling for β-III tubulin to mark (Figure 6).

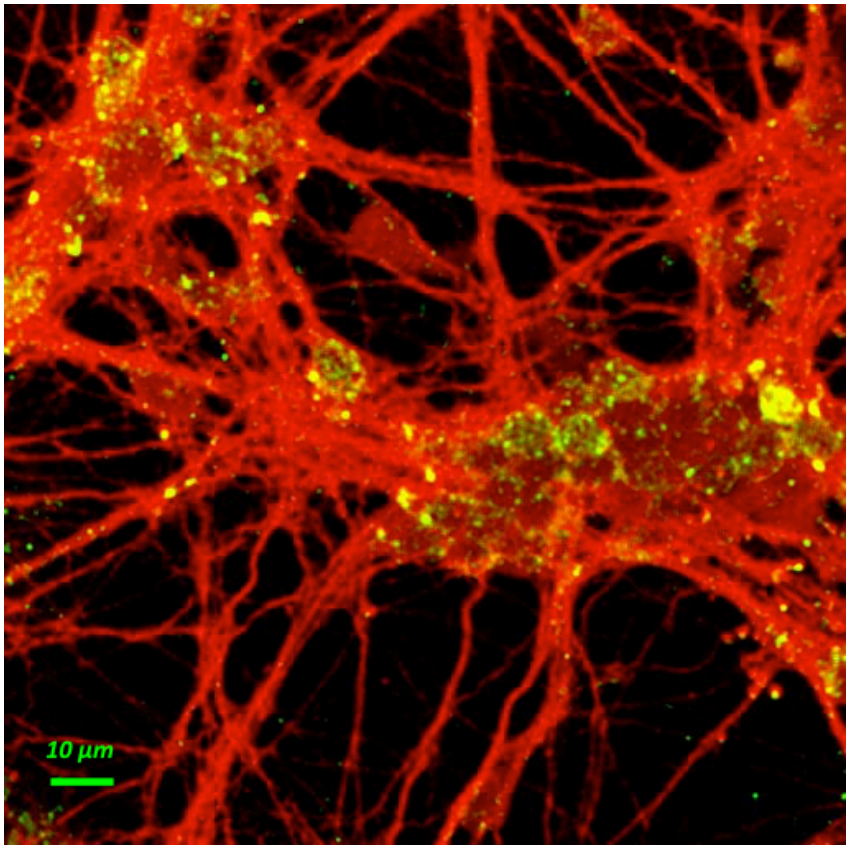

Figure 6: Confocal image of a CGC culture labelled with beta III tubulin, a neuronal marker (red), and BrdU (green), showing small cytoplasmic placement of BrdU in neuronal cell bodies.

TFAM and PicoGreen®

Immunohistochemical labelling of mitochondrial transcription factor A (TFAM) (Figure 7) with neuronal marker NeuN can be used to determine the mitochondrial content in a neurone. However, since TFAM is present on all mitochondrial DNA (Ngo et al., 2014) it is not as sensitive as BrdU in picking up the biogenesis signal. It does not specifically mark 'new' DNA. However, TFAM has the advantage that it is a good quick marker for large changes in mitochondrial biogenesis, and it is a useful tool because it does not require the harsh antigen retrieval steps required for the staining of BrdU and hence it presents an opportunity to counter label with several other antigens.

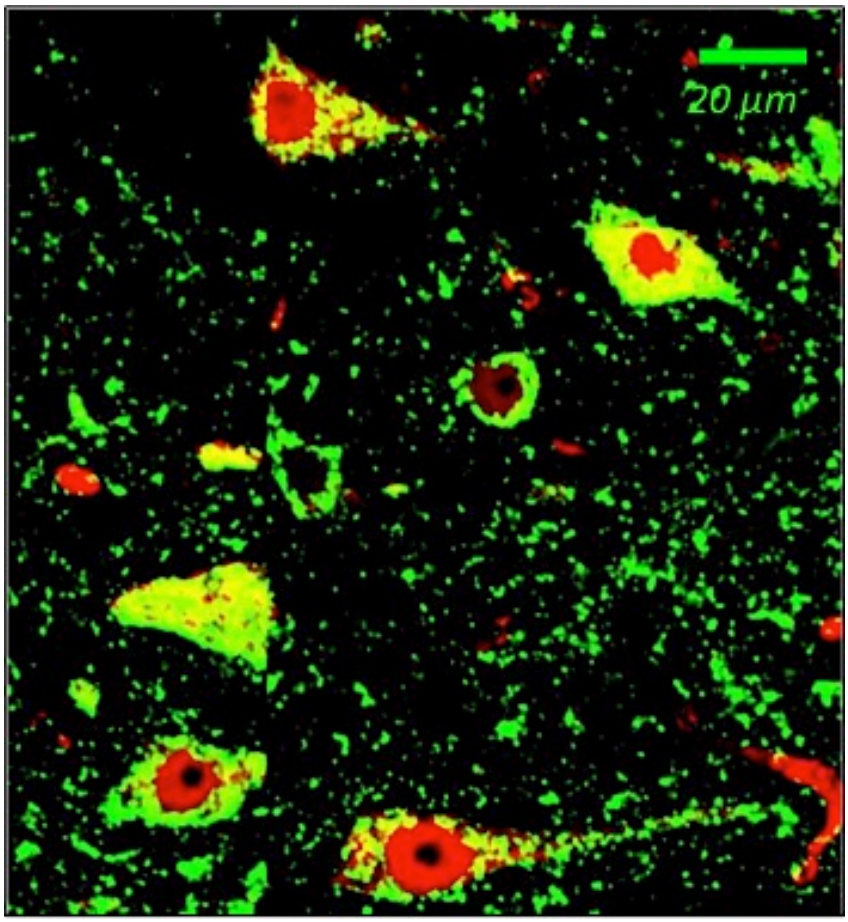

Figure 7: Confocal image of a section through the spinal cord labelled for TFAM (green) and NeuN (red), co-localisation in yellow, showing an abundance of mitochondrial transcription factor in spinal neurones, supporting the possibility of fast turnover of mitochondrial DNA

PicoGreen® is a DNA intercalating fluorescent dye which has a positive charge that allows it to accumulate inside mitochondria and thus specifically label mitochondrial DNA. Due to the nature of the interaction the fluorescence then attained from the cell is directly proportional to the content of DNA. This dye was tried as a way to quantify the amount of mitochondrial DNA content, in order to have an independent control against inherent differences in DNA content. Since the BrdU marks the extent of DNA replication, a change in content of DNA could confound the interpretation of results. However, due to

the loss of mitochondrial membrane potential in the dead tissue, the dye fails to accumulate solely into mitochondria and instead a very large signal appears from nuclear DNA, which overpowers any mitochondrial DNA signal (Figure 8). This dye was found not to be useful in quantifying mitochondrial DNA in post mortem mammalian tissue.

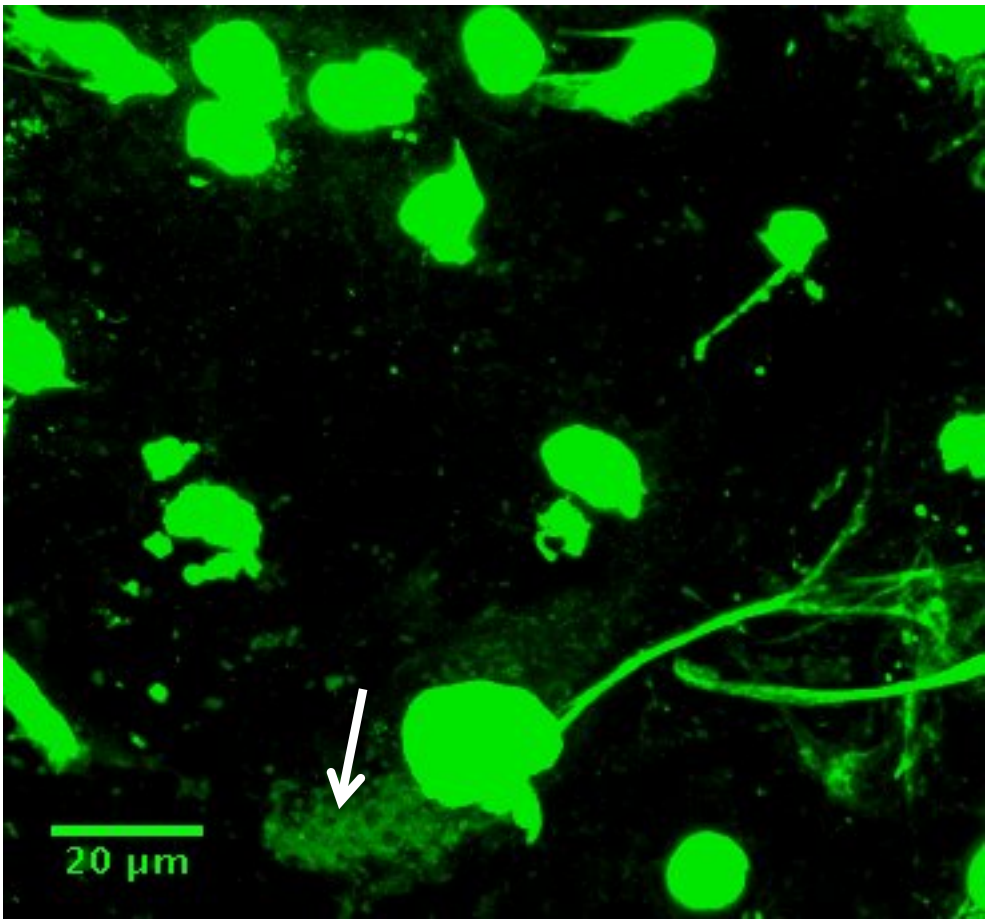

Figure 8: Section of spinal cord stained with PicoGreen®. The signal from the nuclei is overbearing and there is no clear staining of mitochondrial DNA. The white arrow points to cytoplasmic staining of DNA, seen only in sporadic cells. Quantitation of the signal is not possible on account of saturating signal from nuclei and also inconsistent.

Discussion

In the present study we showed that BrdU can be used as a marker for mitochondrial DNA replication and thereby be used as a tool to study the life cycle of mitochondria in the mammalian CNS *in vivo.* While previous studies have used BrdU to target mitochondrial DNA *in vitro* and also *ex vivo* (Ashley et al., 2005), this particular study is the first use of BrdU along with enhancements in immunohistochemical methods, allowing an investigation into the formation of mitochondrial DNA with spatial and temporal resolution *in vivo*.

This tool now presents opportunities to interrogate different aspects of mitochondrial biogenesis with respect to CNS pathology and physiology. In the next few chapters we investigate the extent of mitochondrial biogenesis in response to an inflammatory condition, namely EAE, and speculate about the importance of this process in neuroinflammation and bioenergetics in the CNS. Following that we study the process in physiological processes such as increased electrical activity in the periphery, and the response of the mitochondrial biogenesis cascade to electrical activity.

Co-labelling cells with BrdU and VDAC-1 is a sensitive measure of the growth of the mitochondrial network. In conjunction with new genetic constructs, which mark the age of mitochondrial proteins such as MitoTimer® (Hernandez et al., 2013) this technique can provide powerful insights into the regulation of the mitochondrial network turnover and its implication for neurological diseases. Almost all primary mitochondrial pathology diseases are

neurological in nature and this rather simple technique has presented an opportunity to elucidate aspects of the pathophysiology of these diseases

A more sophisticated thymidine analogue, EdU, which has been previously described to be an alternate method for studying mitochondrial DNA biogenesis (Lentz et al., 2010), could be developed as a way to study the process in vivo just as we have presented in this thesis. This will allow a larger number of cellular markers and antigens to be co-labelled with the DNA replicating signal. This is not possible using BrdU as the staining processes is very harsh and leaves little room for co-labelling other antigens. This is one of the major limitations of this thesis and the antigens presented in this work are more or less the only ones that are able to be co-labelled with BrdU amongst a battery of cellular markers that were tried. While using EdU may ease these problems, the cost of using EdU at a high dose *in vivo* along with the proprietary detection kit is prohibitive for the larger animal studies undertaken in this project.

While TFAM provides a good starting point for detection of mitochondrial content it is not as sensitive as BrdU in detecting subtle changes in mitochondrial biogenesis. PicoGreen® cannot be used in cryo-sections as tested on samples. The BrdU method was found to be the most robust to evaluate mitochondrial biogenesis *in vivo* at an intracellular resolution, and to quantify changes amongst neurones. The technique has definite shortcomings such as, the limitation on the number of antigens which can be

co-labeled with BrdU, generation of unreliable results when tested in a paradigm which inherently changes the mtDNA copy number in mitochondria, and the limitation of sensitivity presented by immunohistochemistry. Considering all these caveats, we used the BrdU method as a surrogate marker for mitochondrial biogenesis and evaluated the cell biology of mitochondrial turnover and the extent of biogenesis in neuroinflammation.

Chapter 3: Mitochondrial biogenesis in neuroinflammation

Introduction

Mitochondria in MS

MS is the most common demyelinating disease of the central nervous system and the most common disabling neurological disease affecting young adults. Demyelination in MS classically occurs with inflammation and is associated with axonal loss, which underlies neurological impairment in MS (Bjartmar and Trapp, 2003). Demyelinated lesions, associated with various degrees of inflammation, are the pathological hallmarks of the disease and they have been studied since the 19th century. Axonal degeneration is most prevalent in active lesions where inflammation is greatest. In chronic lesions, many surviving axons remain chronically demyelinated with only a few undergoing degeneration at any given point in time.

Mitochondria are responsible for supplying the vast amount of ATP produced by oxidative phosphorylation in eukaryotic cells along with performing other key roles in calcium buffering and apoptosis (DiMauro and Schon, 2003). In the CNS mitochondria play a particularly important part because neurons depend on the process of mitochondrial oxidative phosphorylation for most of their supply of ATP (Herrero-Mendez et al., 2009). The observation of increased mitochondrial presence within demyelinated axons raises a number

of important questions regarding how the mitochondrial changes occur (Witte et al., 2014). Possible explanations include an increase in anterograde transport, decrease in retrograde transport, increase in fusion, decrease in fission, and mitochondrial biogenesis within axons. Neurons have developed a highly sophisticated transport system to meet the needs of the axon with machinery for both transport of proteins away from the cell body, into the far reaches of the axon, anterograde transport, and a system to transport aberrant proteins back to the cell body for degradation, retrograde transport (Saxton and Hollenbeck, 2012).

Mitochondrial activity in the form of complex IV has been shown to be increased in inactive areas of chronic lesions associated with an increase of mitochondrial mass (Mahad et al., 2009; Witte et al., 2009). The expression of axon-specific mitochondrial docking protein, syntaphilin, in chronic lesions indicates a potentially immobile reservoir that supplies the necessary energy in demyelinated axons (Mahad et al., 2008). Complex IV defects have been noted in both nonphosphorylated and APP-positive chronically demyelinated axons, with an associated decrease of mitochondrial mass in the former, but not the latter, case, which suggest differing mechanisms. Another study finds agreement with the reduction in ATP synthase expression in MS lesions (Smith and Lassmann, 2002). Enhanced immunoreactivity of the mitochondrial heat shock protein (mtHSP70) in chronic lesions has been noted, indicating an environment of oxidative stress (Volobоueva et al., 2008; Witte et al., 2009). These findings point towards significant changes to the mitochondrial network in MS, and since mitochondrial biogenesis may form a

key element in the life cycle of mitochondria it is important to study this process. In this context, we propose to study mitochondrial biogenesis in neuroinflammation which will help understand in the process in MS.

Mitochondrial Biogenesis

In this study we focussed on studying spinal motor neurones as the pathology of our disease models (EAE and LPS injection) occurs in the grey matter of the spinal cord where these neurones are vulnerable to damage, which is implicated in the manifestation of symptoms. Their dependence on oxidative phosphorylation makes motor neurones especially susceptible to mitochondrial dysfunction, as evidenced by the preferential degeneration of motor neurones in SOD1 motor neurone disease although SOD1 is ubiquitously needed for its protective actions against mitochondria-generated superoxide.

Peroxisome proliferator-activated receptor-1α (PGC-1α), a transcriptional coactivator, has been established to be the key moderator of mitochondrial biogenesis – it regulates the expression of ~19% of genes that are up- or down-regulated in caloric restriction (Corton et al., 2004). PGC-1α is found in brown adipose tissue and skeletal muscle, where it was first found to induce mitochondrial biogenesis, as well as in the brain. The aforementioned stimulators of mitochondrial genesis indirectly increase PGC-1α expression in the nucleus. PGC-1α cannot bind to DNA on its own and instead binds to, and co-activates, nuclear respiratory factors 1 and 2 (NRF-1 and NRF-2). Their activation then induces expression of genes encoding mitochondrial proteins and, via mitochondrial transcription factor A, increases levels of mitochondrial

DNA (Jornayvaz and Shulman, 2010; Ventura-Clapier et al., 2008b). PGC-1α also induces biogenesis by interacting with oestrogen related receptors (ERRs). ERRα then activates transcriptional activity of Mitofusin 2, a mitochondrial membrane protein that is involved in mitochondrial fusion and regulates mitochondrial metabolism (Soriano et al., 2006). The culmination of these events is an increase in overall mitochondrial mass in a cell. Recent studies have demonstrated a link between defective mitochondrial biogenesis and increased risk of a whole host of neurodegenerative diseases such as Huntington's, Parkinson's and Alzheimer's disease, and amyotrophic lateral sclerosis (Katsouri et al., 2012; Tsunemi and La Spada, 2012; Zheng et al., 2010a). Studies have found altered PGC-1α levels in these conditions, pointing towards a possible causal role for dysregulated mitochondrial cell cycles in these diseases as PGC-1α is its master regulator (Liang et al., 2011; Tsunemi and La Spada, 2012). These studies have led to hypotheses that impairment in the regulation of mitochondrial dynamics might underlie other neurological diseases such as multiple sclerosis.

One of the key inducers of mitochondrial biogenesis is hypoxia. Recent studies have shown that active EAE lesions are hypoxic and have increased expression of hypoxia inducible factor 1 α (HIF-1α) (Davies et al., 2013). HIF-1α is a regulator of PGC-1α, which in turn can induce mitochondrial biogenesis. Another inducer of mitochondrial biogenesis of particular interest is oxidative stress. Neurological deficits seen in multiple sclerosis are a consequence of inflammation-induced demyelination of axons. Myelin sheaths are vital for fast and energy-efficient saltatory conduction of impulses down an

axon; when the sheath is compromised, conduction can be restored by redistribution of voltage-gated Na^+ channels (van Horssen et al., 2012). Na^+/K^+ ATPase activity is upregulated to restore intra-axonal Na^+ concentration following Na^+ leakage in previously myelinated segments of the axons; Na^+/K^+ ATPase are the largest consumers of ATP in the CNS, thus, their increased activity results in greatly increased ATP demand (Dutta and Trapp, 2007; van Horssen et al., 2012; Zambonin et al., 2011). This demand, together with the generation by infiltrating microglia and macrophages of reactive oxygen species and nitric oxide, that can react to form peroxynitrite, results in an increase in mitochondrial biogenesis (Marik et al., 2007). At the same time, peroxynitrite-induced damage of mitochondrial DNA results in increased and dysregulated mitochondrial ROS production, impairing the function of new mitochondria and thereby perpetuating a vicious cycle. If mitochondria are suppliers of ROS and of ATP, then here is where a problem lies: does the neurone continue production of mitochondria considering the fact that this in itself is ATP-dependent? If it does not, then this chronic energy deficiency will surely result in neuronal death. The present study has tried to evaluate whether neurones show an increase or decrease in mitochondrial biogenesis under varying extent of inflammation.

EAE as a Model of Multiple Sclerosis

Experimental autoimmune encephalomyelitis (EAE) is an animal model of autoimmune disease of the CNS that has been extensively worked on in the last 60 years. EAE is the most widely used experimental model of human multiple sclerosis, in part because of the resemblance of its pathology to that

of MS: inflammation, demyelination and axonal loss and the occurrence of remyelination and resolution of inflammation (Lavi and Constantinescu, 2005). EAE's susceptibility to variation of its clinical course with mode of induction and host species also makes it favourable for the study of MS as approximations of the different subtypes of MS can be induced and studied (Lavi and Constantinescu, 2005). In this study, a variation in combination of different strains of rats i.e. Dark Agouti and Brown Norway and adjuvant produced a deteriorating form of EAE in one set of animals and a biphasic form in the other. This is detailed in the methods section below. Regardless of the site of inoculation, inflammation always progresses rostrally from the caudal end of the rat spinal cord. These two models showed a different inflammation profile where Brown Norway rats had higher level of inflammatory cells than the Dark Agouti rats at mild to medium neurological deficit. Furthermore, while the mitochondrial biogenesis was reduced in spinal neurones in high inflammation state in Brown Norways, in Dark Agouti rats there was an initial increase in mitochondrial biogenesis at mild to medium inflammation, suggesting a compensatory mechanism for energy deficit. We then followed up on this observation by studying the process of mitochondrial DNA biogenesis in a focal model of neuroinflammation- the intraspinal injection of lipopolysaccharide (LPS).

Intraspinal injection of LPS - model of neuroinflammation:

In a disease such as multiple sclerosis, and its animal model EAE, immune-mediated inflammation can be prominent but it is difficult to distinguish the indirect consequences of the inflammation from other on-going immune-

mediated disease processes. Experimentally, inflammation can be induced in most tissues by the local injection of lipopolysaccharide (LPS), and typically large numbers of neutrophils and monocytes invade the tissue from the bloodstream within minutes, macrophages remaining at the site for a number of days (Issekutz et al., 1981). We have used this local inflammation from which the animals are known to recover as a model of active inflammation close to the site of the sciatic spinal neurones (ventral horn of spinal cord grey matter in the lumbar region) to observe whether there is an increase in mitochondrial biogenesis similar to what was observed in the Dark Agouti rats from EAE experiments.

We hypothesized that the amount of mitochondrial biogenesis in motor neurones in the EAE spinal cord correlates with the severity of inflammation in the CNS. We studied this in both biphasic (Dark Agouti) and deteriorating (Brown Norway) forms of EAE as the pattern of mitochondrial biogenesis could vary according to disease course. We also corroborated our observations in a focal model of inflammation.

Methods

EAE Studies:

EAE was induced as previously established in the laboratory (Davies et al., 2013). The N-terminal sequence (aa 1-125) of rat recombinant myelin oligodendrocyte glycoprotein (rrMOG; C. Linington, University of Aberdeen, UK) was used to induce EAE in young female DA rats (Harlan, UK; 109-150 g). For Dark Agouti rats (DA) a hard emulsion was prepared using 25% 2 mg/ml rMOG, 25% saline and 50% incomplete Freund's adjuvant (IFA). For

Brown Norway rats a similar preparation was made using complete Freund's adjuvant (CFA). Control animals received injections of an emulsion prepared with 50% saline and 50% IFA/CFA alone. Animals were injected with 200 μl of the respective emulsions in the flank near the base of the tail. Therefore, the resulting dose of rMOG received by each animal was 100 μg. Twenty animals were induced with EAE in each strain of rats.

Rats were weighed and examined daily through the course of the experiment. Neurological deficit was assessed using a 10-point scoring system, where the final score is an additive estimate of all the observable neurological signs. Rats were sacrificed at various presentations of neurological score, and were time-matched with controls. All the controls presented with a score of 0 at the time of sacrifice. The animals were injected with BrdU (2x200 mg/kg) 24 h before sacrificing by cardiac perfusion (Figure 1). The following groups were used for analysis:

- Dark Agouti: score 0 (n=4 controls, n=4 asymptomatic), mild score 1-3 (n=6), medium score 4-7 (n=5), severe score 8-9 (n=6) (N=25)
- Brown Norway: score 0 (n=3 controls, n=3 asymptomatic), mild score 1-3 (n=5), medium score 4-7 (n=5), severe score 8-9 (n=5) (N=21)

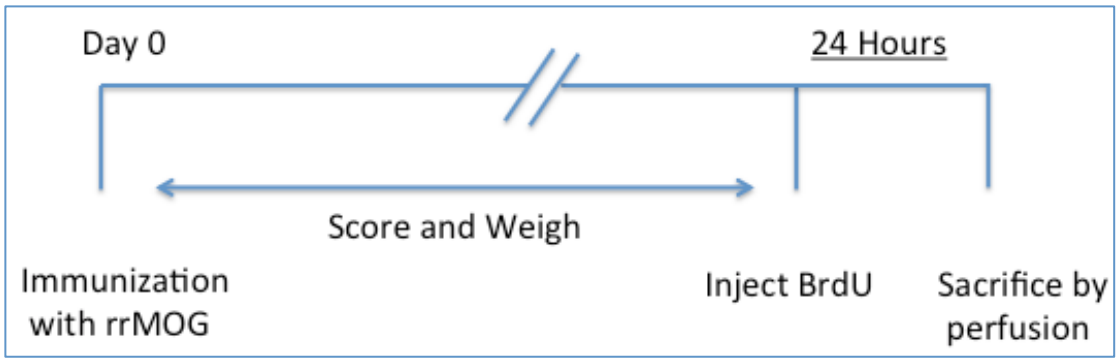

Figure 2: Timeline of conduction of EAE experiments: All animals were injected either with rrMOG or vehicle on the same day. Animals were evaluated for deficit every day. At the first onset of symptoms, or at similar intervals in controls, animals were dosed with 200 mg/kg of i.v. BrdU and sacrificed by cardiac perfusion of rinse and 4% PFA.

Intraspinal LPS injection:

Adult (250-350g) Sprague Dawley (SD) rats were anaesthetised with 2% isoflurane (Merail, Harlow, UK) in 100% oxygen and the site of operation was shaved and sterilised with iodine. Subsequently, animals received a quarter laminectomy of the 13th thoracic (T13-L1) vertebral element, the area where motor neurones of the sciatic nerve are located (Figure 3). Once the spinal cord was exposed, a small incision was made in the dura and pia, and 2 injections of 0.5 µl of LPS (*Salmonella enterica* serotype typhimurium 40 ng/ml Sigma L-6143) were performed at 700 μm distance from the dorsal vein and a depth of 1100 μm (Figure 3). For injections, a glass drawn micropipette held in a micromanipulator with a trajectory of 24 degrees to the vertical was used. Injection sites were marked with a small amount of sterile charcoal. Control animals were injected with sterile PBS. Following this the animals were left to recover from surgery. Cohorts of animals were injected with BrdU (2x200 mg/ml i.p. in saline) at 24, 48, 72 and 96 hours after surgery. Following BrdU, 24 hours later the animals were sacrificed by cardiac

perfusion. The control animals injected with PBS were dosed with BrdU at 72 hours. For injections, a glass drawn micropipette held in a micromanipulator with a trajectory of 24 degrees to the vertical was used. Injection sites were marked with a small amount of sterile charcoal. Control animals were injected with sterile PBS.

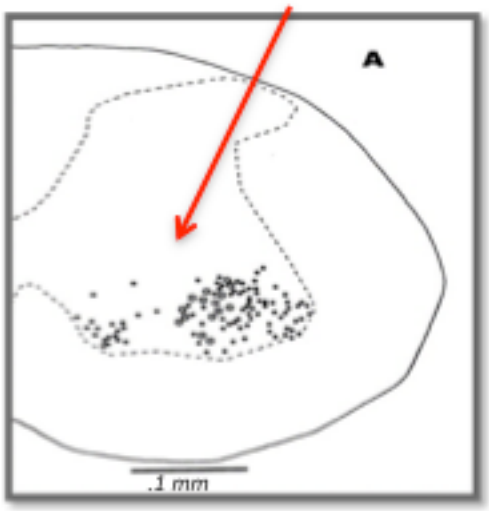

Figure 3: Cross section of spinal cord with a red arrow showing the pathway of the intraspinal injection of LPS into the ventral horn region of the spinal grey matter. The spots represent the motor neurone cell bodies.

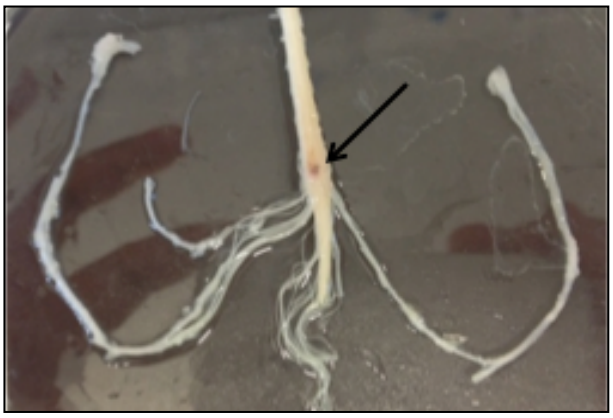

Figure 4: This is a dissected spinal cord, which shows the site of injection of LPS into the lumbar region. The site coincides nicely with the area of the spinal cord that innervates the sciatic nerve.

Tissue Processing:

Tissue processing, fixing and sectioning was performed as described in Chapter 2.

Immunohistochemistry:

Immunohistochemistry was performed as previously described in Chapter 2. Additionally, anti-CD68 (ED1) antibody (Abcam ab31630) was used at a dilution of 1:200 to detect activated microglia and macrophages to evaluate the extent of inflammation in the tissue. Adjacent sections were stained for either a combination of VDAC-1 and BrdU in order to evaluate mitochondrial biogenesis and ED1 and TFAM.

Image Acquisition

Fluorescent labelling was observed through a LSM 5 Pascal confocal microscope (Zeiss, Oberkochen, Germany) and images were recorded with the Pascal software (Zeiss). All image analysis was done using Image J (NCBI, USA) and corresponding plug-ins. All staining was checked for non-specific antibody labeling using control slides without primary antibody or without secondary antibody or without fluorescently labelled streptavidin. None of the controls showed any signs of nonspecific fluorescence. For imaging VDAC-1, BrdU and TFAM sections were imaged using a 63x oil objective with optical sections of 1 μm thickness. To evaluate the extent of ED1 labelling the entire spinal cord section was scanned using a 20x objective to collate tiled images.

Image Analysis

Images of the cell bodies of motor neurones were analysed in 3D stacks collected with optical sections 1 μm apart and analysed using the plugin 3D Object counter using FIJI (ImageJ). The analysis was represented as the

percentage of particles of VDAC-1 which also showed positive labelling for BrdU. Slides from every animal were analysed using the same settings normalised against a positive control section from the intestinal region. Laser power, aperture size and PMT gain were kept consistent for the collection of images across the whole experiment. The threshold used for the analysis of particles was also kept consistent.

To evaluate inflammation in the tiled images of ED1 labelling a threshold was set for fluorescence intensity and the area covered by positive labelling was measured using the 'Measure-Area' function in FIJI. This number was then normalized by the cross sectional area of the spinal cord section as measured by the area calculation after manually drawing the area of the spinal cord.

Statistical analysis:

Up to 80 motor neurone cell bodies were analysed using the above-described method for measuring mitochondrial biogenesis. This percentage value of mitochondrial biogenesis per cell was averaged for each animal. Then one-way ANOVA test was performed with Bonferroni's test to evaluate the significance. Similarly for the ED1 labelling, two sections were counted per animal and then each group of animals was averaged. To analyze the numerical relationship between the extent of inflammation and mitochondrial biogenesis in the Brown Norway rats a scatter plot was made of the extent of inflammation against BrdU content per cell and then a curve was plotted using GraphPad Prism (Version 6) (Figure 9).

Results

Assessing EAE pathology:

Both sets of DA as well as BN rats with rrMOG-induced EAE exhibited severe inflammation in the spinal cord associated with a neurological deficit exhibited as an ascending weakness and paralysis of the tail and hindlimbs, as previously described (Storch et al., 1998). Both sets of animals were only evaluated at first onset of symptoms, however, animals exhibiting a spectrum of neurological deficits were used. The distribution of activated ED1 positive microglia and macrophages was estimated and found to correlate with the severity of neurological symptoms in Dark Agouti Rats (Figure 6). However, in the Brown Norway rats the distribution of ED1 positive cells was far greater at the onset of symptoms in animals presenting mild neurological deficit (Figure 6). An ANOVA test showed a significant difference between the DA and BN rats at mild and medium neurological deficits ($p=0.0091$, $n=35$). In both groups the asymptomatic animals did not have any significant amount of inflammation present in the spinal cord (Figure 6).

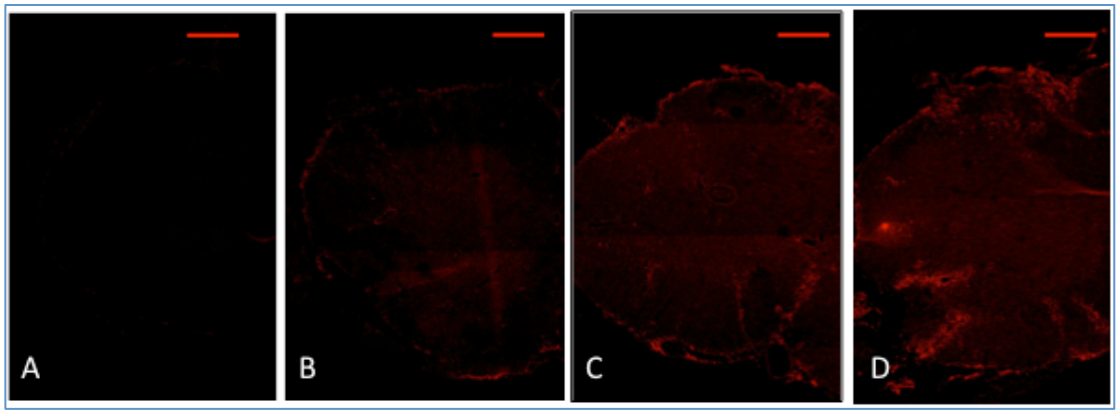

Figure 5: Representative images of spinal cord from the lumbar region showing different degrees of inflammation Dark Agouti rats. Sections were

stained for ED1 marker and secondary antibody conjugated to red Alexafluor 567. Images were captured using confocal microscopy and tiling with a 10x objective lens. (A) Represents an animal with no neurological deficit. (B) Represents an animal with very neurological deficit score 1. (C) Represents an animal with neurological deficit of score 4, and (D) represents an animal with severe deficit scored at 9. The severity of neurological deficit correlates with the degree of inflammation.

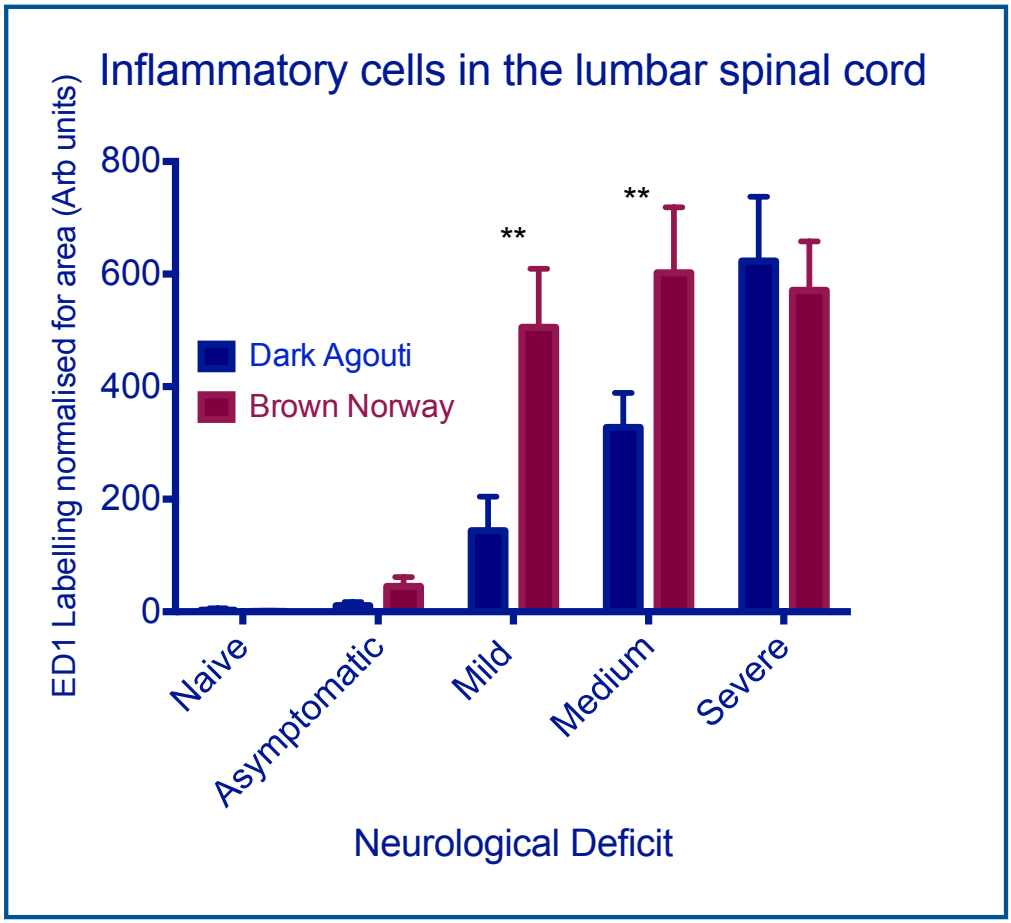

Figure 6: Quantitation of number of ED1 positive cells normalised for cross sectional area of the spinal cord. The blue bars represent an average of 5 animals per group of different neurological deficits (n=5). The naïve and asymptomatic animals had a neurological deficit score of 0. Animals categorised as 'mild' had a neurological score between 1-3. Medium Severity included scores between 4 and 7. Severe deficit was defined as between 8 and 10. A two-way ANOVA test was performed and at the mild and medium neurological deficit the Brown Norway rats showed significantly higher ED1 positive cells compared with Dark Agouti rats. ($p<0.01$).

Mitochondrial DNA replication:

Sections from the lumbar region of the spinal cord were stained for BrdU and VDAC-1 to evaluate the extent of mitochondrial biogenesis in spinal motor neurones as described in the Appendix. The spinal motor neurones showed clear colocalization of both signals in the cytoplasm as depicted in Figure 7A. Figures 7B, and 7C are different optical sections through a single neuron showing that the BrdU signal arises from the cytoplasm and not the hollow nucleus. Figure 7D represents BrdU signal alone arising from nuclei of proliferative cells in the spinal cord such as glial or precursor cells, showing that the signal is specific to replicating DNA.

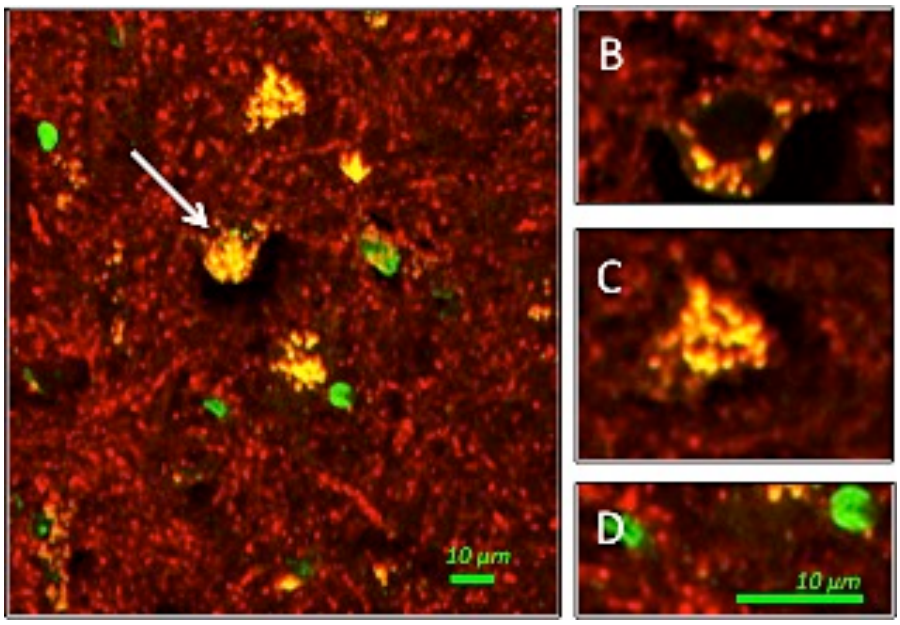

Figure 7: Representative image of VDAC-1(red) and BrdU (green) analysed in the grey matter of the spinal cord for mitochondrial biogenesis evaluation by normalising the yellow colocalization signal against total Porin content. (A) is a full stack of images collapsed into a flat z-project. (B) is a magnified single optical section through the cell indicated in (A) which clearly shows that the staining is perinuclear. (C) is another optical slice showing dense arrangement of BrdU staining in mitochondria. (D) The green only signal appearing in this image represents non-mitochondrial BrdU.

Mitochondrial biogenesis in EAE:

We observed a difference in the profile of change in the signal for mitochondrial DNA biogenesis between the two different EAE models evaluated. The Dark Agouti rats showed an increase in mitochondrial biogenesis in animals with mild, medium or severe neurological deficits and inflammation. In contrast, the Brown Norway rats had a decrease in the mitochondrial biogenesis signal as the neurological deficit increased (Figure 9). The extent of neuroinflammation is relatively lower in the Dark Agouti rats at low neurological deficits and in order to ensure that a drop in the content of mitochondria does not cloud the signal from Brown Norway rats, a plot was made to show the correlation between inflammation and BrdU content and VDAC-1 (whole mitochondrial content) (Figure 9). Although with increasing neuroinflammation the content of mitochondria is reduced (blue line Figure 9), the drop in BrdU is steeper and faster (red line Figure 9) suggesting specifically the production of new mitochondrial DNA has reduced and the observed signal is not just an artifact of a reduced number of mitochondria.

The difference between the neuroinflammation in the Dark Agouti rats, which recover from the deficit from the first peak of disease and the Brown Norway rats, which do not recover from the deficit, was curious and so a second recovery model of focal neuroinflammation was investigated (intraspinal injection of LPS).

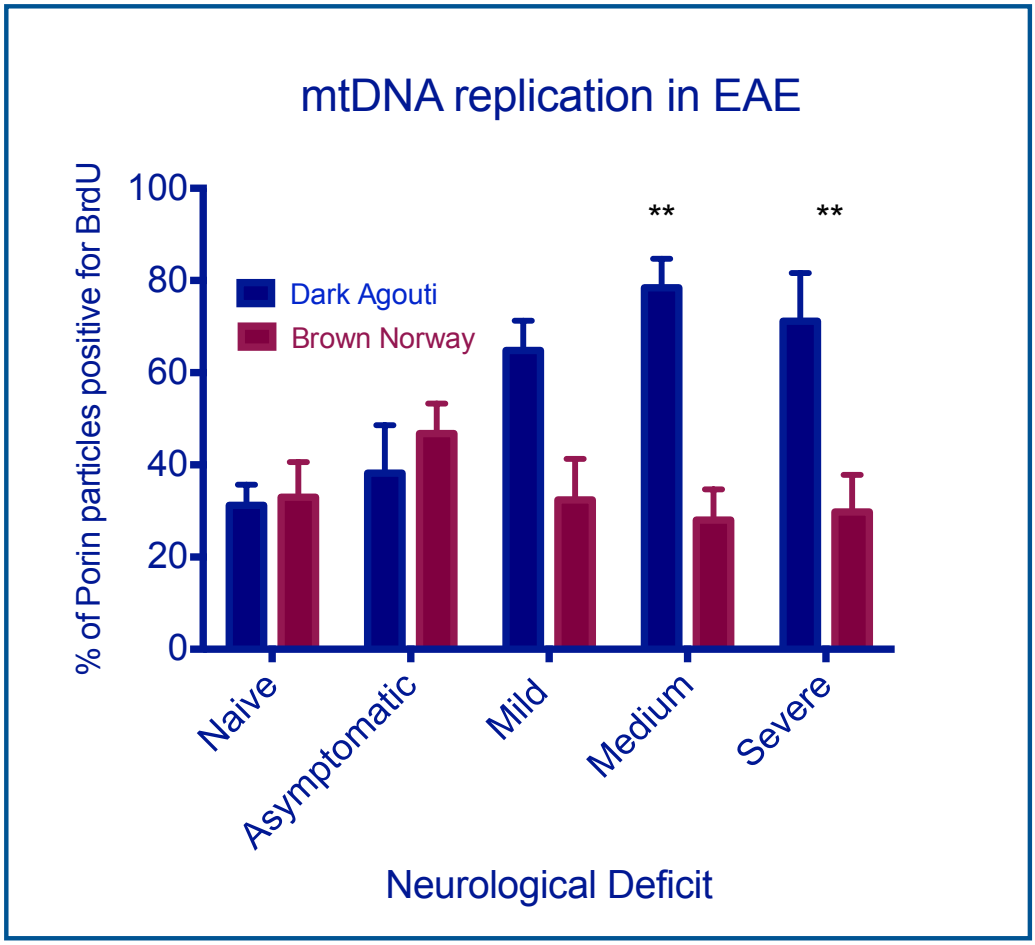

Figure 8: Quantification of mitochondrial biogenesis. The blue bars represent an average of 5 animals per group of different neurological deficits. The naïve and asymptomatic animals had a neurological deficit score of 0. Animals categorized as 'mild' had a neurological score between 1-3. Medium severity included scores between 4 and 7. Severe deficit was defined as between 8 and 10. A two-way ANOVA test was performed and at the mild and medium neurological deficit the Dark Agouti rats showed significantly higher BrdU positive mitochondria normalised for content of Porin and size of the cell compared with Brown Norway rats. ($p<0.0001$)

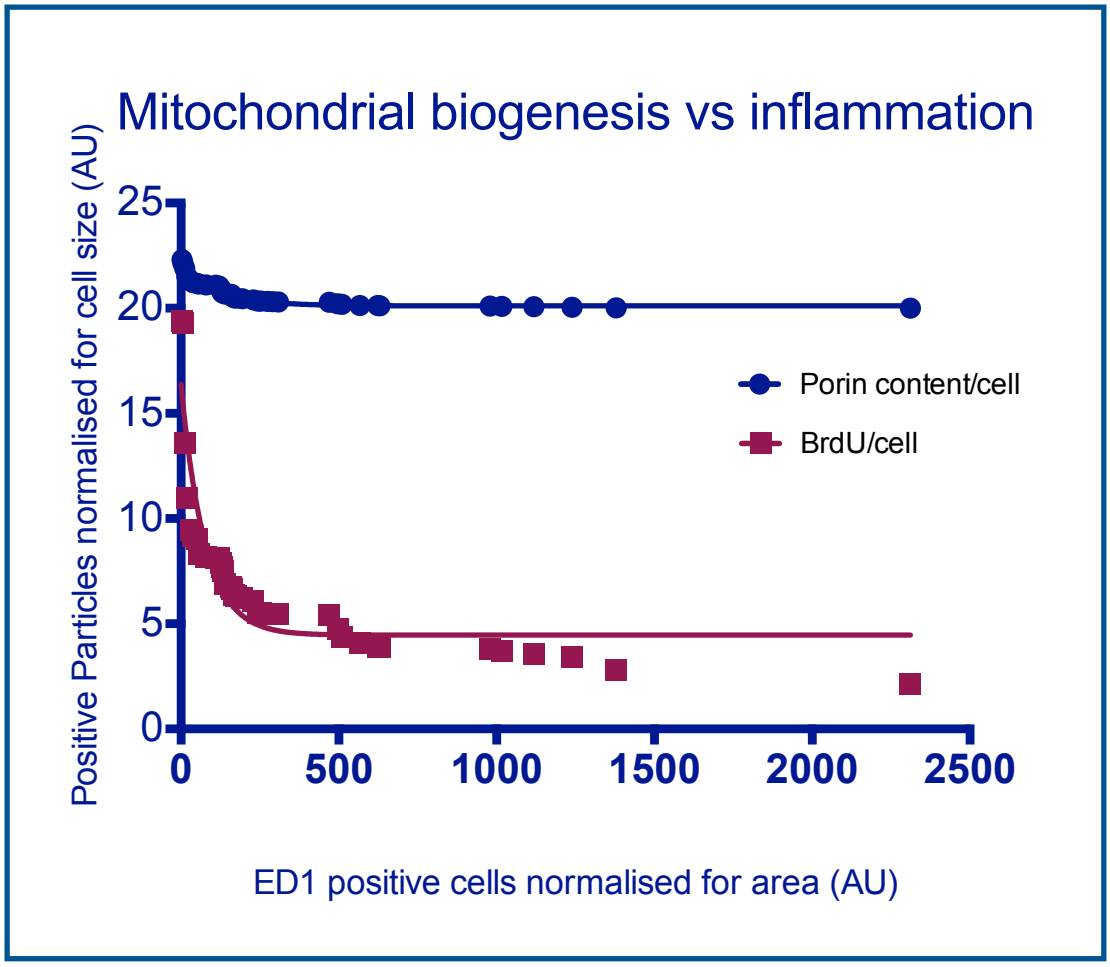

Figure 9: Scatter plot of the average BrdU content per cell in one section across different neurological scores, normalised for the size of cells body in spinal cord sections of Brown Norway EAE rats. The corresponding inflammation in the tissue as measured by ED1 labeling. There is a steep decline of mitochondrial DNA replication as tagged by BrdU (red) but not of the total content of mitochondria as marked by VDAC-1 (blue) in Brown Norway rats.

Intraspinal injection of LPS:

In agreement with previous description (Desai, 2013) of the pathology resulting from intraspinal LPS injections in the ventral horn of the spinal cord of Dark Agouti rats, we observed the gradual build up of neuroinflammation with activated microglia / macrophages (ED1 positive cells) in the first 48 hours after LPS injection (Figure 10) and then this started to subside after 96

hours. On the other hand, mitochondrial biogenesis increased with high levels of neuroinflammation and peaked at 72 hours. A one-way ANOVA test showed a significant increase in mitochondrial DNA biogenesis at 48 hours and 72 hours compared with controls and with levels of biogenesis observed at 24 hours and 96 hours after injection of LPS (Figure 11). This result is similar to the observation of increased mitochondrial biogenesis in the Dark Agouti rats with EAE.

The distribution of mitochondrial content in the neurones of animals that showed an increase in mitochondrial biogenesis was polarized towards the axon hillock (Figure 12) as evaluated by immunohistochemical staining against TFAM.

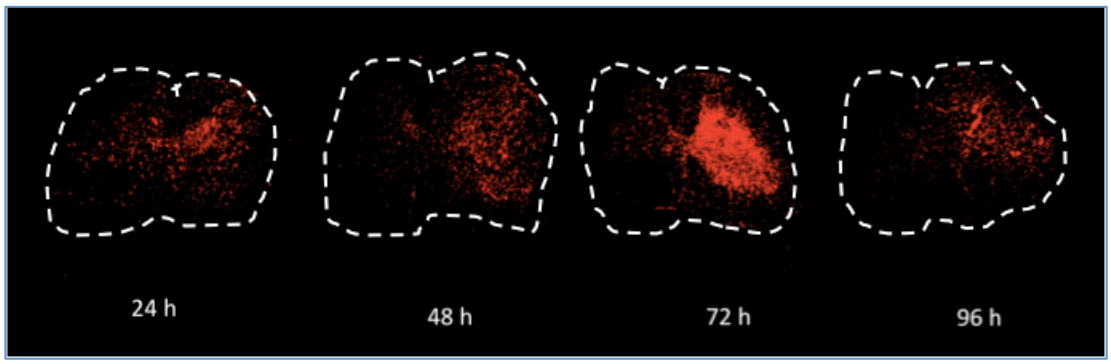

Figure 10: Representative images of spinal cord after LPS injection in the ventral horn labelled with ED1 (red) showing the progression of inflammation after.

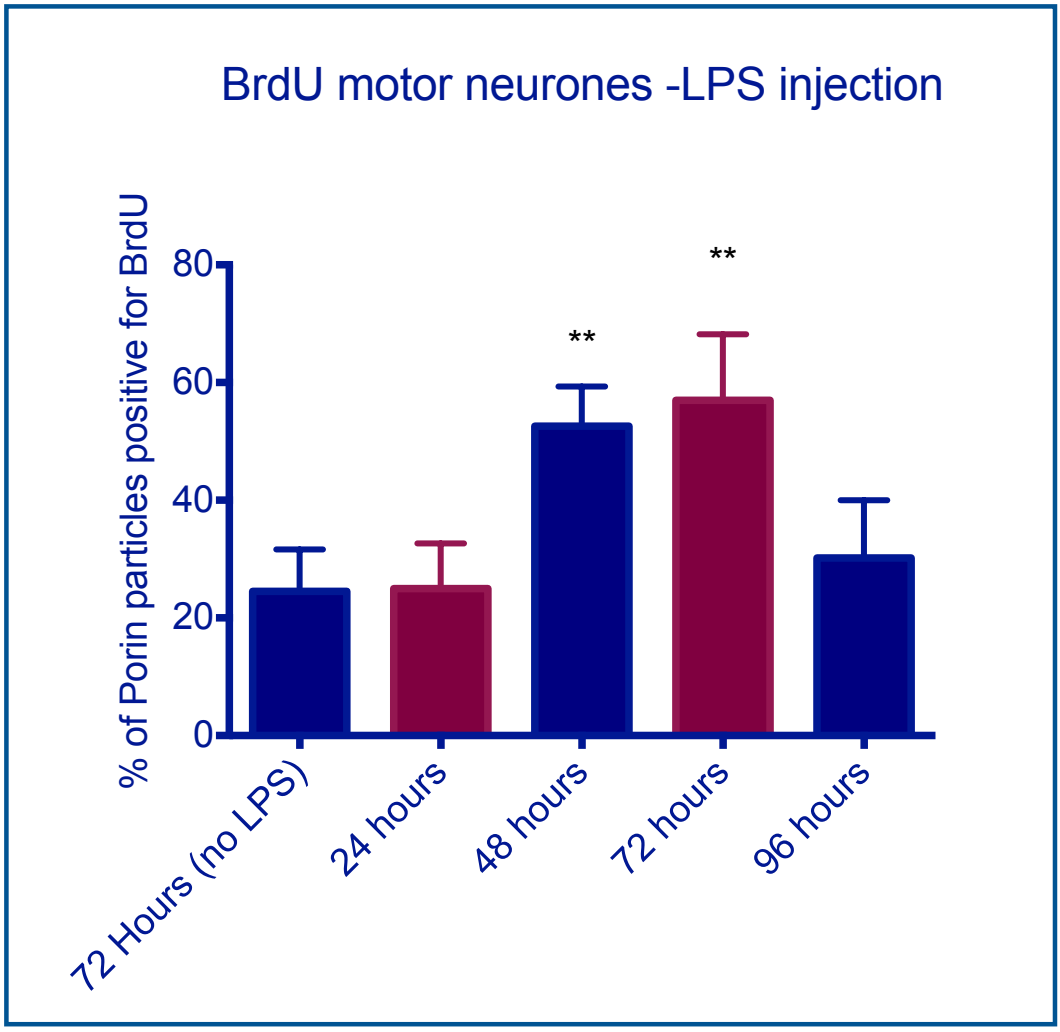

Figure 11: Along with increasing inflammation the amount of mitochondrial biogenesis also increases in the spinal cord of Dark Agouti rats after injection of LPS. A one-way ANOVA test was performed which suggests that at 48 hours and 72 hours the mitochondrial biogenesis signal is significantly higher than at 96 hours and 24 hours and compared with vehicle injected animals ($n=5$, $p<0.0001$)

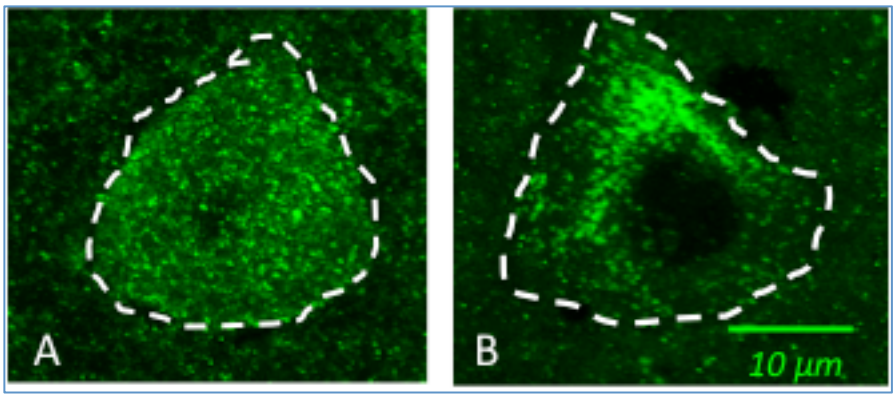

Figure 12: Representative images of motor neurones labeled with TFAM (green). (A) is a motor neurone from tissue with no inflammation. (B) is a motor neurone from a spinal cord with lots of inflammation 72 h after injection of LPS. The mitochondrial content is polarized towards the axon hillock as observed by placement of the cell in the tissue section.

Discussion

It has been reported that mitochondrial DNA deletions at low levels in multiple sclerosis cortical grey matter expands to high levels in a proportion of neurons (Campbell et al., 2011). In primary mitochondrial disorders, the expansion of mitochondrial DNA mutations and respiratory deficiency are most notable in structures that are metabolically highly active, such as muscle fibres, choroid plexus epithelium and neurons (McFarland et al., 2010). An increase in mitochondrial DNA replication rate and expansion of mitochondrial DNA mutations (clonal expansion) has been proposed as a likely mechanism of tissue injury in these disorders. The supposed increase in energy demand of remyelinated and demyelinated axons is likely to influence the expansion of induced mitochondrial DNA deletions in multiple sclerosis. Such an intrinsic process is more likely to render neurons with remyelinated or demyelinated axons respiratory deficient over the course of multiple sclerosis than

myelinated axons. I suggest that my observations in the Dark Agouti rats and intraspinal injection of LPS suggest that an increase in mitochondrial biogenesis concurrent with a neuroinflammatory insult may result in an exacerbation of the clonal expansion of mitochondrial DNA defects. It may be speculated that the imbalance between autophagy and biogenesis might render a cell vulnerable to accumulating mitochondrial damage faster in neuroinflammatory disease.

The changes in axonal mitochondrial content following demyelination were at first thought to be potentially detrimental to axons but now are increasingly recognized as a compensatory mechanism (Campbell and Mahad, 2011; Witte et al., 2014). In light of this, studying the mitochondrial biogenesis regulation and changes in MS are increasingly important.

Several pharmaceutical modulators of mitochondrial biogenesis, most notably PPAR-Y agonists (Chaturvedi and Beal, 2008), are being tested in neurodegenerative diseases such as Parkinson's and are proving to be efficacious enough to warrant clinical trials for neuroprotection. These drugs may prove beneficial in MS as well. The mitochondrial biogenesis tagging by BrdU will enable us to develop a robust *in vivo* pharmacodynamic pre-clinical biomarker model to test the efficacy of these drugs.

It has been found that mitochondrial biogenesis is rapidly increased following neuronal injury resulting from hypoxic-ischaemic (HI) brain injury in rats (Yin et al., 2008). There were increased levels of mitochondrial transcription

factors TFAM and NRF-1 as well as a corresponding increase in relative amount of brain mtDNA in the brain of rats after HI injury. As one of the hallmarks of EAE is inflammation of the CNS, it is likely, then that this endogenous CNS repair mechanism seen in HI brain injury also occurs in EAE. Yin et al. postulated that this increase in mitochondrial biogenesis forms part of an endogenous CNS repair mechanism, which is likely to also be the case in the EAE spinal cord.

MS lesions are characterized by white matter plaques containing activated macrophages and microglia that, in one way or another, cause demyelination and transection of axons (Dutta and Trapp, 2007; Trapp et al., 1998). Axonal demyelination in the early phases of disease results in a large increase in energy utilization to counteract the loss of energy-efficient saltatory conduction. The EAE model of MS can also involve extensive demyelination (Lavi and Constantinescu, 2005), so it may be postulated that this increase in energy demand also occurs in EAE. The increase in mitochondrial number in a cell is likely to increase the metabolic capacity of a cell, thus bringing it out of virtual hypoxia – the condition of energy demand outstripping supply in spite of sufficient perfusion. Mitochondrial biogenesis is increased as if to recover normal function of motor neurones, hence, the more inflammatory damage sustained by neurones, the more mitochondrial biogenesis is upregulated. It is likely that the remission phase of the disease is a manifestation of this mechanism as neurological function is recovered, indicating that widespread neuronal cell death has been averted and recovery has been successful.

One of the reports that supports this hypothesis is the finding that the decreased activity of mitochondrial complex I is accompanied, and possibly compensated, by an increase in complex IV activity in chronic MS lesions (Dutta and Trapp, 2006). Perhaps the upregulation of complex IV activity constitutes part of an endogenous compensatory mechanism aimed at increasing neuronal viability and function by increasing the number of respiratory chains available for oxidative phosphorylation, and that is mimicked in our animal model of MS.

This argument is further strengthened by recent evidence that mitochondrial biogenesis improves neurone viability under ischemic conditions in vitro (Stetler et al., 2012). When deprived of oxygen and glucose, neuronal upregulation of mitochondrial biogenesis by LPS pre-conditioning results in increased viability. These conditions, while not identical to the conditions in inflammation, are a close approximation because energy supply does not meet demand in both situations. The authors showed that inhibiting mitochondrial biogenesis by knocking down TFAM, a transcription factor vital for the initiation of mitochondrial DNA replication, resulted in significantly decreased neuroprotection (Stetler et al., 2012). This mechanism of neuroprotection is likely to have been triggered in the Dark Agouti rats to return the health and function of neurons to baseline. However, it is important to note that the results of Stetler et al.'s study was based on neuronal cell culture, and that it is likely that factors such as multi-cascade interaction could alter the mitochondrial dynamics in an animal spinal cord (Stetler et al., 2012).

While in the study described by Yin and colleagues there is an increase in expression of TFAM very shortly after stimulation (peaks 9 to 24 hours after assault), the timeframe for recovery of neurological function after first peak of disease in EAE is several days. This difference could be due to the acuteness of hypoxia in the Yin et al. experiment compared to chronic nature of inflammation in EAE. Another explanation for this difference in time to recovery could be a result of the complex and multiple processes - removal of damaged proteins, synthesis of new proteins and replacement of damaged oligodendrocytes - that need to occur before neuronal function can be restored.

Mitochondrial biogenesis in progressive EAE

I observed a decrease in mitochondrial DNA biogenesis in symptomatic Brown Norway rats with progressive EAE. A closer look revealed that mitochondrial biogenesis also varied negatively with increasing neurological impairment. These results correlated well with my other demonstration that mitochondrial biogenesis decreased exponentially with increasing inflammation. Dark Agouti rats tend to have episodes of disease interspersed by periods of disease remission whereas Brown Norway rats have a more progressive disease with little to no remission throughout the disease course (Lavi and Constantinescu, 2005).

My demonstration of decreased mitochondrial biogenesis with increasing inflammation might seem to contradict evidence that oxidative stress

stimulates mitochondrial biogenesis (Dai et al., 2014). However, it is important to note that my observations were based on sick animals with EAE and that the conditions within their cells are likely to be very different from those in healthy animals – it is possible that it is this very switch in the direction of inflammation's relationship with mitochondria that results in the progressive worsening of pathology in deteriorating EAE.

The suppression of mitochondrial biogenesis may be a response to increased inflammation and that it functions to minimize neuronal damage. As previously discussed, mitochondria are thought to be important mediators of oxidative damage in EAE and MS. Mitochondria are highly sensitive to damage by reactive oxygen species (ROS) and are therefore especially susceptible to damage within inflammatory lesions in EAE and MS (Perez-Pinzon et al., 2012). This poses a challenge for the production of healthy new mitochondria in inflammatory conditions, as mitochondrial biogenesis involves replication of mitochondrial DNA that are damaged, inadvertently increasing the number of defective mitochondria in a cell. Since the accumulation of damaged mitochondria has been shown to result in cumulative oxidative damage (Gottlieb et al., 2011), it is likely that the suppression of mitochondrial biogenesis serves as a backup mechanism of mitochondrial quality control to limit oxidative damage caused by production of defective new mitochondria.

Not only are mitochondria thought to perpetuate a vicious cycle of ROS production and ROS-induced damage of new mitochondria, but they are also thought to exacerbate pathology by causing apoptosis and necrosis of

neurones (Vosler et al., 2009). Mild mitochondrial membrane damage results in release of apoptosis inducing factor (AIF) and cytochrome c, thus initiating programmed cell death (Vosler et al., 2009). Severe mitochondrial damage, on the other hand, has been linked to Ca^{2+} deregulation and cellular necrotic death (Vosler et al., 2009). Inhibition of the release of apoptotic factors from damaged mitochondria have been demonstrated to be neuroprotective, suggesting that mitochondria might mediate neuronal death in pathological states (Vosler et al., 2009). It is likely that mitochondrial biogenesis is decreased to limit the number of damaged mitochondria in a cell in order to prevent cellular death. In other words, it could be a mechanism to shut down the release of apoptosis-promoting factors in order to salvage neurological function.

Besides preventing the release of apoptotic factors, mitochondrial quality control is also vital to prevent the exacerbation of inflammation. Zhou et al. reported that the accumulation of damaged, ROS-generating mitochondria result in the activation of an inflammasome, potentially worsening any existing inflammation (Zhou et al., 2011).

Decline in mitochondrial quality control has been shown to trigger responses to counteract the effects of poor mitochondrial quality in a cell. Studies conducted on yeast cells have found that the loss of mitochondrial membrane potential triggers a pathway called the retrograde response that, amongst other things, results in the upregulation of mitophagy and autophagy to

remove damaged mitochondria, thus preventing their accumulation (Jazwinski, 2013).

The negative relationship between severity of disease and mitochondrial biogenesis that I demonstrated in Brown Norway rats can also be explained from a bioenergetics point of view. Mitochondrial protein synthesis, transport and assembly are ATP dependent processes (Fox, 2012). In an already energy-deficient neurone, mitochondrial biogenesis will require the expenditure of already scarce ATP. In the severely inflamed CNS of EAE Brown Norway rats, neurones cannot afford to produce new mitochondria but instead prioritize cellular respiration in existing mitochondria to prolong survival. Although neurones attempt to increase their viability by blocking the use of ATP for mitochondrial biogenesis, this will eventually result in cell death as they become more and more hypoxic because existing mitochondria are damaged and cannot keep up with the cell's energy demand. The same is true for the other arguments put forth about suppression of mitochondrial biogenesis as a mechanism to limit CNS damage – they all involve the assumption that the extension of lifespan is prioritized and that cells fail to prevent death. Failure to save neurons could underlie the progressive course of the disease as increasing numbers of motor neurones are lost and function is never recovered.

Another explanation could be that mitochondrial dynamics have simply been derailed in EAE and that this forms part of the disease in Brown Norway rats both being caused by the disease and further exacerbating it. A loss of

mitochondrial regulation in disease is not unprecedented: mitochondrial defects have long been implicated in a range of CNS diseases such as Leber's hereditary optic nerve atrophy (LHON), maternally inherited Leigh's syndrome (MILS) and Pearson syndrome (Kalman, 2006). Other neurodegenerative diseases with close links to EAE have also been reported to be caused by a variety of mitochondrial defects (Beal, 2005; Calkins and Reddy, 2011b).

Clustering of mitochondria towards the axon hillock:

The observation that mitochondria cluster towards the axon hillock of motor neurones in inflamed regions of the spinal cord of the LPS injected animals suggested that there seems to be a localized site of mitochondrial biogenesis in these neurones. This peculiar distribution was only observed in animals examined at the peak of inflammation (48-72 hours after LPS) and which also showed increased mitochondrial biogenesis as evaluated by the BrdU method. Although a few cells in the EAE studies showed this type of distribution it was not as pronounced and wide spread as the LPS studies. This is perhaps due to the precise nature of the LPS injection model where all cells are experiencing a similar tissue environment compared with the stochastic and relatively unpredictable nature of the neuroinflammatory pathology in EAE. This observation along with the localization of BrdU signal to the cell body in previous experiments led to the hypothesis that perhaps mitochondrial biogenesis occurs only in the cell body of long neurones. This observation was investigated further, and is discussed in Chapter 4.

Chapter 4: Cell Biology of mitochondrial biogenesis

Introduction

Mitochondria are key to the survival of neurones (Nicholls, 2002), however, depending on the activity of the network and the biochemical identity of the neurones the energy needs can vary greatly in their demand of energy not just across types of cells but also different compartments within a long neurone (Hollenbeck and Saxton, 2005). Certain areas of long neurones have higher need for energy such as nodes of Ranvier (Berthold et al., 1993; Waxman and Ritchie, 1993), myelination boundaries (Bristow et al., 2002), active synapses or tracts (Bindokas et al., 1998; Kageyama and Wong-Riley, 1982; Wong-Riley and Welt, 1980) and active growth cones or axonal branches (Morris and Hollenbeck, 1993; Ruthel and Hollenbeck, 2003) and these regions accumulate mitochondria. Neurones traffic mitochondria all across distal regions of the cells and continuously carry out fission and fusion to deal with changing energy demands in the cells.

Due to the cyclical nature of mitochondrial lifecycle along with the redistribution the neurons must also regulate the process of organelle biogenesis to replace damaged mitochondria. Most mitochondrial proteins are encoded in the nuclear genome that presents a challenge for carrying out biogenesis in all corners of a large cell such as a motor neurone. In previous

studies in PC-12 cells mtDNA replication has been mainly detected in the perinuclear region (Davis and Clayton, 1996). However, more recently this has been observed to occur in axons of chick sensory neurones in culture (Amiri and Hollenbeck, 2008). Components of the mitochondrial replication apparatus have been found outside of the perinuclear region in both non-neuronal cells (Falkenberg et al., 2002; Larsson et al., 1994; Tiranti et al., 1997) and neuronal cells (Magnusson et al., 2003), which suggests that biogenesis could occur in the distal regions of neurons.

In my initial observations of BrdU signal *in vivo* in spinal motor neurones we found the signal strongly localized to the perinuclear mitochondrial pool. This, along with the observation that when stained with antibodies against TFAM there seemed to appear a clustering of mitochondrial DNA in the axon hillock of motor neurones, which showed higher levels of mitochondrial biogenesis following inflammation (Chapter 3) led us to ask whether these cells primarily perform mitochondrial biogenesis only in the cell body. Here we have tested the hypothesis that *in vivo* neuronal mitochondrial biogenesis largely occurs only in cell bodies of neurons. We have used a sensitive method of BrdU detection to examine mtDNA in motor neurone cell bodies from the grey matter of the spinal cord and then examined the signal in axons, which are contained in the sciatic nerve, after delivering BrdU systemically. The picture that emerged suggested that biogenesis is largely conducted in the soma of the neurones and these newly formed particles are then trafficked along the length of the axons. We have tried to corroborate the speed of movement of mitochondria using an alternate labelling method using the potentiometric dye

MitoTracker® Red. Finally we show that the process of somatic mitochondrial biogenesis is enhanced following the initiation of high demand of energy by electrical stimulation.

Methods

Part 1

In vivo experiment – somatic nursery:

For this first study, we injected two doses of BrdU at 100 mg/kg 5 ml/kg intraperitoneally (systemic administration), 2 hours apart, into adult C57/Bl6 mice weighing between 25-30 g. Cohorts of animals were sacrificed at different times after the injection by cardiac perfusion. Animals were kept for up to 21 days after injection and sacrificed at different time points (Figure 1). Tissue from the animals was stored overnight in 4% PFA and then cryopreserved in 30% sucrose before being processed for immunohistochemistry.

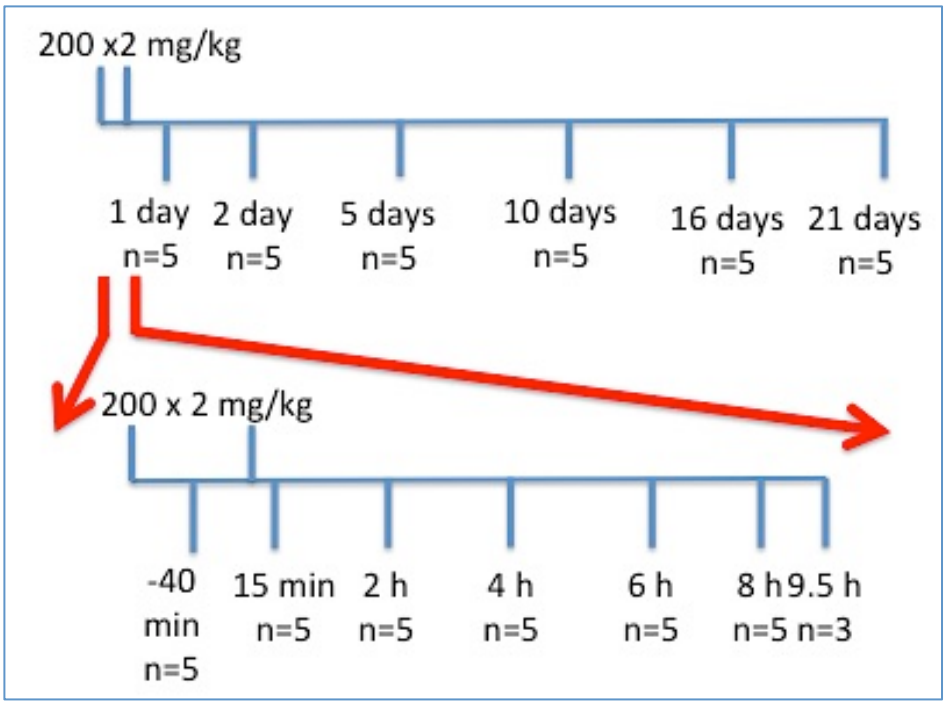

Figure 1:Timeline of pulse chase experiment to determine the location of mitochondrial DNA replication. The first experiment was conducted with sacrificing animals at different days after the injection of BrdU, and the second experiment was conducted where animals were sacrificed at different hours after the second injection of BrdU.

Immunohistochemistry:

Immunohistochemistry was performed as described (Chapter 2). Sections from the region of the spinal cord containing the motor neurons of the sciatic nerve were used for 'cell body analysis', and sections from the first centimeter of the sciatic nerve were used to analyze 'axons'. Both kinds of sections were stained for VDAC-1 in red (Alexa Fluor 546) and BrdU in green (Alexa Fluor 488).

Imaging and Analysis:

Fluorescent labeling was observed through a LSM 5 Pascal confocal microscope (Zeiss, Oberkochen, Germany) and images were recorded with the Pascal software (Zeiss). All image analysis was done using Image J

(NCBI, USA) and corresponding plug-ins. All staining was checked for non-specific antibody labelling using control slides without primary antibody, or without secondary antibody, or without fluorescently labeled streptavidin.

Images of the cell bodies of motor neurones were analysed in 3D stacks collected with 1 μm thick optical sections and analysed using 3D Object counter using FIJI (ImageJ). The analysis was represented as the percentage particles of VDAC-1, which also showed positive staining for BrdU. Slides from every animal were analysed using the same settings normalized against a positive control section from the intestinal region. Laser power, aperture of Iris and PMT gain were kept consistent for the collection of images across the whole experiment. Threshold used for the analysis of particles was also kept consistent.

A similar analysis was performed for the axons of the cells. The analysis on nerves was not performed using 3D because of the frailty of the tissue. 2D particle count was performed on a ‘maximum intensity’ Z projection of the section imaged using 1 μm optical sections. This method may have resulted in the loss of some signal due to missing particles in z-planes other than the one captured. One way of showing qualitatively that the BrdU reached all parts of the body is the mitotic signal which, occurs in the nuclei of proliferating glia in the CNS as well as the PNS and appears as solid green blots in all samples.

Time points were generated such that every time group had 5 animals.

Part 2

Intraspinal LPS injection of MitoTracker® Red:

In order to corroborate the potential speed of movement of newly formed mitochondria which was suggested in the BrdU experiment, we used a second method of labelling mitochondria in the somatic pool. We used the potentiometric dye MitoTracker® Red which, when loaded into mitochondria, sticks to membrane and can be post-fixed with PFA, and imaged.

Adult (250-350 g) Sprague Dawley (SD) rats were anaesthetised with 2% isoflurane (Merail, Harlow, UK) in 100% oxygen and the site of operation was shaved and sterilised with iodine. Subsequently, animals received a quarter laminectomy of the 13th lumbar (T13-L1) vertebral. Once the spinal cord was exposed, a small incision was made in the dura and pia, and 2 injections of 0.5 µl of MitoTracker® Red 0.5 mM (Life technologies M-7512) were performed at 700 μm distance from the dorsal vein and a depth of 1100 μm. For injections, a glass drawn micropipette held in a micromanipulator with a trajectory of 24 degrees to the vertical was used. Injection sites were marked with a small amount of sterile charcoal. Control animals were injected with sterile PBS. Following this the animals were left to recover from surgery and then sacrificed by cardiac perfusion at 4 (n=3) and 8 (n=3) hours after the time of injection.

Tissue preparation for imaging:

After cardiac perfusion the tissue was placed overnight in a 4% solution of PFA and then cryopreserved in 30% sucrose. Tissue blocks were made from regions of the spinal cord with the sciatic motor neurones and the sciatic nerve was collected and cut into 1 cm lengths before being blocked for longitudinal sectioning. Every section of the nerve cut using the cryostat was

collected. A control piece of tissue from the spinal cord 0.5 cm away from the site of injection was also collected in order to determine whether the dye had reached that far in the tissue by simple diffusion. Sections from this region did not show any fluorescence signal. The resulting tissue was embedded and sectioned using a cryostat at a thickness of 12 μm. The tissue was then left to dry and directly mounted with Fluoromount Aqueous Mounting medium (Sigma Aldrich F-4680).

Imaging and analysis:

Images were acquired using a LSM 5 Pascal confocal microscope (Zeiss, Oberkochen, Germany) and images were recorded with the Pascal software (Zeiss). The control animal, which was injected with PBS, did not show any significant fluorescence signal in sections from the spinal cord or sciatic nerve. Motor neurone cell bodies were analysed using an intensity threshold and total content of positive particles of MitoTracker® Red fluorescence containing within the volume of a cell. The sciatic nerve sections were analysed for the area occupied by fluorescence intensity above the threshold normalised for the area of the section. The data were then averaged across the three animals. An ANOVA test was performed for statistical testing.

Part 3

Electrical Stimulation- *in vivo* experiment:

Electrical stimulation was performed in mice adult C57/Bl6 mice weighing between 25-30 g. Animals were given an initial dose of BrdU (100 mg / kg; 5 ml / kg) in saline intraperitoneally. After 105 minutes, the animals were anaesthetised and prepared for surgery. The animals were anaesthetized with isoflurane (5%) and maintained with 1.5%. The sciatic nerves were surgically

exposed on both sides and a Teflon tape was placed under a section of the nerve for electrical isolation as photographed in Figure 2. The preparation was soaked in mineral oil to provide electrical isolation from surrounding tissue and to prevent drying (Figure 2). Electrical stimulation was provided using a constant voltage isolated stimulator (Digitimer, UK). Paired electrodes were placed cupping the sciatic nerve around the hip area. The right side was given stimuli of amplitude 5 V (supramaximal), while the left (control) side was kept at 0 V. Stimuli (0.1ms duration) were delivered at 100 Hz for 2 hours. At the start of stimulation a second dose of BrdU was administered of the same dose. After checking that the stimulation was effective, the sciatic nerves were crushed distally to avoid tetanic stimulation of the muscles. At the end of 2-hour protocol, animals were sacrificed by cardiac perfusion.

Figure 2: Photograph of C57Bl/6 mouse with exposed sciatic nerve prep. Both sides of the nerve are exposed, bathed in mineral oil isolated with Teflon tape and stimulated using custom made silver wire electrode assembly. The right hand side was stimulated at 100 Hz and 5 V and the left at 100 Hz and 0 V as a control.

Tissue preparation for imaging:

After cardiac perfusion the tissue was placed overnight in a 4% solution of PFA and then cryopreserved in 30% sucrose. Tissue blocks were made from regions of the spinal cord with the sciatic motor neurones and also 1 cm above from the thoracic region of the spinal cord as a control. Since the entire electrical pathway was stimulated in this protocol dorsal root ganglia were also collected from these animals. The resulting tissue was embedded and sectioned using a cryostat at a thickness of 12 μm. The tissue was then left

to dry and then directly mounted with Fluoromount Aqueous Mounting medium (Sigma Aldrich F-4680).

Immunohistochemistry:

BrdU was detected with fluorescence immunohistochemistry. Immunohistochemistry was performed as described before (Chapter 2). Briefly, the sections were incubated with primary antibodies: rat anti-BrdU (AbD Serotec, MCA2060) 1:200 dilution in PBS and rabbit anti-VDAC1 (voltage dependent anion channel 1, Abcam) 1:600 dilution, overnight in the fridge. The following day, sections were washed 3 times for 15 minutes with PBS and once with PBS and 0.3% Tween. A secondary antibody was then applied: biotinylated goat anti-rat IgG mouse absorbed (Vector Labs) 1:200, and Alexa Fluor 546 conjugated goat anti- rabbit IgG (Invitrogen) 1:200 for 2 hours at room temperature. The slides were washed 3 times for 15 minutes with PBS and 0.3% Tween, after which the BrdU signal was amplified using Alexa Fluor 488 streptavidin (Invitrogen) 1:200 for 90 minutes at room temperature. The last 3 washes for 15 minutes with PBS were performed and then the slides were mounted with Fluoromount Aqueous Mounting Medium (Sigma). Control animals (no BrdU) for the electrical stimulation experiment were labelled with mitochondrial transcription marker- TFAM (transcriptional factor A, mitochondrial). All the previous steps were the same except using Target Retrieval Solution (Dako) instead of HCl treatment.

1. Primary antibodies: Rabbit anti-TFAM antibody (Sigma) 1:2000 and NeuN (Neuronal Nuclei, Mouse monoclonal; Millipore) 1:500 dilution.
2. Secondary antibodies: Goat anti-rabbit biotinylated mouse absorbed

(Vector Labs); goat anti-mouse IgG conjugated with Alexa Fluor 546 (Invitrogen). TFAM signal was amplified using Alexa Fluor 488 streptavidin (Invitrogen). All dilutions were at 1:200.

Image acquisition

All fluorescently labelled sections were imaged using a Zeiss LSM 5 Pascal confocal microscope (Zeiss, Oberkochen, Germany) at 63x oil immersion magnification. Alexa Fluor 488 and Alexa Fluor 546 were excited with a 488-nm argon laser and 543-nm HeNe laser, respectively. The spinal cord and dorsal root ganglion sections were imaged using a Z-stack mode producing 10-12 slices at 1 μm thick. All the nerve sections and ventral/dorsal roots were imaged using a Tile mode (X=5; Y=2). Mitochondria labelled with BrdU/TFAM and VDAC-1 were assessed with two different channels. All the settings were kept constant throughout imaging, to facilitate direct comparisons.

Image Processing and Analysis:

Images were recorded with Pascal software (Zeiss) and analysed with Image J software (NCBI, USA). Each cell of interest was isolated and analysed individually for BrdU content in BrdU positive mitochondria. A threshold for fluorescence intensity was set manually and kept the same throughout the analysis. The correct threshold settings helped to exclude from the count the BrdU positive nuclear DNA and only counted the BrdU positive mitochondrial DNA. A 3D object-counter plugin was used to count the number of mitochondria labelled with BrdU. The plugin also provided us with read outs of the volume of each particle and the maximum particle fluorescence intensity

of the cell. Then, for each cell of interest, a Z project plug in was applied, and the percentage of BrdU positive particles was calculated per particle count for VDAC-1. This method gives a read out of the percentage of mitochondria undergoing DNA replication.

Due to the high concentration of mitochondria in sensory neurones from the dorsal root ganglion, only a BrdU content analysis was possible in these sections. Threshold fluorescence intensity was used to define positive labelling and then the content was normalised to the size of the cell body.

Statistical analysis

Changes in pattern of mitochondrial biogenesis in short-time series experiments were analysed using GraphPad Prism6 software, a one- way ANOVA analysis ($p<0.5$). The electrical stimulation experiments were assessed using the unpaired two-tailed Student's *t* test ($p<0.05$). The stimulated (right) side was compared to the control (left) side for significant change in mitochondrial biogenesis. Raw data are plotted as dot plots to show the population distribution.

Results

Somatic mitochondrial nursery

All observtaions of the BrdU signal from spinal cord motor neurones were performed in C57Bl/6 mice. Images of at least 80 cell bodies were acquired as z-stacks were analysed for percentage of VDAC-1 positive particles containing a mtDNA replication signal marked with BrdU as represented in Figure 3. This signal was used as a surrogate marker for mitochondrial

biogenesis. All sections analysed showed strong labelling for BrdU in the proliferating nuclei of mitotic cells such as glia. This suggests in terms of the distribution of BrdU in when administered systemically, is available for inclusion into replicating DNA.

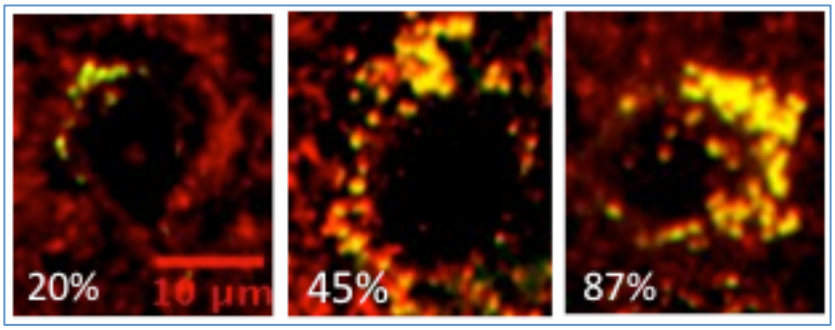

Figure 3: Representative confocal images of sections through individual motor neurone cell bodies of mouse spinal cord showing different amounts of mitochondrial biogenesis or mitochondrial DNA replication as measured with VDAC-1 (red) and BrdU (green). These cells were analysed in 3D via optical stacks to accurately measure the per cent of VDAC-1 positive particles also containing BrdU, where all staining was done together and all images were analysed using the same digital settings of brightness and contrast and threshold of brightness.

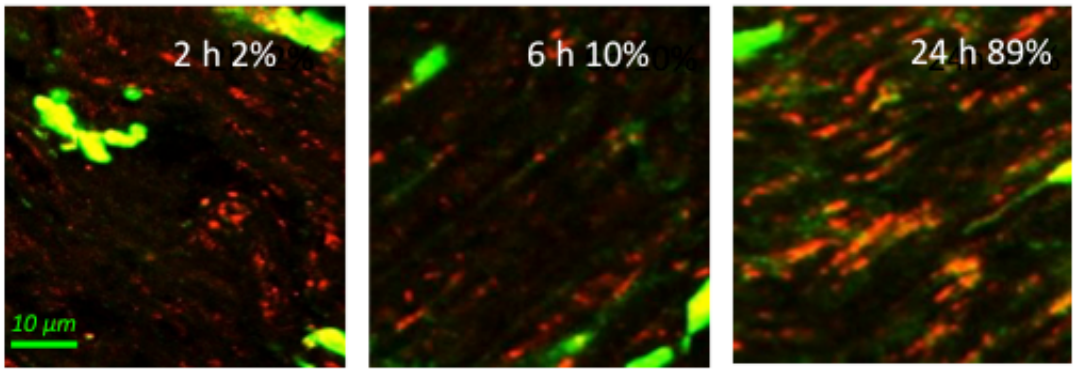

Figure 4: Representative confocal images of sections through individual axons from mouse sciatic nerve sections from the first centimetre of the sciatic nerve. These nerve axons were analysed in 3D via optical stacks to accurately measure the per cent of VDAC-1 positive particles also containing BrdU, where all staining was done together and all images were analysed

using the same digital settings of brightness and contrast and threshold of brightness.

The pulse and chase experiments were analysed over 5 animals at each time point. The averaged percentage points are represented in Figures 5 and 6.

In the early time points the signal of BrdU in the somatic (cell body) mitochondrial rises; reaching a peak at 4 hours. This time represents the pharmacokinetic peak of BrdU. Curiously however, the mitochondrial BrdU signal seemed to be localized to cell bodies of neurones in the grey matter of the spinal cord in the first 6-8 hours, while, the mitotic BrdU signal seems to appear in all the tissue sections, suggesting that only the mitochondria in the cell body are carrying out DNA replication.

The co-localization of VDAC-1 and BrdU in the axonal sections from the sciatic nerve was observed only in the animals sacrificed 6 or more hours after the injection of BrdU. This suggests that most of the mtDNA replication occurs in the mitochondria contained within the soma of motor neurones. The appearance of BrdU in axonal mitochondrial after 6 hours could be explained as an effect of newly formed DNA particles having moved into the axons via a combination of processes i.e. trafficking, fission and fusion. The speed of movement of these potentially new mitochondria was calculated using the distance and the amount of time after the second injection of BrdU and it was determined to be in the range of 0.28 – 0.46 μ m/s. This evidence along with the observation of clustering of mitochondrial particles around the axon hillock (Chapter 3) suggests the presence of a somatic mitochondrial nursery.

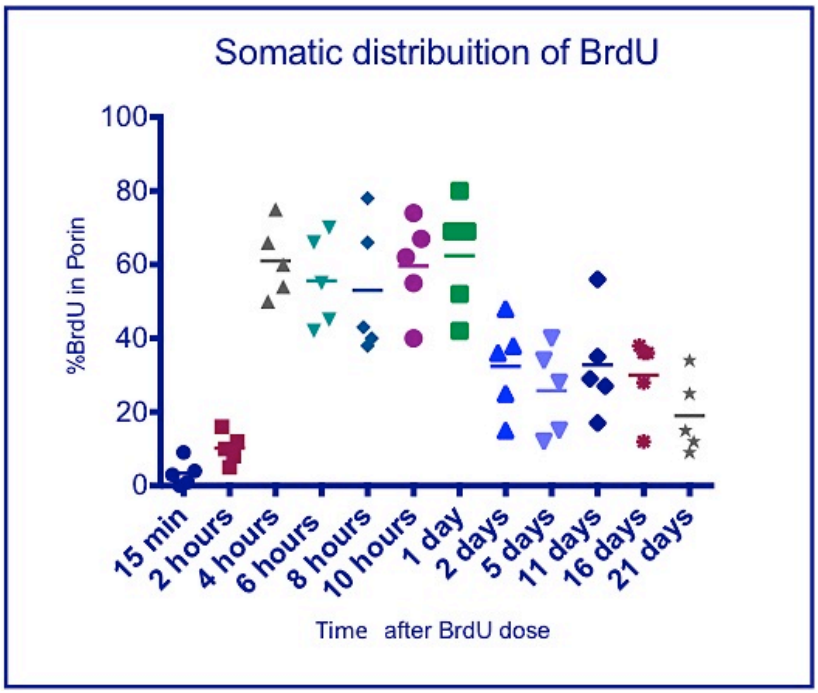

Figure 5: This graph shows the BrdU content in each cell across each animal at each time point. There is a sharp rise of BrdU content after 4 hours, which is representative of the pharmacodynamic peak of BrdU distribution. The fall after 2 days perhaps represents a distribution of newly formed mtDNA or a breakdown of the BrdU signal.

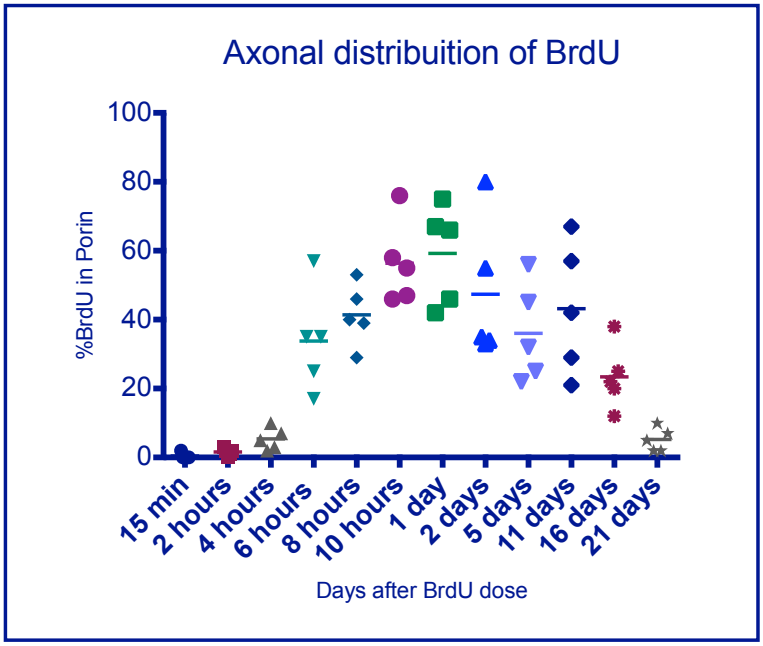

Figure 6: Graph showing the BrdU content in sciatic nerve axons at each animal across each time point. There is a sharp rise of BrdU content after 8 hours, which is representative of the newly formed mitochondrial DNA contained within mitochondria moving down the axon.

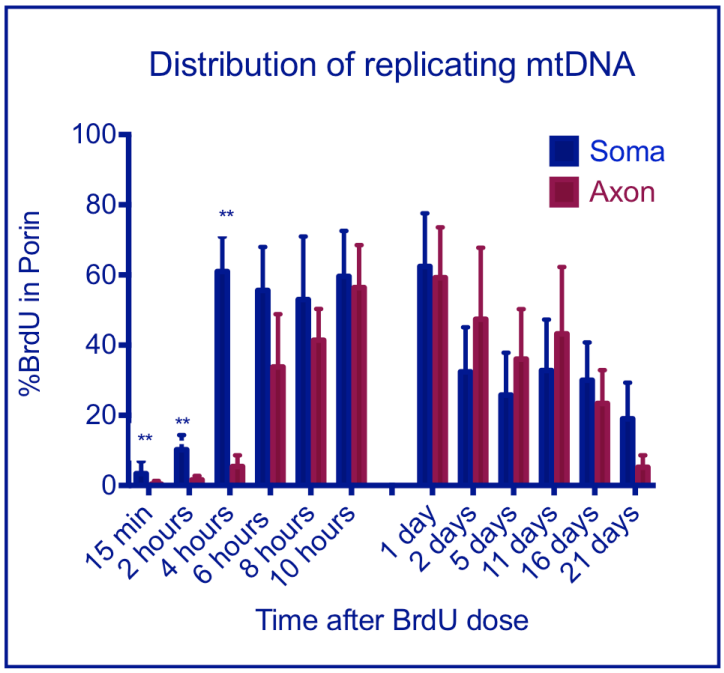

Figure 7: When comparing the mitochondrial BrdU in cell bodies and in axons there is a statistically significant difference at 15 min, 2 hours, 4 hours and 6 hours between the two compartments of the cell. A two-way ANOVA was performed to compare the biogenesis signal between soma and axon ($p<0.0001$). This represents a lag of 6-8 hours, which suggests that most mtDNA replication occurs in the cell bodies and travels down via axonal transport. The velocity of movement is 0.28 – 0.46 μ m/s

MitoTracker® Red

In order to corroborate the speed of movement down the axon using an alternate method of labelling, Mitotracker Red was used as a dye to label mitochondria *in vivo* in Sprague Dawley adult rats and examined in post mortem tissue. The MitoTracker® Red was injected close to the ventral horn where the motor neuron cell bodies are located. The signal was picked up nicely into the mitochondrial in the motor neurone soma as shown in Figures 8a and 8b. The sections from a region 0.5 cm away from the site of injection showed no fluorescence signal, suggesting that by sheer diffusion the concentration of the dye had not been enough to stain mitochondria in that

region. This suggests that it would be unlikely for enough MitoTracker® Red reaching the axon by simple diffusion. The signal, which appeared in different sections of the sciatic nerve after 4 hours and 8 hours of after injection of MitoTracker® Red, is shown in Figures 8 c, d and e. The signal was then averaged over three animals at each time point and the analysis is represented in Figure 9.

We believe that the appearance of these dye containing particles in the axons represents mitochondria which picked up dye from the somatic region while in the somatic region of the motor neurone, and then were trafficked along the axon towards the peripheral regions of the nerve. From these observations we calculated the speed of movement of these particles and was found to be between 0.35 and 1.05 μ m / second.

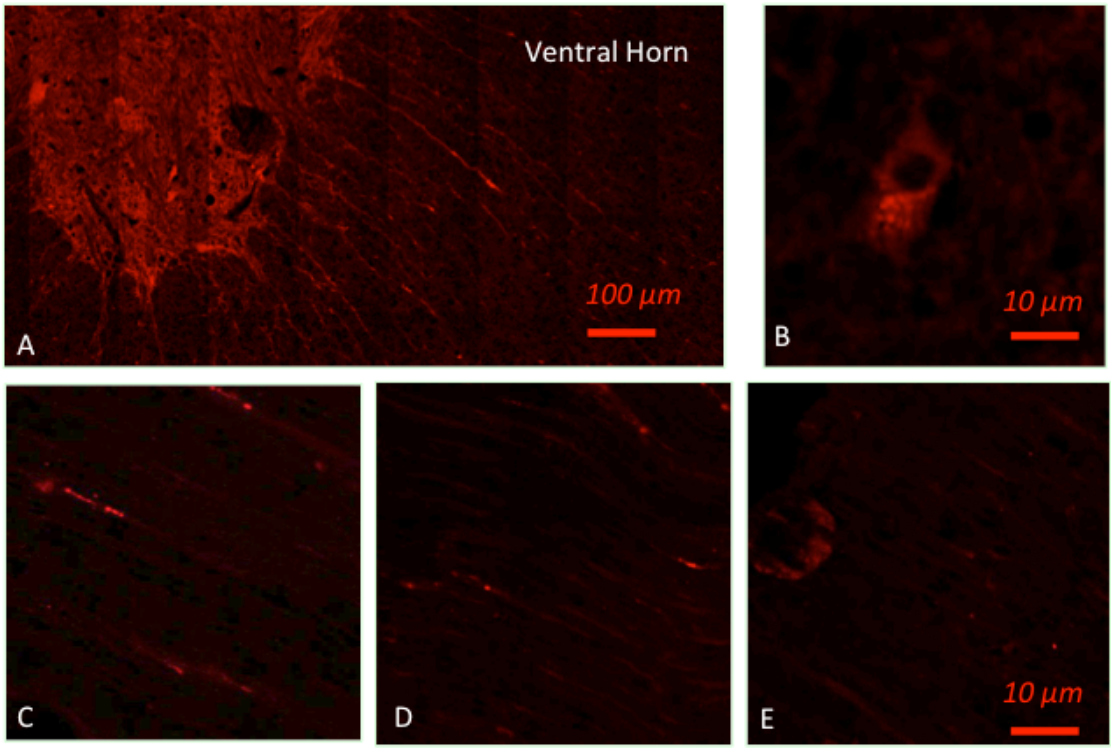

Figure 8: Confocal images of sections spinal cord from adult rat and sciatic nerve after intraspinal injection of MitoTracker® red. (A) is a composite tiled image showing the ventral horn region near the injection site, 4 hours after injection. Dye is clearly collected in cell bodies and projections neat the site. (B) is a high magnification image of one motor neuron with clear punctate labelling of mitochondria with the dye. (C) is a section of the nerve 1 cm from the spinal cord, (D) is 2 cm away and (E) is 3 cm away, 8 hours after injection

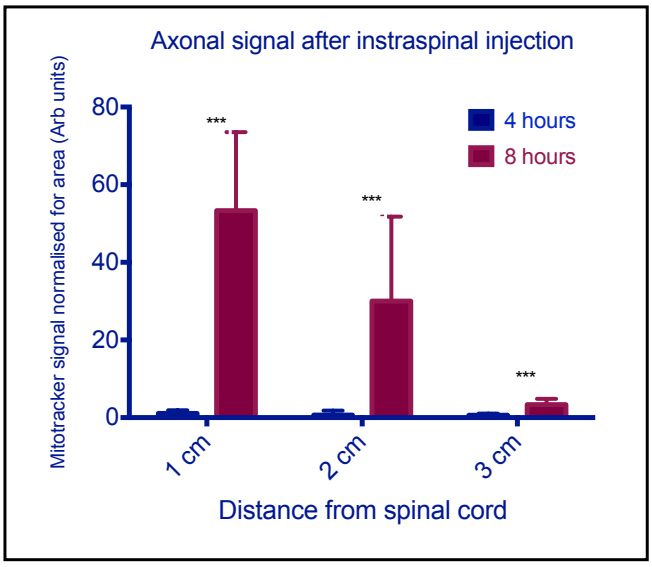

Figure 9: Analysis of MitoTracker® red labelled mitochondrial in 1, 2, and 3 cm away from the spinal cord 4 hours (blue) and 8 hours (red) after the surgery. Virtually no signal appears in sciatic nerve axons after injection of MitoTracker® Red into the ventral horn grey matter until 8 hours after injection. The calculated speed of movement of mitochondria is 0.35 – 1.04 µm/s

Mitochondrial biogenesis responds to electrical stimulation

The observation of a somatic nursery for mitochondrial biogenesis along with the appearance of clustering of mitochondria towards the axon hillock, and the increase of mitochondrial DNA replication, were stepping stones towards testing whether the mitochondrial biogenesis is initiated in cell bodies of neurones following a period of high activity as simulated by external stimulation of the sciatic nerve. Mice which had not been administered BrdU as a control, were sectioned and stained using antibodies against mitochondrial transcription factor A (TFAM), there was a clear increase in signal unilaterally following electrical stimulation (Figure 10).

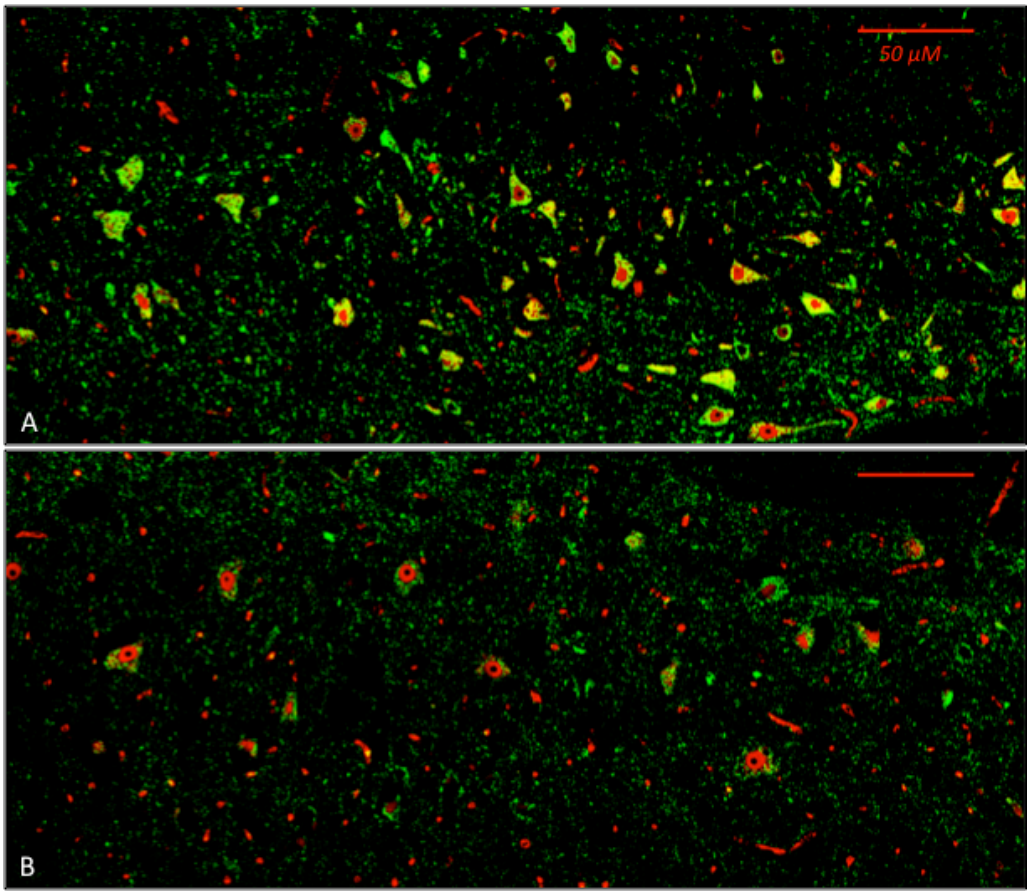

Figure 10: Staining of spinal cord tissue from adult mice to visualise TFAM (green) and NeuN (red). The right side of the animal (upper panel) shows enhanced TFAM staining in neurons following 2 hours of electrical stimulation.

Upon observation of mitochondrial biogenesis signal as measured using previously described methods (Appendix) there was a clear unilateral increase in biogenesis following stimulation of the sciatic nerve on one side, in motor neuron cell bodies (Figures 11 a and b). Furthermore, the a higher signal was observed in the sensory neurons from the right (stimulated) dorsal root ganglion than that in sensory neurones from the left side (Figures 11 c and d). Also when motor neurones from the right (stimulated) were compared with a section of the spinal cord away from the site of stimulation (Figures 11 e and f), it was observed that the site of stimulation contained cell bodies with

a higher biogenesis signal than the ones in a region of the spinal cord which had received no external stimulation.

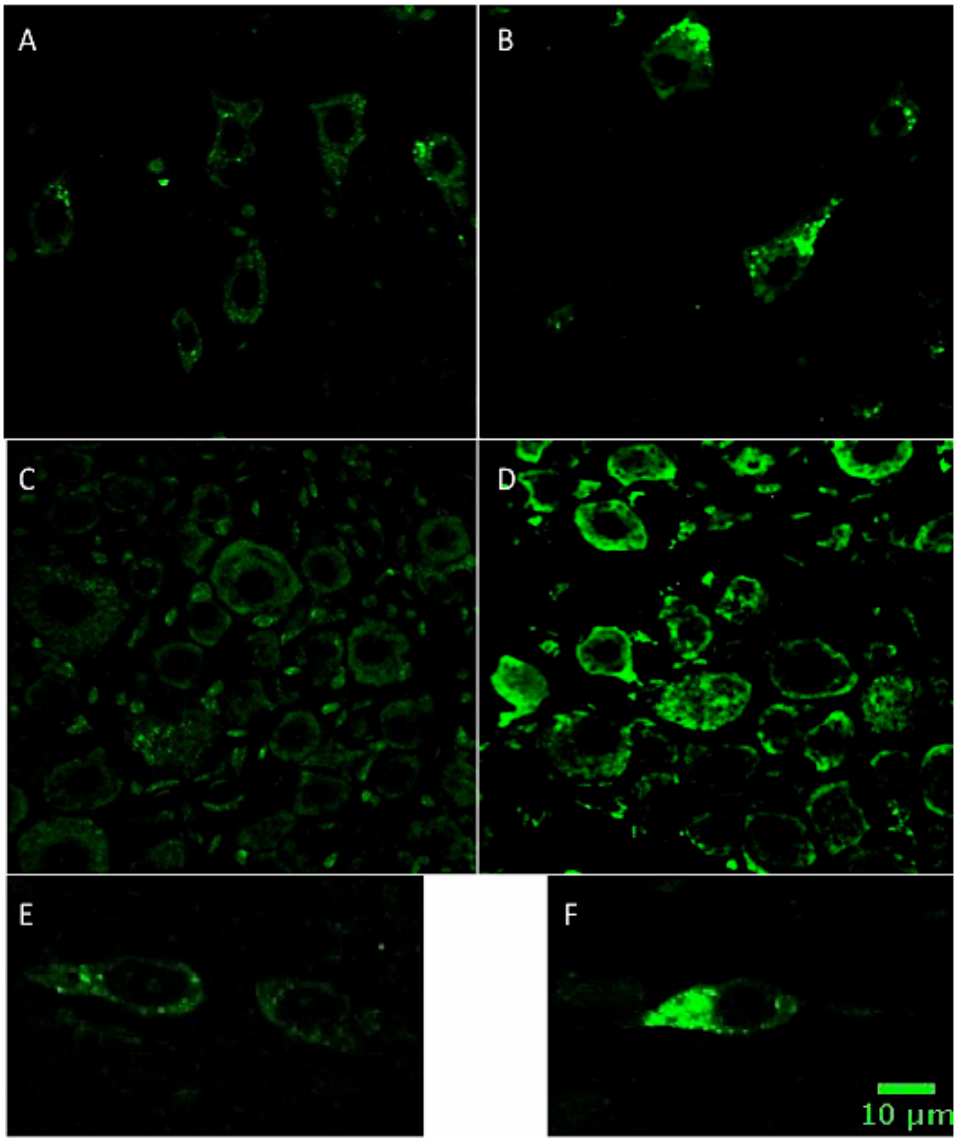

Figure 11: Confocal images comparing the right and left side neurones after unilateral electrical stimulation in mice to increase energy demand labelled for BrdU content (Green). (A) is an image of the sham side motor neurones. (B) is a neurone from the stimulated side. (C) is an image of the dorsal root gangion from sham side and (D) is from the stimulated side. (E) is an image of a motor neuron from the same side as the electrical stimulation but from the thoracic region of the spinal cord which does not containing cell bodies corresponding with the sciatic nerve. (F) is a motor neuron from the lumbar region where the sciatic nerve emerges.

Upon averaging the mitochondrial biogenesis signal from cell bodies across 5 animals, it was observed that the signal was significantly higher on the stimulated side than the control side as tested with a paired t-Test in figures 12 and 13 for motor neurones as well as sensory neurones. Due to the high amount of signal observed in sensory neurones it was not possible to perform the previously described mitochondrial biogenesis signal of percentage of VDAC-1 particles positive for BrdU. Instead, the simple content of BrdU normalised for the size of cell and set threshold for fluorescence intensity was evaluated. Also as represented in Figure 14 the motor neurone cell bodies from the region of the spinal cord 1 cm away from the site of stimulation were found to have far less BrdU signal than the motor neurone cell bodies from the stimulated region of the spinal cord. There is a fair amount of spread observed (Figures 12a, 13a and 14a) which is representative of the diversity of motor neurones, both in size, type and activity.

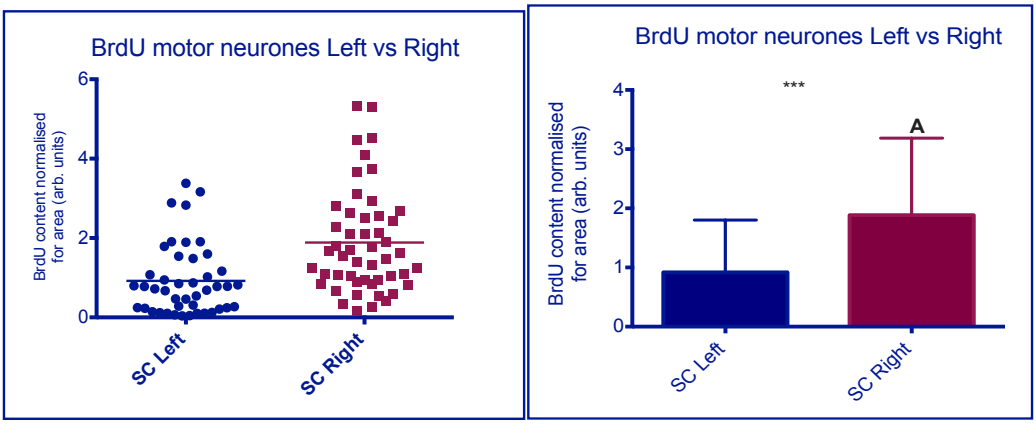

Figure 12: Left graph shows the spread of BrdU signal across different sides of the spinal cord, stimulated (red) and sham (blue) in one animal. Right graph shows averaged over n=5) the result is found to be statistically significant (p=0.00037)

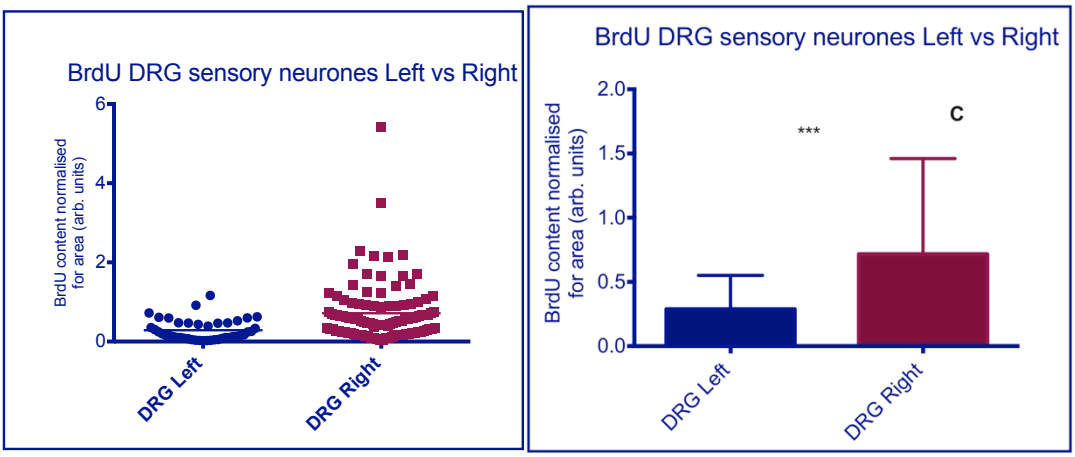

Figure 13: Left graph shows the spread of BrdU signal across sensory neurones of different sided dorsal root ganglia stimulated (red) and sham (blue) in one animal. When averaged over (n=5) the result is found to be statistically significant (p=0.000297)

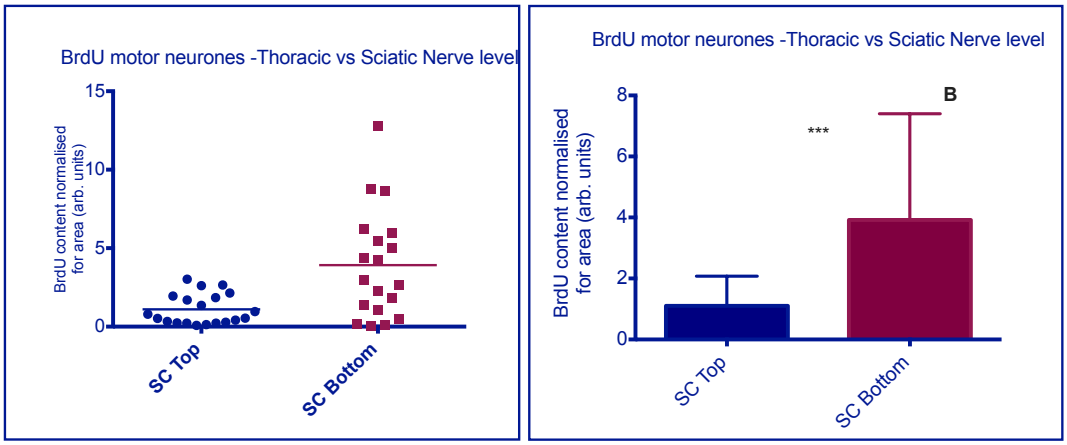

Figure 14: Left graph shows the spread of BrdU signal in motor neurones of the thoracic region and lumbar region stimulated (red) and away from stimulated (blue) in one animal. When averaged over (n=5) the result is found to be statistically significant (p=0.00037)

We suggest that these data demonstrate the presence of a somatic nursery for mitochondrial biogenesis, which increases its rate of growth in response to increases in energy demand, such as resulting from electrical stimulation or in response to damage as in the case of neuroinflammation.

Discussion:

Mitochondrial biogenesis in the soma:

Neurons are large cells that rely on mitochondrial function (Nicholls, 2002) and thus the rapid and versatile distribution of mitochondrial activity over time and space is critical (Hollenbeck and Saxton, 2005). They are also typically long-lived cells in which mitochondria must dilute the products of their error-prone DNA replication (Schapira, 1993) by fission and fusion (Chan, 2006; Chang and Reynolds, 2006; Hoppins et al., 2007; Ono et al., 2001), and renew themselves through biogenesis. The dying-back peripheral neuropathy observed in AIDS patients (Raff et al., 2002) treated with nucleoside inhibitors of mtDNA replication (Dubinsky et al., 1989; Pardo et al., 2001; Raff et al., 2002) emphasizes the importance of mitochondrial biogenesis for the integrity of the axon. Other deficiencies in mitochondrial biogenesis, such as those associated with ageing, affect neurons more than other cell types (Miquel, 1991) and probably underlie neurodegenerative disorders (Linnane et al., 1989). But where in this large and asymmetric cell does mitochondrial biogenesis occur? Because most mitochondrial proteins are encoded in the nuclear genome (Neupert, 1997) it has been suggested that all mitochondrial biogenesis occurs in the cell body, close to the nucleus (Davis and Clayton, 1996). A body of recent work revealing components of the machinery for mitochondrial replication within axons has refocused our attention on this issue, as has the detection of mtDNA replication in neurites of SH-SY5Y neuroblastoma cells (Magnusson et al., 2003). More recent studies have suggested that mtDNA replicates in axons, as well as the cell body, in cultures chick sensory neurones (Amiri and Hollenbeck, 2008)

I have addressed the location of neuronal mitochondrial biogenesis *in vivo* in mammalian neurones that have a particular vulnerability to mitochondrial dysfunction – motor neurones. I find that the majority of mitochondrial DNA replication occurs in the soma of these neurones. It may be postulated that there is a nursery of mitochondria located close to the perinuclear region of motor neurones, which gets activated by a need for new mitochondrial production. This provides quick access to the nuclear machinery, which is necessary for the transcription of mitochondrial genes, and perhaps also isolates the 'mother' mitochondria from mitochondria damaged in the peripheral parts of the neurites. This also presents a new challenge. It maybe speculated that if there is high oxidative stress near the neuronal cell body this may 'poison' the somatic nursery and perhaps manifest in mitochondrial pathology all through the cell more quickly than local changes in the periphery. With support for the existence of clonal expansion of mitochondrial damage in various neurodegenerative diseases and tissues it may be speculated that the poisoning of mitochondrial nursery which is triggered by a variety of pathologies such as a blood barrier breakdown, genetic susceptibility, hypoxia could potentially knock out types of cells where the cell bodies are exposed to the oxidative stress.

Distribution of newly formed mitochondria:

Our understanding of the neuron as a dynamic metabolic system depends critically upon where in the cell mitochondrial biogenesis occurs. If it is limited to the cell body, then axonal mitochondria are purely visitors in the axon whose lifetime prior to turnover will barely equal the time necessary to reach the distal ends of long peripheral axons. In this case, axons could respond to

changes in local need for mitochondrial function only by redistributing or regulating the activity of mitochondria that are already undergoing transport through the axon. This then presents a further importance on the efficient transport of mitochondria to the peripheral regions of the neurone. The speed of movement we estimate using our two methods BrdU (0.28 – 0.46 μ m/s) and MitoTracker® Red (0.35 and 1.05 μ m/s) are both comparable. The MitoTracker® Red studies are carried out in SD rats while the BrdU method was carried out in C57 mice. Furthermore, the BrdU only measures the speed of movement of 'new' mtDNA and the method will not detect any signal if the BrdU has been diluted via the process of fusion and fission below the technical limit of immunohistochemistry. These experimental caveats may account for the difference in the estimated speed of movement. However, our estimates are not very different from previously observed speed of mitochondrial movement estimated by *in vivo* imaging of moving mitochondria in the saphenous nerve of mice (0.3-0.7 μ m/s) (Sajic et al., 2013)

Mitochondrial biogenesis response to electrical stimulation:

I observed a physiological relationship between impulse activity and mitochondrial biogenesis *in vivo*. Earlier studies conducted *in vivo* have reported induced activity was associated with a *increase* in mitochondrial transport, and an accumulation of mitochondrial (Sajic et al., 2013). In conjunction to this change I observe that at high frequency stimulation we a unilateral increase in mitochondrial biogenesis on the side of stimulation in both the motor and sensory neurones occurred. Along with the importance of mitochondrial transport in these neurones this study emphasizes the

importance of mitochondrial turnover. It has been observed in the past that exercise induces mitochondrial biogenesis in skeletal muscle cells (Holloszy, 2011). This paradigm of electrical stimulation suggests a similar type of demand-generated increase of biogenesis in the neurones. This maybe one of the ways the CNS is able to maintain health via the balance of mitochondrial biogenesis and mitophagy following periods of high activity

Chapter 5: Hot-spots of mitochondrial biogenesis

Introduction

The brain is a highly metabolic tissue, and neurons in the central nervous system have an intense demand for mitochondria (Wang et al., 2009). Mitochondria provide most of the ATP for cellular reactions in neurones (Herrero-Mendez et al., 2009). ATP production in mitochondria is coupled to an electron transport system in which the passage of electrons down the various electron carriers is associated with the transport of protons from the matrix into the inter-membrane space. The majority of these protons reenter the mitochondrial matrix by the ATP synthase, thereby generating ATP.

Studies of aging brain mitochondria consistently report reductions of complex I activity, complex IV activity, and increased ROS production (Navarro and Boveris, 2007b). Other age-related mitochondrial changes include reduced membrane potential and increased size. Mitochondrial DNA mutations may contribute to age-related mitochondrial decline. MtDNA deletions accumulate with age in many tissues, especially brain preferentially in certain neuronal niches (Corral-Debrinski et al., 1992).

Mitochondria are altered in the brains of persons with certain neurodegenerative diseases (Navarro and Boveris, 2007a; Swerdlow, 2007b). There are activity reductions of complex I in Parkinson's disease (PD),

cytochrome oxidase in Alzheimer's disease (AD), and multiple electron transport chain (ETC) enzymes in Huntington's disease (HD). Mitochondrial dysfunction occurs in amyotrophic lateral sclerosis (ALS) and progressive supranuclear palsy. Leber's hereditary optic neuropathy (LHON), a focal degeneration of the optic nerves, arises from mutations in mtDNA-encoded complex I genes and is associated with complex I dysfunction.

These observations were crucial in driving the hypothesis that perhaps there is a constitutive activation of mitochondrial biogenesis in certain neuronal niches due to certain factors. These factors include energy metabolism, neurotransmitter identity, size of cell, inherent electrical activity, myelination profile or need for mitochondrial repair and might require an elevated mitochondrial biogenesis. We have used the BrdU mitochondrial biogenesis probe to blindly identify region of the CNS and PNS, which exhibited a high turnover of mitochondrial DNA. Notably, the regions of high turnover we identified match neuronal niches that are susceptible to mitochondrial damage and primary mitochondrial disease.

Methods

In vivo experiment:

Two doses of BrdU were injected at 100 mg/kg intraperitoneally (systemic administration), 2 hours apart, into adult Sprague Dawley rats weighing between 200-250 g. Animals were sacrificed at 24 hours after the injection by cardiac perfusion. Several sets of tissue including brain, spinal cord, peripheral nerves, dorsal root ganglia and eyes were harvested from the

animals and stored overnight in 4% PFA and then cryopreserved in 30% sucrose before being processed for immunohistochemistry.

Immunohistochemistry:

Immunohistochemistry was performed as previously described in Chapter 2. Additionally, antibody to the dopaminergic cell marker tyrosine hydroxylase (TH) Pel-Freez (P40101-0), rabbit polyclonal) was used at dilution of 1:250 to detect the identity of dopaminergic cells in the ventral tegmental area and substantia nigra regions of the brain. Adjacent sections were stained for either a combination of β III Tubulin and BrdU in order to identify neuronal hotspots of mitochondrial biogenesis, or VDAC-1 and BrdU to perform mitochondrial biogenesis analysis as described in Chapter 3. The identity of neuronal niches was determined using histological landmarks.

Image acquisition:

Fluorescent labelling was observed through a LSM 5 Pascal confocal microscope (Zeiss, Oberkochen, Germany) and images were recorded with the Pascal software (Zeiss). All image analysis was done using Image J (NCBI, USA) and corresponding plug-ins. All staining was checked for non-specific antibody labelling using control slides without primary antibody or without secondary antibody or without fluorescently labelled streptavidin. None of the controls showed any signs of nonspecific fluorescence.

Analysis:

The images from the first set of staining using β III Tubulin and BrdU were used to identify neuronal niches containing mitochondrial BrdU signal. Images of section stained with antibody were analysed in 3D stacks collected with

optical sections 1 μ m apart and analysed using 3D Object counter using FIJI (ImageJ). The analysis was represented as the percentage of particles of VDAC-1, which also showed positive staining for BrdU (as described in Appendix). Slides from every animal were analyzed using the same settings normalized against a positive control section from the small intestine. Laser power, aperture of iris and PMT gain were kept consistent for the collection of images across the whole experiment. The threshold used for the analysis of particles was also kept consistent. Samples were processed and analyzed from 5 separate animals treated in exactly the same protocol. The mitochondrial biogenesis signal was then averaged from the 5 animals from comparable neuronal niches and analyzed for statistical significance using ANOVA.

A similar analysis was performed for the dorsal root ganglion sensory cells and retinas. Retinas were not examined using 3D because of the frailty of the tissue. 2D particle count was performed on a 'maximum intensity' Z projection of the section imaged using 1 μ m optical sections. This may have resulted in the loss of some signal. Qualitatively the BrdU reached all parts of the body as suggested by the mitotic signal, which appears in proliferating glia observed in the CNS as well as the PNS.

Results

In order to screen for regions, we scanned sections of rat brains, which had been dosed with BrdU (2 x 200 mg/kg) 24 hours before culling. No signal was detected in non-neuronal cells, and within the neuronal types there were

areas of high levels of mitochondrial biogenesis. We then tried to identify the neuronal types using stereotaxic co-ordinates and neuronal morphology. Neurons were identified using anti-beta III tubulin antibody and then the BrdU analysis was performed in adjacent sections using VDAC-1.

The pharmacokinetic profile of BrdU in the animals allows for the detection of replicating mitochondrial DNA only in certain cells and not at all in all other cells, suggesting a large difference in the turnover occurring in certain cell types. Although most neurones show little to no turnover, a few neuronal niches showed large amounts of BrdU being picked up by mitochondrial DNA. Histological landmarks and cellular morphology were used to identify these regions. Large optical scans which were digitally tiled together, from regions of the brain stained against neuronal marker β III-tubulin and BrdU were used to visualize neuronal niches, which had varying degrees of BrdU in the cytoplasm. Examples of these are shown in Figures 1, 2 and 3.

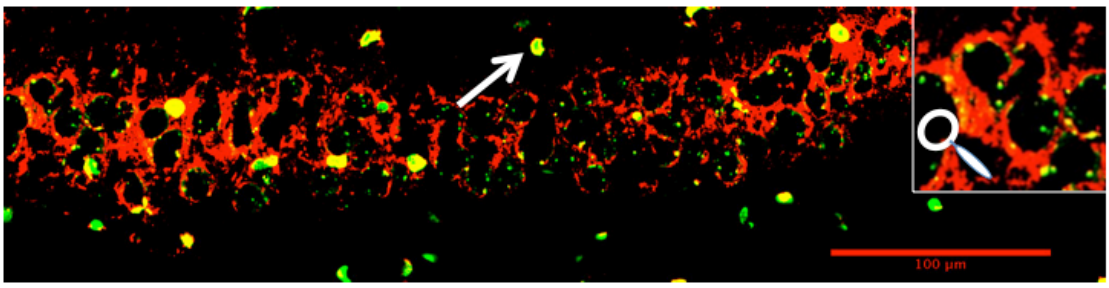

Figure 1: Optical section through a scanned image of the hippocampal CA1 region. βIII-tubulin stained in red and BrdU in green. The inset image shows a high magnification depicting small BrdU-labelled particles in the cytoplasm of cells. Bigger green structures (white arrow) mark proliferating nuclei.

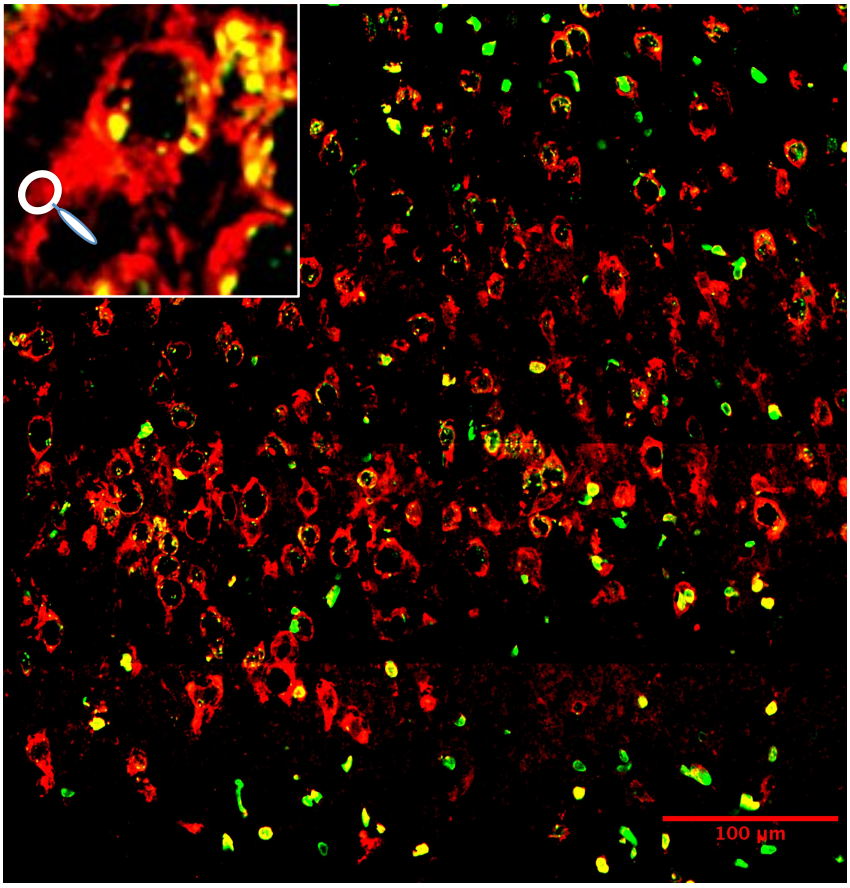

Figure 2: Optical section through a scanned image of the nucleus accumbens stained with anti- β III tubulin antibody (red) and anti-BrdU antibody (green) The small box contains a high magnification image depicting small BrdU-labelled particles in the cytoplasm of cells. Bigger green structures mark proliferating nuclei.

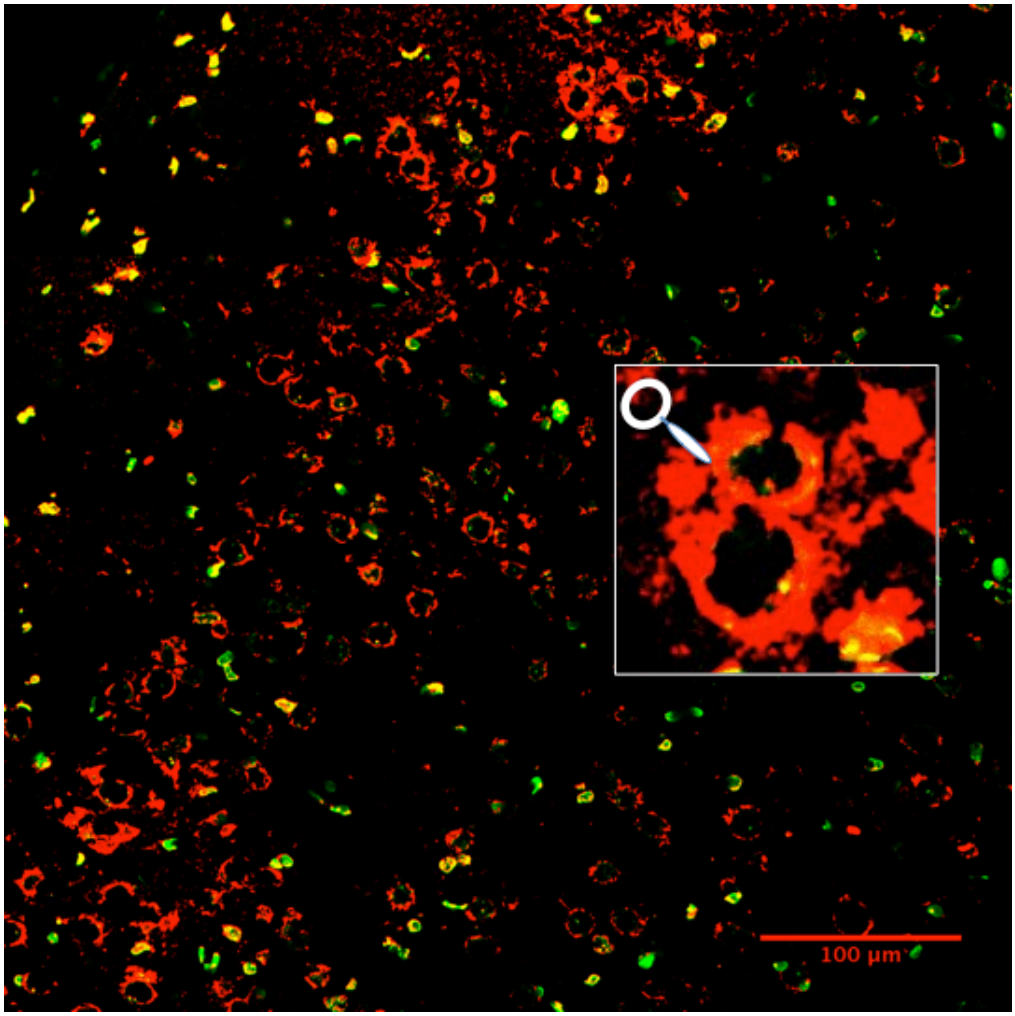

Figure 3: Optical section through a scanned image of the motor cortex region. βIII-tubulin stained in red and BrdU in green. The inset image shows a high magnification depicting very few small BrdU-labelled particles in the cytoplasm of cells.

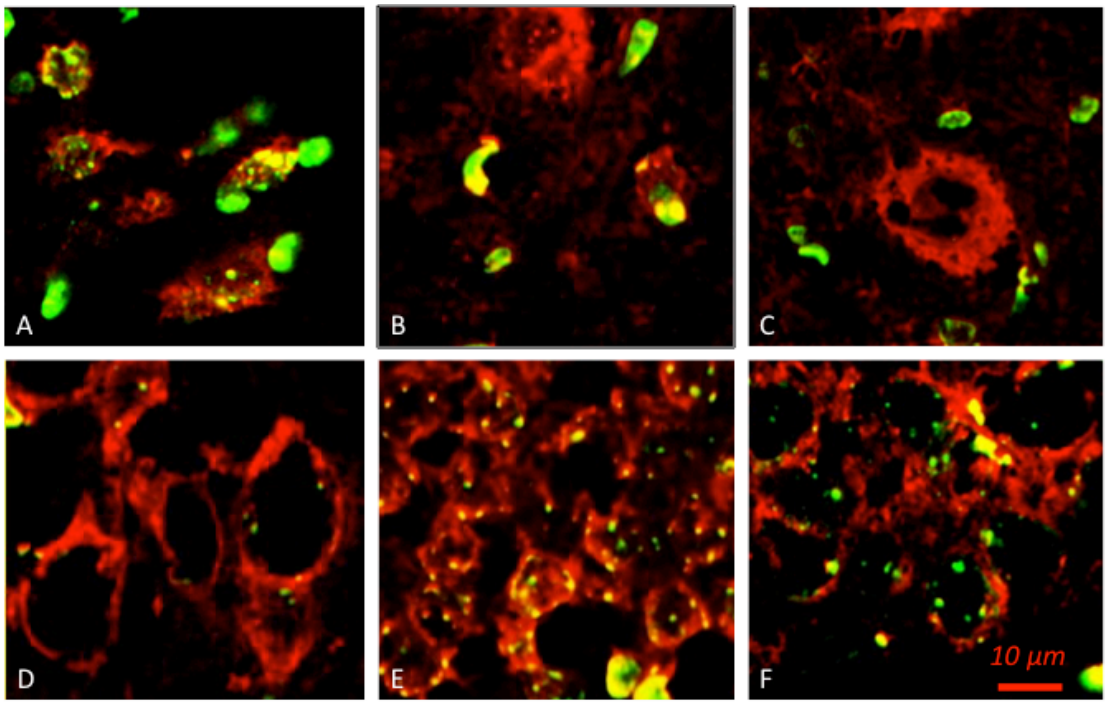

Figure 4 The panel shows confocal images of sections of brain tissue from different regions imaged at the same magnification. The neurones are marked by neuronal marker Beta III Tubulin (red) and BrdU (green). Some regions show more cytoplasmic BrdU than others and some show none at all. (A) substantia nigra, (B) ventral tegmental area (C) raphe nuclei (D) nucleas accumbens, (E) dentate gyrus of the hippocampus (F) CA1 region of the hippocampus

Other neuronal cell types outside the brain were also processed and imaged, specifically, the retina and dorsal root ganglion. Samples of these tissue regions were selected because they are susceptible to neurodegenerative pathology mediated by mitochondrial damage, such as in Leber's hereditary optic neuropathy and diabetic neuropathy. Certain regions of the brain that showed large mitochondrial DNA biogenesis include the hippocampus, nucleus accumbens core, substantia nigra in the brain. Other regions showed very little labelling such as in the motor cortex (Figure 4).

Certain layers of the eye such as the retinal ganglion layer and outer layer show mitochondrial DNA biogenesis (Figure 5). In previous chapters motor neurones have been shown to pick up large mitochondrial biogenesis signal with this dosing regimen of BrdU. Additionally, the sensory neurons contained in the dorsal root ganglion also exhibited large BrdU signal in the cytoplasm as shown in Figure 5.

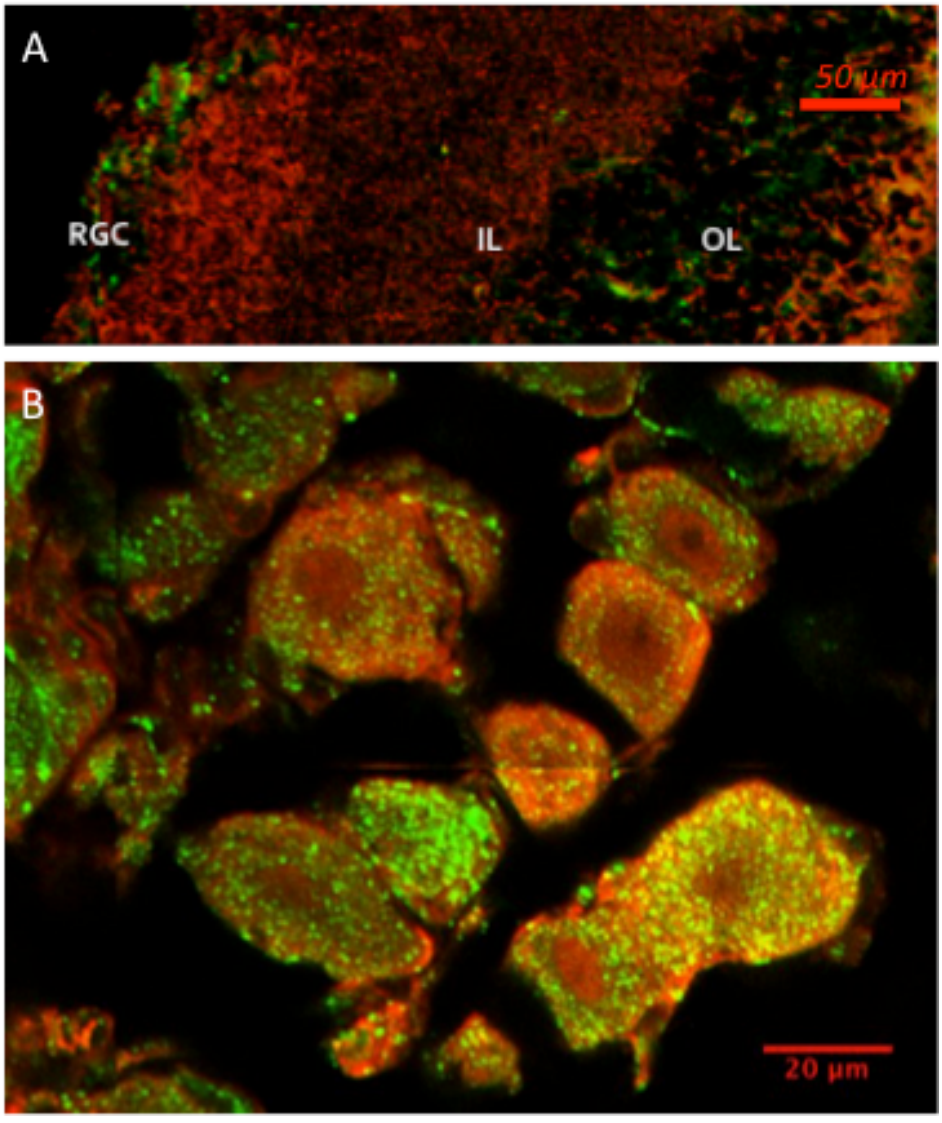

Figure 5: Sensory neurons also show incorporation of BrdU (Green) in beta III-tubulin marked neurones (red). (A) shows a section through the retinal layers. The retinal ganglion cells (RGC) and outer later (OL) show the most

BrdU labelling. (B) Shows sensory cells in the dorsal root ganglion with also a large turnover signal.

The dopaminergic neuronal niches were of particular interest as they have been implicated in primary mitochondrial disease such as Parkinson's disease. However, the dopaminergic neurones of the substantia nigra (SN) are susceptible to more degeneration than those of the ventral tegmental area (VTa). This mitochondrial biogenesis signal from these two regions is observed to be vastly different (Figure 6). Tissue sections from these regions were stained for the dopaminergic marker tyrosine hydroxylase and BrdU to confirm the identity of the neurones and the SN showed far more mtDNA replication signal than the VTa. It may be postulated that a constitutively higher rate of mitochondrial biogenesis in the SN compared with the VTa could underlie the accumulation of mitochondrial damage. That is to say that when faced with a defect in the mitophagy pathway, as observed with many genetic forms of Parkinson's disease, the SN neurones may be rendered vulnerable to accumulating clonally expanded dysfunctional mitochondria

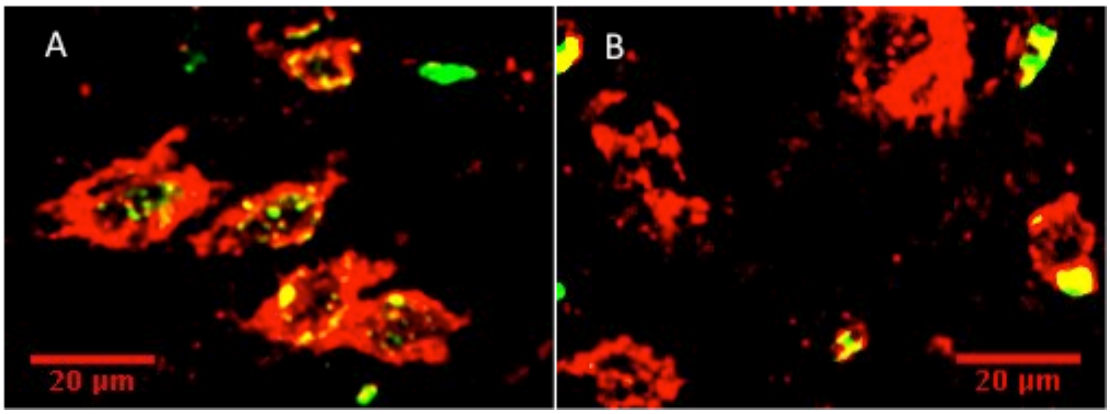

Figure 6: Section from brain tissue from the Substantia Nigra (A) and Ventral Tegmental Area (B). Immunohistochemical labelling for dopaminergic marker tyrosine hydroxylase (TH) in red and BrdU (green)

Tissue sections from the CNS and PNS were tested for mitochondrial biogenesis signal as described in Appendix. We found that the percentage of mitochondria picking up BrdU signal in different regions of the CNS was consistent across tissue harvested from several animals (Figure 7). Including the complete lack of signal from certain types of neurones. A good example were the sertonergic neurones of the raphe nuclei. Raphe nuclei neurones (Figure 9) are of similar size as the SN neurones. However, no mitochondrial biogenesis signal was detected in the cell bodies. These observations suggest that the rate of mitochondrial biogenesis is defined by the metabolism and cellular identity of a neuron.

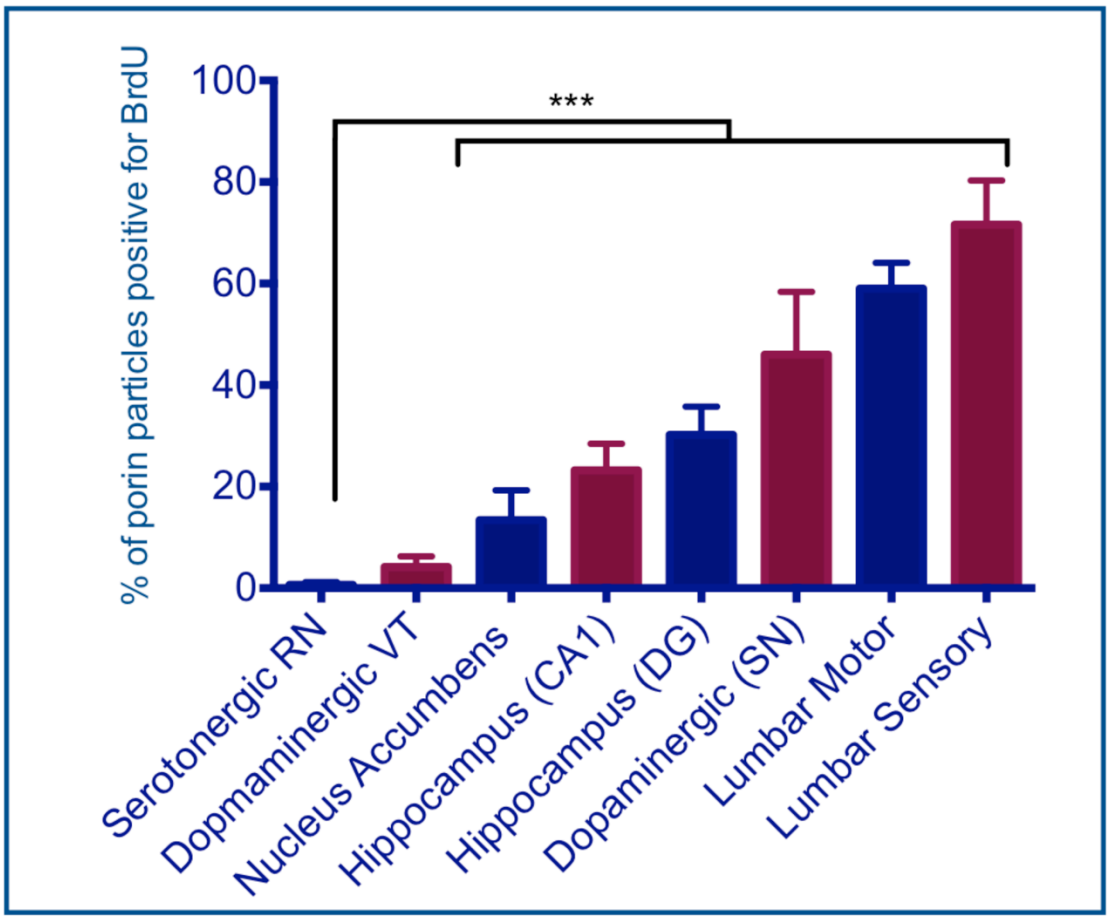

Figure 7: When averaged over 5 animals, a few regions emerge as having statistically more BrdU tagged biogenesis compared with control regions. nucleus accumbens, hippocampus, substantia nigra, motor neurones, sensory neurones. showed significantly higher mitochondrial biogenesis than serotonergic neurones of the raphe nuclei; tested by one –way ANOVA, p=0.00045

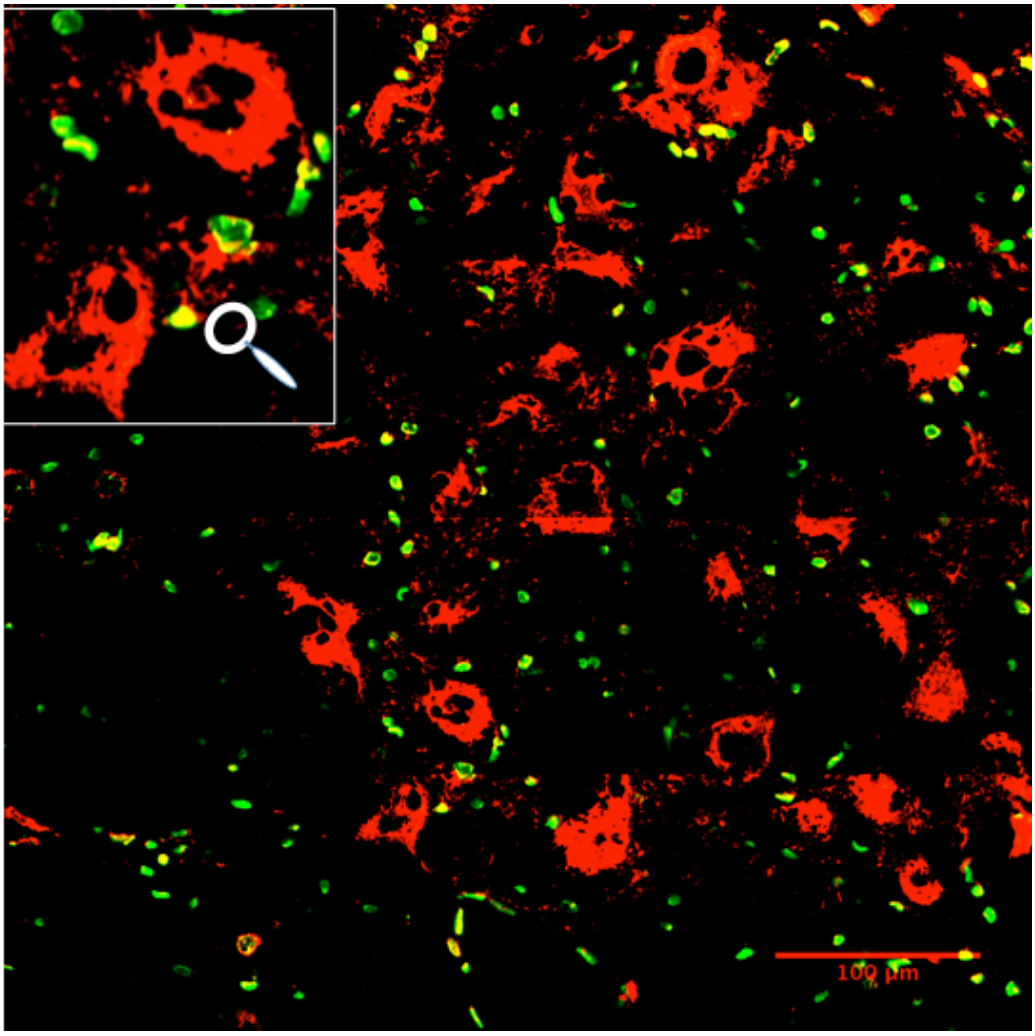

Figure 8: Optical section through a scanned image of Raphe Nuclei. β III-tubulin stained in red and BrdU in green. The inlaid image shows a high magnification depicting very few small BrdU labelled particles in the cytoplasm of cells. Bigger green structures mark proliferating nuclei.

Due to the highly compact nature of retinal cell layers and cellular anatomy, the mitochondrial biogenesis analysis using the previously described method was not possible in this tissue. However, by qualitative observation we believe that the level of mtDNA replication in the retinal ganglion cell is high (Figure 5A).

Discussion

Studies of mitochondrial biology in have shown that mitochondrial activities go beyond bioenergetics. A picture emerges in which mitochondrial biogenesis, mitophagy, migration, and morphogenesis are crucial for brain function. Understanding of these new aspects of mitochondrial function will provide insights into brain development and neurological disease, and enable discovery and development of new strategies for treatment.

Our observation that the dopaminergic niches show high levels of mitochondrial DNA biogenesis is is particularly important from the perspective of understanding mitochondrial dysfunction in Parkinson's disease. Parkinson's disease (PD) is a chronic neurodegenerative movement disorder characterized by the progressive and massive loss of dopaminergic neurons by neuronal apoptosis in the substantia nigra pars compacta and depletion of dopamine in the striatum, which lead to pathological and clinical abnormalities. Cellular processes including oxidative stress, mitochondrial dysfunction, and accumulation of α-synuclein aggregates are considered to contribute to the pathogenesis of Parkinson's disease.

Accumulation of mitochondrial DNA deletions is observed especially in dopaminergic neurons of the substantia nigra during ageing and even more in Parkinson's disease (Bender et al., 2006; Kraytsberg et al., 2006). The resulting mitochondrial dysfunction is suspected to play an important role in

neurodegeneration. Recently it has been shown that catecholamine metabolism drives the generation and accumulation of these mitochondrial DNA mutations (Neuhaus et al., 2014). Dopamine treatment of terminally differentiated neuroblastoma cells, as well as stimulation of dopamine turnover in mice over-expressing monoamine oxidase B, both induce multiple mitochondrial DNA deletions. These mechanisms identify catecholamine metabolism as the driving force behind mitochondrial DNA deletions, probably being an important factor in the ageing-associated degeneration of dopaminergic neurons.

Mitochondrial dysfunction in the form of reduced bioenergetic capacity, increased oxidative stress and reduced resistance to stress, is observed in several Parkinson's disease models. However, identification of the recessive genes implicated in Parkinson's disease has revealed a common pathway involving mitochondrial dynamics, transport, turnover and mitophagy. While the mtDNA mutations are shown to occur in both dopaminergic niches, it is evident that the substantia nigra neurones are more susceptible to neurodegeneration.

Our observation suggests that the dopaminergic SN cells maintain a higher mitochondrial biogenesis rate compared with dopaminergic VTa neurones (Figure 6). This may suggest that by the sheer replicative rate these neurones are more susceptible to accumulating clonal expansion of mutant deletions.

Or that, as suggested by Mosharov et al (Mosharov et al., 2009), the higher dopaminergic concentrations in the SN result in more mitochondrial damage, which needs to be compensated for, and hence the mitochondrial biogenesis rate is high. Unless the rate of biogenesis is very strongly coupled to the mitophagy pathway this system will remain susceptible to degeneration. In addition, it is conceivable that, with mitochondrial dysfunction induced by higher mitochondrial DNA deletions levels in substantia nigra pars compacta neurons, the Ca^{2+} buffering capacity of the organelles may well be impaired, thus worsening the situation. Alternatively, levels of mitochondrial DNA deletions and ensuing mitochondrial dysfunction may be similar in ventral tegmental area and substantia nigra pars compacta neurons, however, the high energy requirement of Ca^{2+} homeostasis in the latter, and the resulting reliance on mitochondria, could make them more vulnerable (Surmeier and Schumacker, 2013). There is recent evidence suggesting that PPAR-γ (peroxisome proliferator-activated receptor - gamma) agonist fenofibrate is effective in alleviating the effects of damage in the rodent MPTP model of Parkinson's disease (Barbiero et al., 2014). While PPAR-γ agonists are messy drugs with several molecular targets, a major target is the induction of mitochondrial biogenesis via the PPAR-γ receptor. This along with our observation of the substantia nigra cells having high mitochondrial biogenesis opens up a potential therapeutic avenue.

Leber's hereditary optic neuropathy is a maternally inherited blinding disease caused as a result of homoplasmic point mutations in complex I subunit genes

of mitochondrial DNA. It is characterized by incomplete penetrance, as only some mutation carriers become affected. There is recent evidence which supports increased mitochondrial biogenesis in carriers may overcome some of the pathogenic effect of mitochondrial DNA mutations (Giordano et al., 2014). We have observed that normally the retinal ganglion layer, which is susceptible to damage in LHON, shows high mitochondrial biogenesis.

Mitochondria in motor neurones are also observed to have high biogenesis signal. These neurones are susceptible to damage in the SOD1 mutation which leads to amyotrophic lateral sclerosis (ALS). This enzyme is an antioxidant in the matrix of mitochondria, which protects ROS induced damage to mitochondrial DNA, proteins and lipids. Recent evidence suggests that resveratrol is effective in reducing some of the damage in a SOD1 knockout model of ALS. Resveratrol protects neurones by increasing activation and expression of Sirtuin 1 (SIRT1) and AMPK in the spinal cord and inducing mitochondrial biogenesis (Mancuso et al., 2014)

In Alzheimer's disease, where a complicated pathology results in large scale degeneration, the hippocampus is known to be affected quite early on and strongly in the disease. In a recent study which highlighted the differences in gene expression amongst Alzheimer's affected brains, mild cognitive impairment brains and healthy brains, the mitochondrial genes were implicated strongly (Berchtold et al., 2014). Furthermore, mtDNA copy number is reduced and mitochondrial biogenesis is disrupted in the hippocampi (Rice

et al., 2014). This is corroborated in our observation that the hippocampus has a constitutively high level of mitochondrial biogenesis and we postulate that this may be reduced in affected brains.

Sensory neurones are affected in peripheral neuropathies such as diabetic neuropathy. Literature suggests that the pathology is manifested by an imbalance of mitochondrial lifecycle (Vincent et al., 2010). We also observe a high turnover rate of mitochondrial biogenesis in doral root ganglion sensory neurones.

The emerging theme is that niches of neurons which show constitutively high mitochondrial biogenesis have a susceptibility to degeneration which can be precipitated by a variety of external insults- genetic, inflammatory, energetic demands. The data represented in this study are the first visualization of the unique nature of the high turnover of mitochondrial DNA in certain neuronal populations. The niches identified can be targets for mitochondrial lifecycle modulating drugs in diseases in which the neurones degenerate. Furthermore, I have described an effective method in being able to evaluate changes in mitochondrial biogenesis rate using BrdU if indeed these therapeutic strategies need to be assessed at a cellular level.

The question about why certain populations of neurons degenerate in genetic forms of neurodegenerative diseases while all cells carry the mutations has long plagued neuroscientists. We speculate the rate of mitochondrial biogenesis and in turn the ‘dependence’ of the cell on mitochondrial function

may be one aspect of predicting which cells are susceptible to degenerative pathology as a consequence of mitochondrial dysfunction.

Chapter 6: Discussion

New method showing somatic mitochondrial nursery

The overall aim of this thesis was to profile the process of mitochondrial biogenesis in the mammalian nervous system. To quantify the percentage of mitochondrial undergoing active growth, I developed a method using mtDNA replication as a surrogate marker for mitochondrial biogenesis. In this study I showed that BrdU could be used as a marker for mitochondrial DNA replication and present a tool to study the life cycle of mitochondria in the mammalian CNS in vivo. I have described a precise method for conducting these studies. Furthermore, I have investigated the birth of new mitochondria in motor neurons in the spinal cord. This work is an important step towards understanding conditions under which the balance of mitochondrial biogenesis and mitophagy (Figure 1) is disturbed.

While previous studies have used BrdU to target mitochondrial DNA *in vitro* (Calkins et al., 2011; Calkins and Reddy, 2011b; Magnusson et al., 2003), this is the first reported use of BrdU and enhanced immunohistochemistry investigating mitochondrial DNA with spatial and temporal resolution *in vivo*. I found that with 6-hour exposure to a reasonable blood plasma concentration of BrdU, I can achieve clear labelling of replicating DNA in mitochondria and validate this methodology reproducibly *in vitro*. The methodology established here, is relevant for not just MS but also other neurological disorders in which

mitochondrial pathology manifests. It can also helps identify cellular niches in the CNS with high turnover of mitochondria.

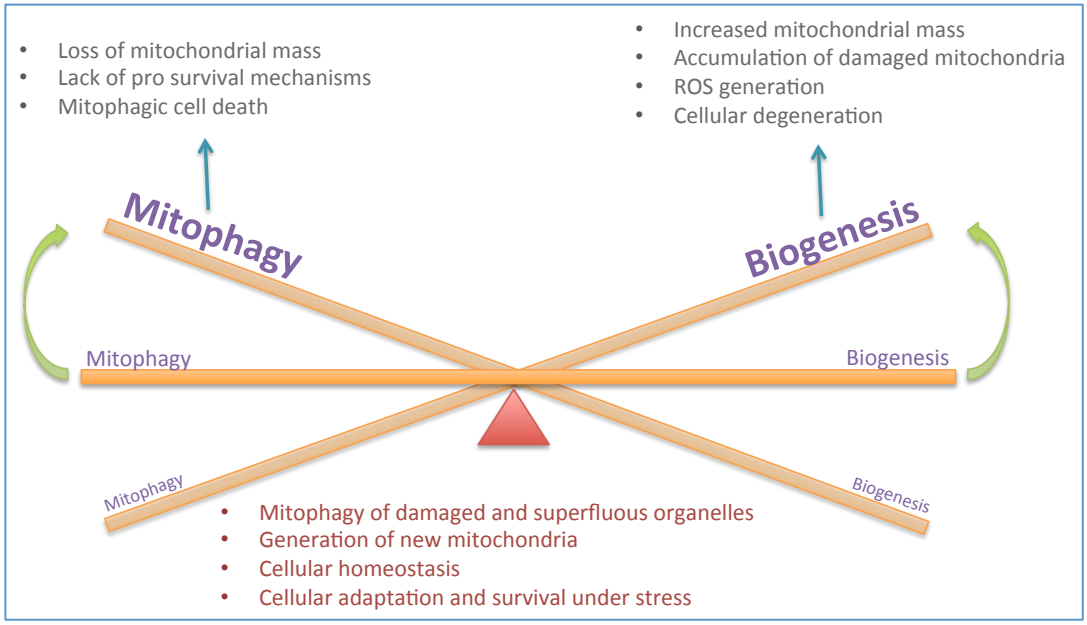

Figure 1: Overview of the balance of mitochondrial biogenesis and mitophagy, the modulation of which determines the mitochondrial content and turnover in a cell. The balance of both is what should be achieved for optimum health of the mitochondrial network. Future efforts are needed to identify the signalling pathways which can be modulated to maintain this balance and also the changes that occur under pathological conditions.

From our study of BrdU incorporation into motor neurons of the spinal cord, we observed that a distinct pattern emerged. We interpret these time dependent changes in new mitochondrial DNA as representative of the biogenesis of mitochondria in these cells. We observed an increase in BrdU labelling in the first four hours after injection of BrdU, which we suggest is the period over which incorporation of BrdU into mitochondrial DNA takes place. Following which, we observed a progressive decrease in labelling to 9.5 hours post injection of BrdU (the longest period examined in this experiment). These data suggest that the newly formed DNA has begun to be distributed into the rest of the mitochondrial network outside of the cell body. Accordingly, when

some of the sciatic nerve sections were labeled for BrdU and porin, the BrdU label appeared only in the sections from animals, which were sacrificed 9.5 hours after the BrdU injections. We interpret this to indicate newly formed mitochondrial DNA getting distributed through the network. We did not see new mitochondrial DNA in the sciatic nerve in the early time points of the study. This suggests that in these spinal neurons the mitochondria are only being formed in cell bodies; contrary to what has been observed in vitro (Amiri and Hollenbeck, 2008)

Over the longer time period (21 days), we observed that the amount of BrdU labelled mitochondrial DNA in the cell body reduced over time up to five days, and then seemed to go up again at 11 days (but not statistically significant). If correct, this finding may suggest that this newly formed mitochondrial DNA has been moved away from the cell bodies, as part of the process by which new mitochondria are supplied to distal parts of cells. Further investigation is needed to confirm whether these mitochondria return to cell body for autophagy in due course of time. The duration of the mitochondrial life cycle is likely to be different in different types of cells and with the BrdU tag we now have a method to study this temporally. There is a possibility that DNA containing BrdU is targeted for autophagy earlier than the wild type DNA. Since we did not observe any obvious cellular death or atrophy at any of the time points, we assume that at the least, BrdU containing mitochondria did not result in cell death.

The process of mitochondrial biosynthesis is highly interlinked with mitochondrial fission, and therefore BrdU-labelled mitochondrial DNA content reflects both mitochondrial biosynthesis and fission. Mitochondrial DNA replication occurs in existing organelles largely within the cell soma. After DNA replication, the organelle will undergo Drp1 mediated fission to produce two daughter mitochondria. Both of these daughter mitochondria are expected to carry the BrdU-labelled DNA. Without a fission event to separate the mitochondria, BrdU-labelling would occur as a single punctum with high intensity. Under conditions of enhanced Drp1 activation and normal mtDNA synthesis, the number of BrdU puncta would be increased.

MtDNA synthesis is known to occur largely in the cell body but there is evidence that it occurs in neurites as well (Amiri and Hollenbeck, 2008). Presented data showed that the majority of BrdU-labeled mitochondria occur within or very near the cell body, supporting the notion that mitochondrial biogenesis is largely dependent on factors within the soma. When healthy, newly formed mitochondria are available for anterograde transport to the distal regions of the neuron, where they will supply the necessary ATP to satisfy the high-energy demands of synaptic activity. However, as in this study, in diseased neurones or in neurons exposed to toxins, mitochondria are excessively fragmented and produce large numbers of small, defective mitochondria. These defective mitochondria stay mostly in the soma and do not (or perhaps are unable to transport) to distal regions of the neurons, hence depriving nerve terminals of ATP. This ATP deprivation may ultimately

decrease synaptic activities and increase synaptic degeneration. The presence of the somatic nursery could also present a peculiar phenomenon in diseases of the spinal cord. The motor neurone cell bodies are contained in the grey matter of the spinal cord. If indeed the 'mother' mitochondria are present in the soma, damage to this pool of mitochondria can have devastating effects on the population of mitochondria in the cell. This process could be postulated as a towards clonal expansion of damaged mtDNA.

In summary, BrdU-labelling of mtDNA synthesis allowed us to assess newly synthesized mtDNA in the cell body neurones. Previous studies have established clonal expansion of mutant mtDNA as a feature of MS (Campbell et al., 2011). While high oxidative stress, hypoxia, inflammation and high levels of cytokines might be present in different parts of the brain and CNS, the proximity of a tissue insult to the somatic mitochondrial nursery could render a neurone vulnerable to accumulating mitochondrial DNA damage. It maybe postulated then that protecting the somatic pool of mitochondria from damage in the long run more effective in therapy.

Hot-spots of neuronal mitochondrial biogenesis

Several neuronal niches have been identified in this thesis, which maintain a constitutively high rate of mitochondrial biogenesis. As such, this presents an opportunity to identify molecular players, which modulate and maintain this high level of mitochondrial biogenesis. For instance, in the future, a combination of laser dissection microscopy and microarray technology can be used to find genes that help maintain a high rate of mitochondrial biogenesis.

These then become targets for modulation from the perspective of not just therapeutic intervention but also understanding the signalling pathways.

The high-biogenesis neuronal niches identified in this study were found to be tightly associated with neurodegenerative disease. This presents an opportunity to understand why these cells maintain this high rate of mitochondrial biogenesis. Whether it is simply related to the size of neurites, or also to other constraints to metabolism.

Reactivity to bioenergetic changes

Previously, in cultured muscle cells it was found that an increase in electrical activity could quickly initial mitochondrial biogenesis (Ding et al., 2012). We described a similar observation in motor neurones and sensory neurones. It has been observed that following electrical activity; mitochondria are trafficked to the peripheral regions of the neurone (Sajic et al., 2013). Also, the phenomenon of transmitophagy has been observed in retinal neurones, where mitochondria move from neurones to astrocytes for degradation (Davis et al., 2014). Together, these three observations present a picture that the mitochondrial network in long neurones may be a combination of an assembly line and a recycling unit, where mitochondria are made in the cell body, trafficked down the axons to distal parts and then damaged mitochondria do not return to the cell body for degradation but rather are degraded by locally present astrocytes.

Transcriptional modulation of mitochondrial biogenesis

PGC-1α is now increasingly being recognized as an important therapeutic target for neurodegenerative disorders. As discussed above, PGC-1α expression and/or function is impaired in many major neurodegenerative diseases; therefore, pharmacologic/transcriptional activation of the PGC-1α pathway is expected to have neuroprotective effects. Recently, Da Cruz et al. (2012) showed that increasing PGC-1α activity in muscle in a transgenic mouse model of ALS caused by a mutation in SOD1 is able to sustain muscle function throughout the disease course, although survival was not extended (Da Cruz et al., 2012). Another potential approach to activating the PGC-1α pathway, and thereby improving mitochondrial function, is via activation of PPARs. The PPARs are a subfamily of nuclear receptors that are ligand-modulated transcription factors that regulate gene expression programmes of metabolic pathways. PPAR agonists increase oxidative phosphorylation capacity in mouse and human cells and enhance mitochondrial biogenesis. Both pioglitazone and rosiglitazone, which are PPAR-γ agonists, were shown to exert beneficial effects in *in vitro* and *in vivo* models of PD and AD (Chaturvedi and Beal, 2008).

Sirtuins (silent information regulators, SIRT) are members of the NAD+-dependent histone deacetylase family of proteins in yeast, and its homologs in mice and humans participate in a variety of cellular processes, including mitochondrial functions, cellular metabolism, energy metabolism, gluconeogenesis, cell survival, and aging. Although the role of sirtuins in

promoting lifespan extension in non-mammalian organisms has been contested recently, there is strong evidence to suggest that sirtuins are an integrative link between metabolic control and transcriptional regulation, and the role of SIRT1 in activating the master regulator PGC-1α is largely accepted. Increased intracellular NAD+ concentrations activate SIRT1 in brain after caloric restriction resulting in a reduction in amyloid pathology in a mouse model of AD; increased SIRT1 protects against hippocampal degeneration in a mouse model of AD, and direct injection of SIRT1 lentivirus in the hippocampus of AD transgenic mice produces significant neuroprotection (Chaturvedi and Beal, 2008). SIRT1 activation by resveratrol increases the survival of motor neurons in transgenic ALS mice and reduces learning impairments and neurodegeneration in AD mouse models, by decreasing the acetylation of the SIRT1 substrates PGC-1α and p53 (Song et al., 2014). Overexpression of SIRT1 improves motor function and reduces brain atrophy, in transgenic mouse models of HD (Jiang et al., 2012a).

AMP-activated protein kinase (AMPK) is a Ser/Thr kinase that is activated as a consequence of increased AMP levels, reflecting low ATP availability and low energy reserve. AMPK activation results in a cascade of phosphorylation-dependent adaptive modifications of several factors, including PGC-1α, to switch on the catabolic pathways (such as fatty acid oxidation and mitochondrial respiratory chain activity) to produce ATP, while simultaneously shutting down energy-consuming anabolic processes. 5-Aminoimidazole-4-carboxamide ribonucleoside (AICAR) is a compound that has been used to activate PGC-1α through AMPK. It does so by generating inosine

monophosphate, which acts as an AMPK agonist by mimicking AMP. AICAR was shown to inhibit tau phosphorylation in an in vitro model of AD; however, AMPK activation by AICAR was shown to produce adverse effects in R6/2 HD mice in that it enhanced brain atrophy, neuronal loss, and aggregate formation in the striatum. Recently, it was shown that AMPK activity is increased in spinal cord cultures expressing mutant SOD1, as well as in spinal cord lysates from mutant SOD1 mice (Lim et al., 2012b). Reducing AMPK activity either pharmacologically or genetically prevented mutant SOD1-induced motor neuron death in vitro (Lim et al., 2012b). Metformin is another AMPK activator and known inducer of mitochondrial biogenesis was shown to be effective in male HD transgenic mice in that it prolonged survival and decreased hind limb clasping (Ma et al., 2007).

ROS damage to mitochondria is well known in all of the major neurodegenerative disorders; therefore, therapies targeting the Nrf2/antioxidant response element (ARE) pathway are of particular interest. Neuronal cultures derived from Nrf2 knockout mice show increased susceptibility to oxidative damage, as well as damage produced by mitochondrial electron transport gene complex inhibitors such as MPP+ and rotenone. Nrf2-deficient mice show increased susceptibility to the mitochondrial toxins MPTP and 3-NP. The synthetic triterpenoid CDDO methylamide (CDDO-MA), which is a potent activator of the Nrf2/ARE signalling pathway was tested (Yang et al., 2009). CDDO-MA produced marked protection in the 3-NP rat model and both the acute and chronic MPTP mouse models. CDDO-MA exerted significant protection against

tertbutylhydroperoxide-induced ROS in vitro. It increased the expression of genes involved in mitochondrial biogenesis, as well as those involved in glutathione synthesis and in the expression of antioxidant enzymes. Triterpenoids also protect in transgenic mouse models of HD (Escartin and Brouillet, 2010; Stack et al., 2010).

The beneficial effects of resveratrol and SIRT1 that were observed in several mouse models of neurodegenerative diseases cannot be overlooked, and the quest for small-molecule activators of sirtuins with potential neuroprotective effects should continue along with other avenues of initiating mitochondrial biogenesis. The collective observations and findings described in this thesis present an opportunity to identify molecular targets which modulate mitochondrial biogenesis, assess the level of mitochondrial biogenesis under different conditions and explore the possibility of protecting certain neuronal niches against damage by mitochondrial life cycle changes.

Appendix

Materials

1. Phosphate Buffered Saline (PBS)

0.1 M PBS was prepared either in a stock solution of 10 times concentration and then diluted 1:10 with deionised water just before use or made at isotonic concentration just before use. All salts were measured on a chemical balance, and then dissolved in deionised water using a magnetic stirrer. The following table describes the concentration of different components used.

Salt	**Molarity (mM)**	**g/l for 1x solution**	**g/l for 10x solution**
NaCl	137	8.01	80.1
KCl	2.7	0.2	2
$Na_2HPO_4.2H_2O$	10	1.78	17.8
KH_2HPO_4	2	0.27	2.7
pH 7.4			

For convenience, small quantities of PBS were made by dissolving PBS tablets (Sigma Aldrich) in deionised water – 1 tablet per 200 ml.

2. Phosphate Buffer (PB)

0.1 M Phosphate buffer was made by dissolving 3.1 g of $NaH_2PO_4.H_2O$ and 10.9 g of Na_2HPO_4 in 1 l of deionised water.

3. Saline for Injection

For small quantities packaged sterile saline was used from plastic vials. For experiments requiring a large amount saline was prepared by dissolving 0.9 g of NaCl in 1 l of deionised water and then autoclaving the solution to render it sterile.

4. 4% Parafomaldehyde (PFA)

For 1 l of 4% PFA, 600 ml of deionised water was placed in a glass beaker on a stir plate in a ventilated hood along with a temperature probe. The water was heated to about 50°C and then 40 g of paraformaldehyde powder was added. The mixture was heated and stirred up to 60 °C. The pH was slowly raised by added 1 N NaOH solution drop-wise with continuous stirring. Once the solution cleared, the mixture was cooled and filtered. This filtered solution was mixed with 300 ml of deionised water into which the full salt composition of 1 l PBS (either from salts as described above or 5 PBS tablets) had already been dissolved. The full mixture was then checked for pH and the volume made up to 1 l in a volumetric flask. This solution was made up fresh for all perfusions or split in aliquots of 50 ml and stored at -80°C for fixing slides before immunohistochemistry.

5. Sucrose solution for cryoprotection

Sucrose was dissolved in PB in increasing concentrations to make solutions for graded cryoprotection of post fixed neural tissue. 10, 20 or 30 g of sucrose was dissolved in PB and made up to a volume of 100 ml.

6. Triton X solution for immunohistochemistry

For permeabilization of tissue 0.3% Triton x-100 was prepared by dissolving 300 μl of Triton X-100 (Sigma Aldrich) in 100 ml of PBS by gentle stirring on a magnetic stirrer or roller.

7. Tween 80 solution for immunohistochemistry

0.3% Tween solution was prepared by dissolving 300 μl of Tween 80 (Sigma Aldrich) in 100 ml of PBS by gentle stirring on a magnetic stirrer or roller.

8. Blocking Buffer

Blocking buffer was prepared by gently mixing a secondary antibody matched animal sera in 5% concentration. For instance 1 ml of goat serum made up to a volume of 20 ml using PBS, stirred gently. Where two different sera were required the quantity of each was halved to make up a total of 5% volume in the solution. All sera were purchased either from Vector Labs or Sigma

Method for detecting mitochondrial biogenesis

Mitochondrial biogenesis was analysed using 3D confocal images of sections from rodent tissue stained for detecting BrdU and VDAC-1 as described. In experiments described in chapters 3, 4, and 5, the percentage of VDAC-1 positive particles that also showed BrdU staining was used as a measure of

mitochondrial biogenesis. Images were acquired using similar imaging parameters and individual neurones of interest were scored for mitochondrial biogenesis using particle analysis. Neurones presented mitochondrial particles with small BrdU staining within those particles as seen in the series of images shown in Figure 1. These images represent one single motor neuron from the ventral horn of spinal cord. VDAC-1 signal is seen in red, the BrdU signal is seen in and colocolization is digitally visualized in yellow. The series of images is of a 3D reconstruction of the neurones made from 1 μm thick optical sections acquired in two colour channels. Each consecutive image from A to J is rotated 40° from the previous image in the series.

Analysis was performed on individual spectral channels. First the neuron was identified manually by defining a region of interest as shown in Image 1 A. A fluorescence intensity threshold was set manually as shown in Image 2A and 2B which collected only positive signal and not the background signal. This threshold was maintained for all images. Then the Image J plugin, 3D particle count, was used to count the number of particles across the stack of optical sections (Image 2C- Green, Image 2D- Red). These numbers were then used to calculate the extent of mitochondrial biogenesis. In this particular case the signal is (12/18) x 100 – 66.67%.

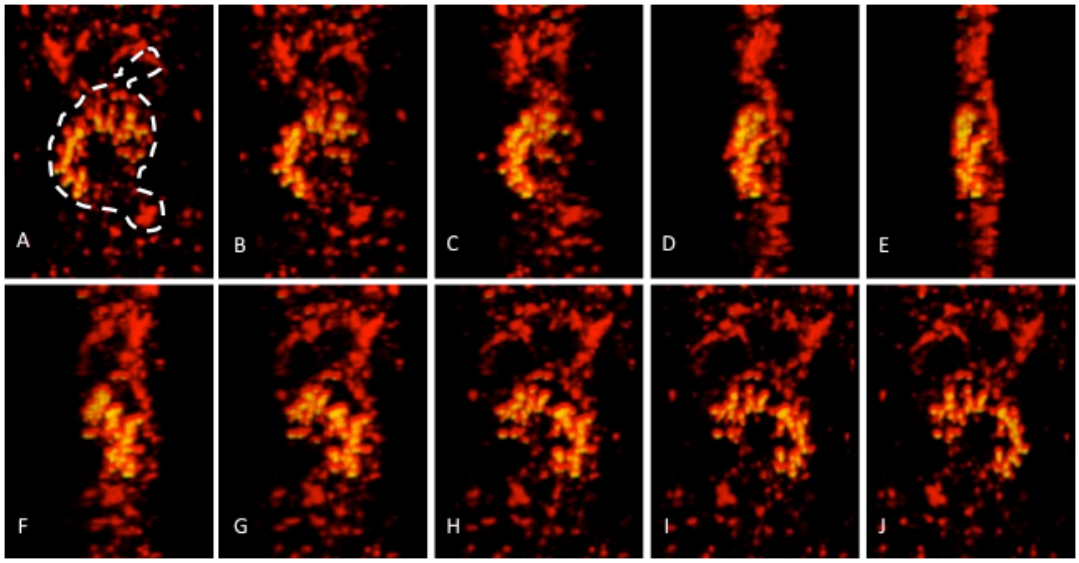

Figure 1: 3D rotation in series of one motor neurone in a spinal cord section from mouse. The section was labelled for VDAC-1 (red) and BrdU (green) and colocalization is seen in yellow. The white dashed line in panel A is a representation of how a cell body was identified for analysis.

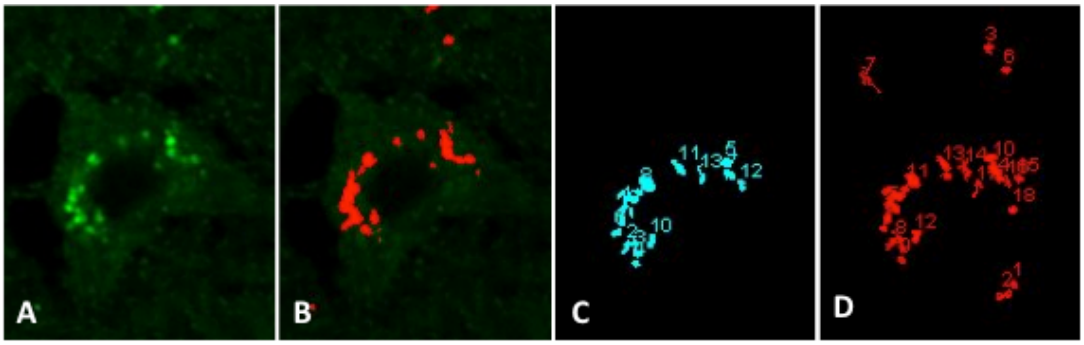

Figure 2: The Image J plugin 'particle count' generates images as shown in this panel. Panel A is the raw pseudocolored image, which then gets thresholded for intensity (panel B). The particles are counted in 3D and a count is generated. Panel C is the count for the BrdU signal and panel D shows count for the VDAC-1 signal for the same motor neurone cell body.

Bibliography

Amiri, M., and Hollenbeck, P.J. (2008). Mitochondrial biogenesis in the axons of vertebrate peripheral neurons. Dev Neurobiol *68*, 1348-1361.

Ashley, N., Harris, D., and Poulton, J. (2005). Detection of mitochondrial DNA depletion in living human cells using PicoGreen staining. Experimental cell research *303*, 432-446.

Barbiero, J.K., Santiago, R., Tonin, F.S., Boschen, S., da Silva, L.M., de Paula Werner, M.F., da Cunha, C., Lima, M.M., and Vital, M.A. (2014). PPAR-alpha agonist fenofibrate protects against the damaging effects of MPTP in a rat model of Parkinson's disease. Progress in neuro-psychopharmacology & biological psychiatry *53C*, 35-44.

Beal, M.F. (2005). Mitochondria take center stage in aging and neurodegeneration. Ann Neurol *58*, 495-505.

Bender, A., Krishnan, K.J., Morris, C.M., Taylor, G.A., Reeve, A.K., Perry, R.H., Jaros, E., Hersheson, J.S., Betts, J., Klopstock, T.*, et al.* (2006). High levels of mitochondrial DNA deletions in substantia nigra neurons in aging and Parkinson disease. Nature genetics *38*, 515-517.

Berchtold, N.C., Sabbagh, M.N., Beach, T.G., Kim, R.C., Cribbs, D.H., and Cotman, C.W. (2014). Brain gene expression patterns differentiate mild cognitive impairment from normal aged and Alzheimer's disease. Neurobiology of aging. Volume 35, Issue 9, Pages 1961–1972

Berthold, C.H., Fabricius, C., Rydmark, M., and Andersen, B. (1993). Axoplasmic organelles at nodes of Ranvier. I. Occurrence and distribution in

large myelinated spinal root axons of the adult cat. Journal of neurocytology *22*, 925-940.

Bindokas, V.P., Lee, C.C., Colmers, W.F., and Miller, R.J. (1998). Changes in mitochondrial function resulting from synaptic activity in the rat hippocampal slice. The Journal of neuroscience : the official journal of the Society for Neuroscience *18*, 4570-4587.

Bjartmar, C., and Trapp, B.D. (2003). Axonal degeneration and progressive neurologic disability in multiple sclerosis. Neurotoxicity research *5*, 157-164.

Bogenhagen, D.F. (2009). Biochemical isolation of mtDNA nucleoids from animal cells. Methods in Molecular Biology (Clifton, NJ) *554*, 3-14.

Bristow, E.A., Griffiths, P.G., Andrews, R.M., Johnson, M.A., and Turnbull, D.M. (2002). The distribution of mitochondrial activity in relation to optic nerve structure. Archives of ophthalmology *120*, 791-796.

Calkins, M., and Reddy, P. (2011a). Assessment of newly synthesized mitochondrial DNA using BrdU labeling in primary neurons from Alzheimer's disease mice: Implications for impaired mitochondrial biogenesis and synaptic damage. Biochimica et biophysica acta *1812*, 1182-1191.

Calkins, M.J., Manczak, M., Mao, P., Shirendeb, U., and Reddy, P.H. (2011b). Impaired mitochondrial biogenesis, defective axonal transport of mitochondria, abnormal mitochondrial dynamics and synaptic degeneration in a mouse model of Alzheimer's disease. Human molecular genetics *20*, 4515-4529.

Campbell, G.R., and Mahad, D.J. (2011). Mitochondria as crucial players in demyelinated axons: lessons from neuropathology and experimental demyelination. Autoimmune diseases *2011*, 262847.

Campbell, G.R., Ziabreva, I., Reeve, A.K., Krishnan, K.J., Reynolds, R., Howell, O., Lassmann, H., Turnbull, D.M., and Mahad, D.J. (2011). Mitochondrial DNA deletions and neurodegeneration in multiple sclerosis. Annals of neurology *69*, 481-492.

Chan, D.C. (2006). Mitochondrial fusion and fission in mammals. Annual review of cell and developmental biology *22*, 79-99.

Chang, D.T., and Reynolds, I.J. (2006). Mitochondrial trafficking and morphology in healthy and injured neurons. Progress in neurobiology *80*, 241-268.

Chaturvedi, R.K., Adhihetty, P., Shukla, S., Hennessy, T., Calingasan, N., Yang, L., Starkov, A., Kiaei, M., Cannella, M., Sassone, J.*, et al.* (2009). Impaired PGC-1alpha function in muscle in Huntington's disease. Human molecular genetics *18*, 3048-3065.

Chaturvedi, R.K., and Beal, M.F. (2008). Mitochondrial approaches for neuroprotection. Annals of the New York Academy of Sciences *1147*, 395-412.

Chen, H., McCaffery, J.M., and Chan, D.C. (2007a). Mitochondrial fusion protects against neurodegeneration in the cerebellum. Cell *130*, 548-562.

Chen, S., Zhang, Y., Wang, Y., Li, W., Huang, S., Chu, X., Wang, L., Zhang, M., and Liu, Z. (2007b). A novel OPA1 mutation responsible for autosomal dominant optic atrophy with high frequency hearing loss in a Chinese family. American Journal of Ophthalmology *143*, 186-188.

Chen, Y., Liu, Y., and Dorn, G.W., 2nd (2011). Mitochondrial fusion is essential for organelle function and cardiac homeostasis. Circulation research *109*, 1327-1331.

Chen, Z.R., Xiong, Y., Wang, S.B., and Dong, Y. (1991). Inhibition of mitochondrial respiratory function by an organic solvent extractable component from an extract of burn eschar. Burns : journal of the International Society for Burn Injuries *17*, 282-287.

Clark, J., Reddy, S., Zheng, K., Betensky, R.A., and Simon, D.K. (2011). Association of PGC-1alpha polymorphisms with age of onset and risk of Parkinson's disease. BMC medical genetics *12*, 69.

Corral-Debrinski, M., Horton, T., Lott, M.T., Shoffner, J.M., Beal, M.F., and Wallace, D.C. (1992). Mitochondrial DNA deletions in human brain: regional variability and increase with advanced age. Nature genetics *2*, 324-329.

Corton, J.C., Apte, U., Anderson, S.P., Limaye, P., Yoon, L., Latendresse, J., Dunn, C., Everitt, J.I., Voss, K.A., Swanson, C.*, et al.* (2004). Mimetics of Caloric Restriction Include Agonists of Lipid-activated Nuclear Receptors. Journal of Biological Chemistry *279*, 46204-46212.

Courtney, M.J., Lambert, J.J., and Nicholls, D.G. (1990). Glutamate-receptor-mediated regulation of the cytoplasmic free calcium level in cultured cerebellar granule cells. Biochemical Society transactions *18*, 420-421.

Cui, L., Jeong, H., Borovecki, F., Parkhurst, C.N., Tanese, N., and Krainc, D. (2006). Transcriptional repression of PGC-1alpha by mutant huntingtin leads to mitochondrial dysfunction and neurodegeneration. Cell *127*, 59-69.

Da Cruz, S., Parone, P.A., Lopes, V.S., Lillo, C., McAlonis-Downes, M., Lee, S.K., Vetto, A.P., Petrosyan, S., Marsala, M., Murphy, A.N.*, et al.* (2012). Elevated PGC-1alpha activity sustains mitochondrial biogenesis and muscle function without extending survival in a mouse model of inherited ALS. Cell Metab *15*, 778-786.

Dai, S.H., Chen, T., Wang, Y.H., Zhu, J., Luo, P., Rao, W., Yang, Y.F., Fei, Z., and Jiang, X.F. (2014). Sirt3 protects cortical neurons against oxidative stress via regulating mitochondrial Ca2+ and mitochondrial biogenesis. International journal of molecular sciences *15*, 14591-14609.

Davies, A.L., Desai, R.A., Bloomfield, P.S., McIntosh, P.R., Chapple, K.J., Linington, C., Fairless, R., Diem, R., Kasti, M., Murphy, M.P.*, et al.* (2013). Neurological deficits caused by tissue hypoxia in neuroinflammatory disease. Annals of neurology *74*, 815-825.

Davis, A.F., and Clayton, D.A. (1996). In situ localization of mitochondrial DNA replication in intact mammalian cells. The Journal of cell biology *135*, 883-893.

Davis, C.H., Kim, K.Y., Bushong, E.A., Mills, E.A., Boassa, D., Shih, T., Kinebuchi, M., Phan, S., Zhou, Y., Bihlmeyer, N.A.*, et al.* (2014). Transcellular degradation of axonal mitochondria. Proceedings of the National Academy of Sciences of the United States of America *111*, 9633-9638.

Davis, R.E., and Williams, M. (2012). Mitochondrial function and dysfunction: an update. The Journal of pharmacology and experimental therapeutics *342*, 598-607.

Dennis, E.A., and Kennedy, E.P. (1972). Intracellular sites of lipid synthesis and the biogenesis of mitochondria. Journal of lipid research *13*, 263-267.

Desai, R. (2013). The role of hypoxia in neuroinflammatory disease. In Institute of Neurology (London: University College London), pp. 356.

DiMauro, S., and Schon, E.A. (2003). Mitochondrial respiratory-chain diseases. The New England Journal of Medicine *348*, 2656-2668.

Ding, S., Riddoch-Contreras, J., Abramov, A.Y., Qi, Z., and Duchen, M.R. (2012). Mild stress of caffeine increased mtDNA content in skeletal muscle cells: the interplay between Ca2+ transients and nitric oxide. Journal of muscle research and cell motility *33*, 327-337.

Dubinsky, R.M., Yarchoan, R., Dalakas, M., and Broder, S. (1989). Reversible axonal neuropathy from the treatment of AIDS and related disorders with 2',3'-dideoxycytidine (ddC). Muscle & nerve *12*, 856-860.

Duque, A., and Rakic, P. (2011). Different effects of bromodeoxyuridine and [3H]thymidine incorporation into DNA on cell proliferation, position, and fate. The Journal of neuroscience : the official journal of the Society for Neuroscience *31*, 15205-15217.

Dutta, R., McDonough, J., Yin, X., Peterson, J., Chang, A., Torres, T., Gudz, T., Macklin, W.B., Lewis, D.A., Fox, R.J.*, et al.* (2006). Mitochondrial dysfunction as a cause of axonal degeneration in multiple sclerosis patients. Annals of neurology *59*, 478-489.

Dutta, R., and Trapp, B.D. (2006). [Pathology and definition of multiple sclerosis]. La Revue du praticien *56*, 1293-1298.

Dutta, R., and Trapp, B.D. (2007). Pathogenesis of axonal and neuronal damage in multiple sclerosis. Neurology *68*, S22-31; discussion S43-54.

Escartin, C., and Brouillet, E. (2010). The Nrf2 pathway as a potential therapeutic target for Huntington disease A commentary on "Triterpenoids CDDO-ethyl amide and CDDO-trifluoroethyl amide improve the behavioral phenotype and brain pathology in a transgenic mouse model of Huntington disease". Free radical biology & medicine *49*, 144-146.

Falkenberg, M., Gaspari, M., Rantanen, A., Trifunovic, A., Larsson, N.G., and Gustafsson, C.M. (2002). Mitochondrial transcription factors B1 and B2 activate transcription of human mtDNA. Nature genetics *31*, 289-294.

Falkenberg, M., Larsson, N.G., and Gustafsson, C.M. (2007). DNA replication and transcription in mammalian mitochondria. Annual review of biochemistry *76*, 679-699.

Fox, T.D. (2012). Mitochondrial Protein Synthesis, Import, and Assembly. Genetics *192*, 1203-1234.

Giordano, C., Iommarini, L., Giordano, L., Maresca, A., Pisano, A., Valentino, M.L., Caporali, L., Liguori, R., Deceglie, S., Roberti, M.*, et al.* (2014). Efficient mitochondrial biogenesis drives incomplete penetrance in Leber's hereditary optic neuropathy. Brain : a journal of neurology *137*, 335-353.

Goldstein, A., Bhatia, P., and Vento, J.M. (2012). Update on nuclear mitochondrial genes and neurologic disorders. Seminars in pediatric neurology *19*, 181-193.

Gottlieb, R.A., Mentzer, R.M., and Linton, P.-J. (2011). Impaired mitophagy at the heart of injury. Autophagy *7*, 1573-1574.

Gratzner, H.G. (1982). Monoclonal antibody to 5-bromo- and 5-iododeoxyuridine: A new reagent for detection of DNA replication. Science *218*, 474-475.

Handschin, C., and Spiegelman, B.M. (2006). Peroxisome proliferator-activated receptor gamma coactivator 1 coactivators, energy homeostasis, and metabolism. Endocrine reviews *27*, 728-735.

Hermann, G.J., and Shaw, J.M. (1998). Mitochondrial dynamics in yeast. Annual review of cell and developmental biology *14*, 265-303.

Hernandez, G., Thornton, C., Stotland, A., Lui, D., Sin, J., Ramil, J., Magee, N., Andres, A., Quarato, G., Carreira, R.S.*, et al.* (2013). MitoTimer: a novel tool for monitoring mitochondrial turnover. Autophagy *9*, 1852-1861.

Herrero-Mendez, A., Almeida, A., Fernandez, E., Maestre, C., Moncada, S., and Bolanos, J.P. (2009). The bioenergetic and antioxidant status of neurons is controlled by continuous degradation of a key glycolytic enzyme by APC/C-Cdh1. Nature cell biology *11*, 747-752.

Hollenbeck, P.J., and Saxton, W.M. (2005). The axonal transport of mitochondria. Journal of cell science *118*, 5411-5419.

Holloszy, J.O. (2011). Regulation of mitochondrial biogenesis and GLUT4 expression by exercise. Comprehensive Physiology *1*, 921-940.

Hoppins, S., Lackner, L., and Nunnari, J. (2007). The machines that divide and fuse mitochondria. Annual review of biochemistry *76*, 751-780.

Issekutz, T.B., Chin, G.W., and Hay, J.B. (1981). Lymphocyte traffic through chronic inflammatory lesions: differential migration versus differential retention. Clinical and experimental immunology *45*, 604-614.

Jazwinski, S.M. (2013). The retrograde response: When mitochondrial quality control is not enough. Biochimica et Biophysica Acta (BBA) - Molecular Cell Research *1833*, 400-409.

Jeong, J.K., Moon, M.H., Lee, Y.J., Seol, J.W., and Park, S.Y. (2013). Autophagy induced by the class III histone deacetylase Sirt1 prevents prion peptide neurotoxicity. Neurobiology of aging *34*, 146-156.

Jiang, M., Wang, J., Fu, J., Du, L., Jeong, H., West, T., Xiang, L., Peng, Q., Hou, Z., Cai, H.*, et al.* (2012a). Neuroprotective role of Sirt1 in mammalian models of Huntington's disease through activation of multiple Sirt1 targets. Nature medicine *18*, 153-158.

Jiang, S., Wang, W., Miner, J., and Fromm, M. (2012b). Cross regulation of sirtuin 1, AMPK, and PPARgamma in conjugated linoleic acid treated adipocytes. PloS one *7*, e48874.

Johri, A., Calingasan, N.Y., Hennessey, T.M., Sharma, A., Yang, L., Wille, E., Chandra, A., and Beal, M.F. (2012). Pharmacologic activation of mitochondrial biogenesis exerts widespread beneficial effects in a transgenic mouse model of Huntington's disease. Human molecular genetics *21*, 1124-1137.

Jornayvaz, F.R., and Shulman, G.I. (2010). Regulation of mitochondrial biogenesis. Essays in biochemistry *47*, 69-84.

Kageyama, G.H., and Wong-Riley, M.T. (1982). Histochemical localization of cytochrome oxidase in the hippocampus: correlation with specific neuronal types and afferent pathways. Neuroscience *7*, 2337-2361.

Kalman, B. (2006). Role of mitochondria in multiple sclerosis. Curr Neurol Neurosci Rep *6*, 244-252.

Kalman, B., Li, S., Chatterjee, D., O'Connor, J., Voehl, M.R., Brown, M.D., and Alder, H. (1999). Large scale screening of the mitochondrial DNA reveals no pathogenic mutations but a haplotype associated with multiple sclerosis in Caucasians. Acta neurologica Scandinavica *99*, 16-25.

Kanki, T., Nakayama, H., Sasaki, N., Takio, K., Alam, T.I., Hamasaki, N., and Kang, D. (2004). Mitochondrial nucleoid and transcription factor A. Annals of the New York Academy of Sciences *1011*, 61-68.

Katsouri, L., Blondrath, K., and Sastre, M. (2012). Peroxisome proliferator-activated receptor-γ cofactors in neurodegeneration. IUBMB Life *64*, 958-964.

Kee, N., Sivalingam, S., Boonstra, R., and Wojtowicz, J.M. (2002). The utility of Ki-67 and BrdU as proliferative markers of adult neurogenesis. Journal of neuroscience methods *115*, 97-105.

Kelly, D.P., and Scarpulla, R.C. (2004). Transcriptional regulatory circuits controlling mitochondrial biogenesis and function. Genes & development *18*, 357-368.

Kim, D., Nguyen, M.D., Dobbin, M.M., Fischer, A., Sananbenesi, F., Rodgers, J.T., Delalle, I., Baur, J.A., Sui, G., Armour, S.M.*, et al.* (2007). SIRT1 deacetylase protects against neurodegeneration in models for Alzheimer's disease and amyotrophic lateral sclerosis. The EMBO journal *26*, 3169-3179.

Kraytsberg, Y., Kudryavtseva, E., McKee, A.C., Geula, C., Kowall, N.W., and Khrapko, K. (2006). Mitochondrial DNA deletions are abundant and cause functional impairment in aged human substantia nigra neurons. Nature genetics *38*, 518-520.

Larsson, N.G., Oldfors, A., Holme, E., and Clayton, D.A. (1994). Low levels of mitochondrial transcription factor A in mitochondrial DNA depletion. Biochemical and biophysical research communications *200*, 1374-1381.

Lavi, E., and Constantinescu, C.S. (2005). Experimental Models of Multiple Sclerosis (Springer).

Lentz, S.I., Edwards, J.L., Backus, C., McLean, L.L., Haines, K.M., and Feldman, E.L. (2010). Mitochondrial DNA (mtDNA) biogenesis: visualization and duel incorporation of BrdU and EdU into newly synthesized mtDNA in

vitro. The journal of histochemistry and cytochemistry : official journal of the Histochemistry Society *58*, 207-218.

Liang, H., and Ward, W.F. (2006). PGC-1alpha: a key regulator of energy metabolism. Advances in physiology education *30*, 145-151.

Liang, H., Ward, W.F., Jang, Y.C., Bhattacharya, A., Bokov, A.F., Li, Y., Jernigan, A., Richardson, A., and Van Remmen, H. (2011). PGC-1alpha protects neurons and alters disease progression in an amyotrophic lateral sclerosis mouse model. Muscle & nerve *44*, 947-956.

Lim, H.D., Kim, Y.S., Ko, S.H., Yoon, I.J., Cho, S.G., Chun, Y.H., Choi, B.J., and Kim, E.C. (2012a). Cytoprotective and anti-inflammatory effects of melatonin in hydrogen peroxide-stimulated CHON-001 human chondrocyte cell line and rabbit model of osteoarthritis via the SIRT1 pathway. Journal of pineal research *53*, 225-237.

Lim, M.A., Selak, M.A., Xiang, Z., Krainc, D., Neve, R.L., Kraemer, B.C., Watts, J.L., and Kalb, R.G. (2012b). Reduced activity of AMP-activated protein kinase protects against genetic models of motor neuron disease. The Journal of neuroscience : the official journal of the Society for Neuroscience *32*, 1123-1141.

Lin, J., Tarr, P.T., Yang, R., Rhee, J., Puigserver, P., Newgard, C.B., and Spiegelman, B.M. (2003). PGC-1beta in the regulation of hepatic glucose and energy metabolism. The Journal of biological chemistry *278*, 30843-30848.

Linker, R.A., Lee, D.H., Ryan, S., van Dam, A.M., Conrad, R., Bista, P., Zeng, W., Hronowsky, X., Buko, A., Chollate, S.*, et al.* (2011). Fumaric acid esters exert neuroprotective effects in neuroinflammation via activation of the Nrf2 antioxidant pathway. Brain : a journal of neurology *134*, 678-692.

Linnane, A.W., Marzuki, S., Ozawa, T., and Tanaka, M. (1989). Mitochondrial DNA mutations as an important contributor to ageing and degenerative diseases. Lancet *1*, 642-645.

Ma, T.C., Buescher, J.L., Oatis, B., Funk, J.A., Nash, A.J., Carrier, R.L., and Hoyt, K.R. (2007). Metformin therapy in a transgenic mouse model of Huntington's disease. Neuroscience letters *411*, 98-103.

Magnusson, J., Orth, M., Lestienne, P., and Taanman, J.W. (2003). Replication of mitochondrial DNA occurs throughout the mitochondria of cultured human cells. Experimental cell research *289*, 133-142.

Mahad, D., Lassmann, H., and Turnbull, D. (2008). Review: Mitochondria and disease progression in multiple sclerosis. Neuropathology and Applied Neurobiology *34*, 577-589.

Mahad, D.J., Ziabreva, I., Campbell, G., Lax, N., White, K., Hanson, P.S., Lassmann, H., and Turnbull, D.M. (2009). Mitochondrial changes within axons in multiple sclerosis. Brain: A Journal of Neurology *132*, 1161-1174.

Mancuso, R., Del Valle, J., Modol, L., Martinez, A., Granado-Serrano, A.B., Ramirez-Nunez, O., Pallas, M., Portero-Otin, M., Osta, R., and Navarro, X. (2014). Resveratrol Improves Motoneuron Function and Extends Survival in SOD1(G93A) ALS Mice. Neurotherapeutics : the journal of the American Society for Experimental NeuroTherapeutics *11*, 419-432.

Marik, C., Felts, P.A., Bauer, J., Lassmann, H., and Smith, K.J. (2007). Lesion genesis in a subset of patients with multiple sclerosis: a role for innate immunity? Brain : a journal of neurology *130*, 2800-2815.

McFarland, R., Taylor, R.W., and Turnbull, D.M. (2010). A neurological perspective on mitochondrial disease. Lancet neurology *9*, 829-840.

Mendelev, N., Mehta, S.L., Witherspoon, S., He, Q., Sexton, J.Z., and Li, P.A. (2011). Upregulation of human selenoprotein H in murine hippocampal neuronal cells promotes mitochondrial biogenesis and functional performance. Mitochondrion *11*, 76-82.

Michel, S., Wanet, A., De Pauw, A., Rommelaere, G., Arnould, T., and Renard, P. (2012). Crosstalk between mitochondrial (dys)function and mitochondrial abundance. Journal of cellular physiology *227*, 2297-2310.

Miller, M.L., Andringa, A., and Baxter, C.S. (1988). Critical comparison of histological and morphometric changes in SENCAR mouse epidermis in response to n-dodecane, 12-O-tetradecanoylphorbol-13-acetate and mezerein. Carcinogenesis *9*, 1959-1965.

Miquel, J. (1991). An integrated theory of aging as the result of mitochondrial-DNA mutation in differentiated cells. Archives of gerontology and geriatrics *12*, 99-117.

Morris, R.L., and Hollenbeck, P.J. (1993). The regulation of bidirectional mitochondrial transport is coordinated with axonal outgrowth. Journal of cell science *104 (Pt 3)*, 917-927.

Mosharov, E.V., Larsen, K.E., Kanter, E., Phillips, K.A., Wilson, K., Schmitz, Y., Krantz, D.E., Kobayashi, K., Edwards, R.H., and Sulzer, D. (2009). Interplay between cytosolic dopamine, calcium, and alpha-synuclein causes selective death of substantia nigra neurons. Neuron *62*, 218-229.

Mudo, G., Makela, J., Di Liberto, V., Tselykh, T.V., Olivieri, M., Piepponen, P., Eriksson, O., Malkia, A., Bonomo, A., Kairisalo, M.*, et al.* (2012). Transgenic expression and activation of PGC-1alpha protect dopaminergic neurons in the MPTP mouse model of Parkinson's disease. Cellular and molecular life sciences : CMLS *69*, 1153-1165.

Navarro, A., and Boveris, A. (2007a). Brain mitochondrial dysfunction in aging: conditions that improve survival, neurological performance and mitochondrial function. Frontiers in bioscience : a journal and virtual library *12*, 1154-1163.

Navarro, A., and Boveris, A. (2007b). The mitochondrial energy transduction system and the aging process. American journal of physiology Cell physiology *292*, C670-686.

Neuhaus, J.F., Baris, O.R., Hess, S., Moser, N., Schroder, H., Chinta, S.J., Andersen, J.K., Kloppenburg, P., and Wiesner, R.J. (2014). Catecholamine metabolism drives generation of mitochondrial DNA deletions in dopaminergic neurons. Brain : a journal of neurology *137*, 354-365.

Neupert, W. (1997). Protein import into mitochondria. Annual review of biochemistry *66*, 863-917.

Ngo, H.B., Lovely, G.A., Phillips, R., and Chan, D.C. (2014). Distinct structural features of TFAM drive mitochondrial DNA packaging versus transcriptional activation. Nature communications *5*, 3077.

Nicholls, D. (2002). Mitochondrial bioenergetics, aging, and aging-related disease. Science of aging knowledge environment : SAGE KE *2002*, pe12.

Olsen, N.K., Hansen, A.W., Norby, S., Edal, A.L., Jorgensen, J.R., and Rosenberg, T. (1995). Leber's hereditary optic neuropathy associated with a disorder indistinguishable from multiple sclerosis in a male harbouring the mitochondrial DNA 11778 mutation. Acta neurologica Scandinavica *91*, 326-329.

Ono, T., Isobe, K., Nakada, K., and Hayashi, J.I. (2001). Human cells are protected from mitochondrial dysfunction by complementation of DNA products in fused mitochondria. Nature genetics *28*, 272-275.

Pardo, J., Perez-Galan, P., Gamen, S., Marzo, I., Monleon, I., Kaspar, A.A., Susin, S.A., Kroemer, G., Krensky, A.M., Naval, J.*, et al.* (2001). A role of the mitochondrial apoptosis-inducing factor in granulysin-induced apoptosis. J Immunol *167*, 1222-1229.

Perez-Pinzon, M.A., Stetler, R.A., and Fiskum, G. (2012). Novel mitochondrial targets for neuroprotection. J Cereb Blood Flow Metab *32*, 1362-1376.

Puigserver, P., and Spiegelman, B.M. (2003). Peroxisome proliferator-activated receptor-gamma coactivator 1 alpha (PGC-1 alpha): transcriptional coactivator and metabolic regulator. Endocrine reviews *24*, 78-90.

Qin, W., Haroutunian, V., Katsel, P., Cardozo, C.P., Ho, L., Buxbaum, J.D., and Pasinetti, G.M. (2009). PGC-1alpha expression decreases in the Alzheimer disease brain as a function of dementia. Archives of neurology *66*, 352-361.

Raff, M.C., Whitmore, A.V., and Finn, J.T. (2002). Axonal self-destruction and neurodegeneration. Science *296*, 868-871.

Rapaport, D., Kunkele, K.P., Dembowski, M., Ahting, U., Nargang, F.E., Neupert, W., and Lill, R. (1998). Dynamics of the TOM complex of mitochondria during binding and translocation of preproteins. Molecular and cellular biology *18*, 5256-5262.

Rice, A.C., Keeney, P.M., Algarzae, N.K., Ladd, A.C., Thomas, R.R., and Bennett, J.P., Jr. (2014). Mitochondrial DNA Copy Numbers in Pyramidal Neurons are Decreased and Mitochondrial Biogenesis Transcriptome

Signaling is Disrupted in Alzheimer's Disease Hippocampi. Journal of Alzheimer's disease : JAD *40*, 319-330.

Ruthel, G., and Hollenbeck, P.J. (2003). Response of mitochondrial traffic to axon determination and differential branch growth. The Journal of neuroscience : the official journal of the Society for Neuroscience *23*, 8618-8624.

Sajic, M., Mastrolia, V., Lee, C.Y., Trigo, D., Sadeghian, M., Mosley, A.J., Gregson, N.A., Duchen, M.R., and Smith, K.J. (2013). Impulse conduction increases mitochondrial transport in adult mammalian peripheral nerves in vivo. PLoS biology *11*, e1001754.

Salic, A., and Mitchison, T.J. (2008). A chemical method for fast and sensitive detection of DNA synthesis in vivo. Proceedings of the National Academy of Sciences of the United States of America *105*, 2415-2420.

Sanders, L.H., McCoy, J., Hu, X., Mastroberardino, P.G., Dickinson, B.C., Chang, C.J., Chu, C.T., Van Houten, B., and Greenamyre, J.T. (2014). Mitochondrial DNA damage: Molecular marker of vulnerable nigral neurons in Parkinson's disease. Neurobiology of disease *70*, 214-223.

Sato, A., Nakada, K., and Hayashi, J.-I. (2006). Mitochondrial dynamics and aging: Mitochondrial interaction preventing individuals from expression of respiratory deficiency caused by mutant mtDNA. Biochimica et biophysica acta *1763*, 473-481.

Sato, A., Nakada, K., and Hayashi, J.-I. (2009). Mitochondrial complementation preventing respiratory dysfunction caused by mutant mtDNA. BioFactors (Oxford, England) *35*, 130-137.

Saxton, W.M., and Hollenbeck, P.J. (2012). The axonal transport of mitochondria. Journal of cell science *125*, 2095-2104.

Schapira, A.H. (1993). Mitochondrial cytopathies. Current opinion in neurobiology *3*, 760-767.

Shin, J.H., Ko, H.S., Kang, H., Lee, Y., Lee, Y.I., Pletinkova, O., Troconso, J.C., Dawson, V.L., and Dawson, T.M. (2011). PARIS (ZNF746) repression of PGC-1alpha contributes to neurodegeneration in Parkinson's disease. Cell *144*, 689-702.

Smith, K.J., and Lassmann, H. (2002). The role of nitric oxide in multiple sclerosis. Lancet neurology *1*, 232-241.

Song, L., Chen, L., Zhang, X., Li, J., and Le, W. (2014). Resveratrol ameliorates motor neuron degeneration and improves survival in SOD1(G93A) mouse model of amyotrophic lateral sclerosis. BioMed research international *2014*, 483501.

Soriano, F.X., Liesa, M., Bach, D., Chan, D.C., Palacín, M., and Zorzano, A. (2006). Evidence for a Mitochondrial Regulatory Pathway Defined by Peroxisome Proliferator–Activated Receptor-γ Coactivator-1α, Estrogen-Related Receptor-α, and Mitofusin 2. Diabetes *55*, 1783-1791.

St-Pierre, J., Drori, S., Uldry, M., Silvaggi, J.M., Rhee, J., Jager, S., Handschin, C., Zheng, K., Lin, J., Yang, W.*, et al.* (2006). Suppression of reactive oxygen species and neurodegeneration by the PGC-1 transcriptional coactivators. Cell *127*, 397-408.

Stack, C., Ho, D., Wille, E., Calingasan, N.Y., Williams, C., Liby, K., Sporn, M., Dumont, M., and Beal, M.F. (2010). Triterpenoids CDDO-ethyl amide and CDDO-trifluoroethyl amide improve the behavioral phenotype and brain

pathology in a transgenic mouse model of Huntington's disease. Free radical biology & medicine *49*, 147-158.

Stetler, R.A., Leak, R.K., Yin, W., Zhang, L., Wang, S., Gao, Y., and Chen, J. (2012). Mitochondrial biogenesis contributes to ischemic neuroprotection afforded by LPS pre-conditioning. Journal of neurochemistry *123 Suppl 2*, 125-137.

Storch, M.K., Stefferl, A., Brehm, U., Weissert, R., Wallstrom, E., Kerschensteiner, M., Olsson, T., Linington, C., and Lassmann, H. (1998). Autoimmunity to myelin oligodendrocyte glycoprotein in rats mimics the spectrum of multiple sclerosis pathology. Brain pathology *8*, 681-694.

Surmeier, D.J., and Schumacker, P.T. (2013). Calcium, bioenergetics, and neuronal vulnerability in Parkinson's disease. The Journal of biological chemistry *288*, 10736-10741.

Swerdlow, R.H. (2007a). Mitochondria in cybrids containing mtDNA from persons with mitochondriopathies. Journal of neuroscience research *85*, 3416-3428.

Swerdlow, R.H. (2007b). Treating neurodegeneration by modifying mitochondria: potential solutions to a "complex" problem. Antioxidants & redox signaling *9*, 1591-1603.

Taylor, R.W., He, L., Proctor, S.J., Middleton, P.G., and Turnbull, D.M. (2004). Mitochondrial DNA mutations in the haematopoietic system. Leukemia *18*, 169-170.

Tiranti, V., Savoia, A., Forti, F., D'Apolito, M.F., Centra, M., Rocchi, M., and Zeviani, M. (1997). Identification of the gene encoding the human

mitochondrial RNA polymerase (h-mtRPOL) by cyberscreening of the Expressed Sequence Tags database. Human molecular genetics *6*, 615-625.

Trapp, B.D., Peterson, J., Ransohoff, R.M., Rudick, R., Mork, S., and Bo, L. (1998). Axonal transection in the lesions of multiple sclerosis. The New England journal of medicine *338*, 278-285.

Tsunemi, T., and La Spada, A.R. (2012). PGC-1α at the intersection of bioenergetics regulation and neuron function: From Huntington's disease to Parkinson's disease and beyond. Progress in Neurobiology *97*, 142-151.

van Horssen, J., Witte, M., and Ciccarelli, O. (2012). The role of mitochondria in axonal degeneration and tissue repair in MS. Multiple Sclerosis Journal *18*, 1058-1067.

Ventura-Clapier, R., Garnier, A., and Veksler, V. (2008a). Transcriptional control of mitochondrial biogenesis: the central role of PGC-1alpha. Cardiovascular research *79*, 208-217.

Vidoni, S., Zanna, C., Rugolo, M., Sarzi, E., and Lenaers, G. (2013). Why mitochondria must fuse to maintain their genome integrity. Antioxidants & redox signaling *19*, 379-388.

Vincent, A.M., Edwards, J.L., McLean, L.L., Hong, Y., Cerri, F., Lopez, I., Quattrini, A., and Feldman, E.L. (2010). Mitochondrial biogenesis and fission in axons in cell culture and animal models of diabetic neuropathy. Acta neuropathologica *120*, 477-489.

Vogler, S., Goedde, R., Miterski, B., Gold, R., Kroner, A., Koczan, D., Zettl, U.K., Rieckmann, P., Epplen, J.T., and Ibrahim, S.M. (2005). Association of a common polymorphism in the promoter of UCP2 with susceptibility to multiple sclerosis. J Mol Med (Berl) *83*, 806-811.

Voloboueva, L.A., Duan, M., Ouyang, Y., Emery, J.F., Stoy, C., and Giffard, R.G. (2008). Overexpression of mitochondrial Hsp70/Hsp75 protects astrocytes against ischemic injury in vitro. Journal of Cerebral Blood Flow and Metabolism: Official Journal of the International Society of Cerebral Blood Flow and Metabolism *28*, 1009-1016.

Vosler, P.S., Graham, S.H., Wechsler, L.R., and Chen, J. (2009). Mitochondrial Targets for Stroke: Focusing Basic Science Research Toward Development of Clinically Translatable Therapeutics. Stroke *40*, 3149-3155.

Wallace, D.C., and Fan, W. (2009). The pathophysiology of mitochondrial disease as modeled in the mouse. Genes & development *23*, 1714-1736.

Wallace, D.C., Singh, G., Lott, M.T., Hodge, J.A., Schurr, T.G., Lezza, A.M., Elsas, L.J., 2nd, and Nikoskelainen, E.K. (1988). Mitochondrial DNA mutation associated with Leber's hereditary optic neuropathy. Science *242*, 1427-1430.

Wang, X., Su, B., Zheng, L., Perry, G., Smith, M.A., and Zhu, X. (2009). The role of abnormal mitochondrial dynamics in the pathogenesis of Alzheimer's disease. Journal of neurochemistry *109 Suppl 1*, 153-159.

Waxman, S.G., and Ritchie, J.M. (1993). Molecular dissection of the myelinated axon. Annals of neurology *33*, 121-136.

Weydt, P., Pineda, V.V., Torrence, A.E., Libby, R.T., Satterfield, T.F., Lazarowski, E.R., Gilbert, M.L., Morton, G.J., Bammler, T.K., Strand, A.D.*, et al.* (2006). Thermoregulatory and metabolic defects in Huntington's disease transgenic mice implicate PGC-1alpha in Huntington's disease neurodegeneration. Cell Metab *4*, 349-362.

Witte, M.E., Bø, L., Rodenburg, R.J., Belien, J.A., Musters, R., Hazes, T., Wintjes, L.T., Smeitink, J.A., Geurts, J.J.G., De Vries, H.E.*, et al.* (2009).

Enhanced number and activity of mitochondria in multiple sclerosis lesions. The Journal of Pathology *219*, 193-204.

Witte, M.E., Mahad, D.J., Lassmann, H., and van Horssen, J. (2014). Mitochondrial dysfunction contributes to neurodegeneration in multiple sclerosis. Trends in molecular medicine *20*, 179-187.

Wong-Riley, M.T., and Welt, C. (1980). Histochemical changes in cytochrome oxidase of cortical barrels after vibrissal removal in neonatal and adult mice. Proceedings of the National Academy of Sciences of the United States of America *77*, 2333-2337.

Yang, L., Calingasan, N.Y., Thomas, B., Chaturvedi, R.K., Kiaei, M., Wille, E.J., Liby, K.T., Williams, C., Royce, D., Risingsong, R.*, et al.* (2009). Neuroprotective effects of the triterpenoid, CDDO methyl amide, a potent inducer of Nrf2-mediated transcription. PloS one *4*, e5757.

Yin, W., Signore, A.P., Iwai, M., Cao, G., Gao, Y., and Chen, J. (2008). Rapidly increased neuronal mitochondrial biogenesis after hypoxic-ischemic brain injury. Stroke; a journal of cerebral circulation *39*, 3057-3063.

Ylikallio, E., Tyynismaa, H., Tsutsui, H., Ide, T., and Suomalainen, A. (2010). High mitochondrial DNA copy number has detrimental effects in mice. Human molecular genetics *19*, 2695-2705.

Zambonin, J.L., Zhao, C., Ohno, N., Campbell, G.R., Engeham, S., Ziabreva, I., Schwarz, N., Lee, S.E., Frischer, J.M., Turnbull, D.M.*, et al.* (2011). Increased mitochondrial content in remyelinated axons: implications for multiple sclerosis. Brain : a journal of neurology *134*, 1901-1913.

Zhao, W., Varghese, M., Yemul, S., Pan, Y., Cheng, A., Marano, P., Hassan, S., Vempati, P., Chen, F., Qian, X.*, et al.* (2011). Peroxisome proliferator

activator receptor gamma coactivator-1alpha (PGC-1alpha) improves motor performance and survival in a mouse model of amyotrophic lateral sclerosis. Molecular neurodegeneration *6*, 51.

Zheng, B., Liao, Z., Locascio, J.J., Lesniak, K.A., Roderick, S.S., Watt, M.L., Eklund, A.C., Zhang-James, Y., Kim, P.D., Hauser, M.A.*, et al.* (2010). PGC-1alpha, a potential therapeutic target for early intervention in Parkinson's disease. Science translational medicine *2*, 52ra73.

Zhou, R., Yazdi, A.S., Menu, P., and Tschopp, J. (2011). A role for mitochondria in NLRP3 inflammasome activation. Nature *469*, 221-225.

Zsurka, G., and Kunz, W.S. (2013). Mitochondrial involvement in neurodegenerative diseases. IUBMB life *65*, 263-272.